SEDIMENTARY PROCESSES AND PALEOENVIRONMENTAL SIGNIFICANCE OF LAMINATED DIATOMACEOUS SEDIMENTS FROM THE MIOCENE MONTEREY FORMATION, CALIFORNIA, USA

by

ALICE S. CHANG

B. Sc., The University of British Columbia, 1995

A THESIS SUBMITTED IN PARTIAL FULFILLMENT OF THE REQUIREMENTS

FOR THE DEGREE OF MASTER OF SCIENCE

in

THE FACULTY OF GRADUATE STUDIES

(Department of Earth and Ocean Sciences)

We accept this thesis as conforming to the required standard

THE UNIVERSITY OF BRITISH COLUMBIA

October, 1997

In presenting this thesis in partial fulfilment of the requirements for an advanced degree at the University of British Columbia, I agree that the Library shall make it freely available for reference and study. I further agree that permission for extensive copying of this thesis for scholarly purposes may be granted by the head of my department or by his or her representatives. It is understood that copying or publication of this thesis for financial gain shall not be allowed without my written permission.

Department of _Earth & Ocean Sciences_

The University of British Columbia
Vancouver, Canada

Date _October 15, 1997_

ABSTRACT

Diatomaceous sediments from the Miocene Monterey Formation in Santa Barbara County, California, were investigated to gain a better understanding of sedimentary processes, diatom paleoecology, and the paleoenvironmental significance of laminated organic-rich hemipelagites. Sedimentary couplets and individual laminae from laminated intervals were described and classified to assess paleoenvironmental settings and interannual processes of hemipelagic sedimentation. Speckled beds, a type of non-laminated interval, were studied to understand physical properties of laminated diatomaceous sediments and slope failure processes. We utilized field observations, hand sample descriptions, x-radiography, optical microscopy and scanning electron microscopy to examine the composition and interpret the origins of laminae and speckled beds.

Laminated intervals, sedimentary couplets and individual laminae were classified on the basis of bimodality, thickness, mud-diatom domination, spacing, and cyclicity. Five main lamina types were defined, based on composition and microfossil content. These laminae were termed detrital, thin biosiliceous, thick continuous diatomaceous, thick discontinuous diatomaceous and macerated biosilica. We focused on diatom paleoecology and biologically mediated sedimentary processes to interpret the origin of laminae and distinct couplet types, concluding that various diatom blooms—including self-sedimentation of conspicuous blooms and diatom mats—preserve a unique and high resolution paleoenvironmental record.

A study of distinct, non-laminated intervals termed speckled beds gives insights to the physical properties of organic-rich hemipelagites. Speckled beds are sharply based and are abruptly overlain by undisturbed laminated diatomite. The speckled fabric is derived from discrete detritus-rich and diatom-rich aggregates ranked in size and termed speckles, blebs and lozenges. Four types of speckled beds were classified: unimodal, bimodal, amalgamated, and speckled beds with laminated intraclasts. Failure of cohesive laminated sediments deposited on a slope within the oxygen minimum zone is prerequisite for speckled bed formation. We postulate a gravity flow hypothesis that describes the deposition of speckled beds from viscous, high-density turbidity flows.

A thorough understanding of the processes by which individual lamina types and speckled beds are produced provides refining insights into Miocene paleoenvironments. The approaches developed in this study can also be applied to other subannually deposited hemipelagic sediments accumulating beneath productive coastal upwelling regions.

TABLE OF CONTENTS

LIST OF TABLES

LIST OF FIGURES

CHAPTER 2

CHAPTER 3

ACKNOWLEDGEMENTS

CHAPTER 1

INTRODUCTORY STATEMENTS

1.1   Introduction

Finely laminated hemipelagic sediments are recorders of *and* participants in Earth's environmental history. The importance of this aspect is two-fold: biological, oceanographic and environmental information is recorded at an extremely high resolution (Brodie and Kemp 1994; Kemp 1995; Kemp et al. 1995; Pearce et al. 1995; Pike and Kemp 1997); the accumulation of unrecycled organic carbon and opal within hemipelagites affects biogeochemical cycles within the local, regional and global environments (Grimm et al. 1997). Thus, laminated hemipelagic sediments are increasingly being sought as paleoenvironmental archives. Past studies have focused on broad trends in the presence and/or absence of laminated intervals and bulk sediment composition, yielding paleoenvironmental interpretations on millennial to longer time scales (cf. Garrison et al. 1981; Govean and Garrison 1981; Anderson 1986). But with the relatively recent application of refined imaging techniques such as backscattered electron microscopy (Kemp 1990; Grimm 1992a; Bull and Kemp 1995), collimated-beam x-radiography (Algeo et al. 1994; Collins 1996), and computerized axial tomography (Behl 1997), exploring short-term environmental signals recorded in laminated sediments has become more accessible and scientifically rewarding.

Diatomaceous sediments from the Monterey Formation offer an excellent opportunity to explore subseasonal and subannual sedimentary processes in the southern California Borderland during the Miocene. In this study, two aspects of diatomaceous sediments from the Monterey Formation are considered. The first is a lamination-scale assessment of the composition and paleoenvironmental settings of rhythmic sedimentary couplets and individual laminae. Lamination-scale paleoecological and geochemical examinations of laminated hemipelagic sediments is a method that has been recently applied to studying fine-scale subannual sedimentary processes. This has been attempted on sediments from areas such as the Gulf of California (e.g. Pike and Kemp 1996a) and modern-day off-shore

1

California Borderland Basins (e.g. Bull and Kemp 1995; Grimm et al. 1996). Few studies of this kind have been attempted on Monterey Formation diatomites (cf. Chang 1995; Johnson et al. 1997).

In the second aspect, we explore slope destabilization and sediment failure processes from the Monterey Formation, and their relationship with organic-rich diatomaceous sediments. We introduce the concept of speckled beds as a distinctive type of non-laminated interval. Although there is plenty of literature regarding other non-laminated intervals, including muddy turbidites, flood suspensate layers, and bioturbated beds (Stow and Bowen 1980; Behl 1995; Ozalas et al. 1994), no literature has described speckled beds and their paleoenvironmental significance.

1.2 Structure of Thesis

This thesis was written as two independent papers to be submitted to journals. Due to the similarity in setting and methodology of the two studies, there is minor redundancy in content, particularly in the introductory sections.

Chapter 2 is titled "Diatomaceous sediments from the Miocene Monterey Formation, California, USA—a lamina-scale investigation of biological, ecological, and sedimentary processes." In this chapter, classification of laminated diatomites is presented, and descriptions and interpretations of individual laminae are discussed. This chapter is co-authored by Kurt A. Grimm and Lisa D. White and will be submitted to *Palaios*.

Chapter 3 is titled "Speckled beds in the Miocene Monterey Formation, California, USA: distinctive gravity flow deposits in finely laminated diatomaceous sediments." In this chapter, we describe the texture and composition of speckled beds, consider their origin by slope failure processes, and develop a gravity flow hypothesis to describe the formation of these unique deposits. This chapter is co-authored by Kurt A. Grimm and has been submitted to the *Journal of Sedimentary Research*.

CHAPTER 2

DIATOMACEOUS SEDIMENTS FROM THE MIOCENE MONTEREY FORMATION, CALIFORNIA, USA—A LAMINA-SCALE INVESTIGATION OF BIOLOGICAL, ECOLOGICAL, AND SEDIMENTOLOGICAL PROCESSES

2.1   Abstract

In this study, we utilize outcrop and hand sample observations, x-radiography, optical microscopy and scanning electron imaging to determine the composition and paleoecology of laminated diatomaceous hemipelagites from the Miocene Monterey Formation at Lompoc, California. We elucidate paleoenvironmental settings, paleoecological associations and biologically mediated sedimentary processes to understand submillimetre event stratigraphies in these subannually deposited laminites.

We present a new method of classifying lamination styles based on bimodality, thickness, domination, spacing and cyclicity. We also describe five types of laminae with emphasis on diatom ecology. (1) Detrital laminae consist of detrital silt and clay and robust diatom species, and are considered to have been deposited during the autumn and winter rainy seasons. (2) Most thin biosiliceous laminae are composed of poorly preserved high diversity diatom assemblages although some laminae consist of pristine monospecific diatom or silicoflagellate assemblages. (3) Thick continuous diatomaceous laminae consist mainly of well preserved low diversity diatom assemblages interpreted to have been deposited via post-bloom self-sedimentation during the spring and summer. (4) Thick discontinuous diatomaceous laminae are composed of either *Thalassiothrix longissima* mat laminae or flocs of *Chaetoceros* setae. One lensoid *Chaetoceros* setae lamina measured 15 cm in length and 5 mm in thickness. (5) Macerated biosilica laminae consist exclusively of highly fragmented and/or dissolved biosilica from a variety of taxa. Interpreting the origins of submillimetre event stratigraphies from laminated diatomaceous hemipelagites are important for understanding sedimentary processes in the coastal upwelling region of the Miocene California margin.

2.2   Introduction

Laminated diatomites of the Miocene Monterey Formation are a unique and underutilized paleoenvironmental archive, providing an excellent opportunity to explore paleoecology and fine-scale sedimentary processes in the California Borderland region (Chang 1995; Pearce et al. 1995; Chang et al. 1997). Because laminae are deposited at subannual and subseasonal time scales, a historical record of ocean and climate variability at high temporal resolutions can be compiled (Brodie and Kemp 1994; Kemp 1995; Hagadorn et al. 1995; Pearce et al. 1995; Pike and Kemp 1997). Past studies of the Monterey Formation and modern analogues focused on broad comparisons between laminated and non-laminated intervals where broad-scale origin, composition and paleoenvironmental significance had been assessed (Hülsemann and Emery 1961; Soutar and Crill 1977; Schrader et al. 1980; Garrison et al. 1981; Baumgartner et al. 1985; Anderson et al. 1987; Schimmelmann et al. 1992). Further progression of these studies led to the analysis of lamina types and interpretations of paleoecology from ODP cores (e.g. Kemp 1990; Grimm et al. 1996). In this study, we examine couplets and laminae from the outcrop and classify them in a stratigraphic context, provide lamination-scale descriptions, and interpret paleoecology and sedimentary processes. To understand broad, long-term changes in paleoenvironment and their effects on hemipelagic sedimentation, we must first investigate the composition and origins of individual laminae.

Recent studies involving high-resolution backscattered electron microscopy of laminated hemipelagites from highly productive regions such as the Santa Barbara Basin (e.g. Bull and Kemp 1995; Grimm et al. 1996, 1997), the Gulf of California (Pike and Kemp 1996a), and the Peruvian margin (Kemp 1990; Brodie and Kemp 1994) have shed light on ecological assemblages, biological activity and interannual sedimentary processes. These studies have important implications for furthering the understanding of biologically mediated sedimentary processes (Alldredge and Gottschalk 1989; Grimm et al. 1996) and ocean-biogeochemical cycles (i.e. biological pump; Grimm et al. 1997). Lamination-scale examinations of paleoecology and geochemistry are also useful for assessing the paleoenvironment of the Monterey Formation and Monterey-type deposits for hydrocarbon source rock analysis (e.g. Isaacs and Garrison 1983; Isaacs and Petersen 1987; Johnson et al. 1997).

4

For this study, we will be surveying the general sedimentology of diatomaceous sediments from the Celite diatomite quarry in Lompoc, Santa Barbara County, California (Fig. 2.1). We will develop and apply a new classification and description scheme for laminated sediments. We will also focus on the paleoecological associations, origins and paleoenvironmental significance of individual lamina types.

2.3   Methods and Materials

Approximately 218 m of laminated diatomite are exposed at Celite quarry. According to updated chronostratigraphic data, the diatomaceous sediments date at 8.2 Ma at the base of the exposed section to 7.3 Ma at the top of the economically mineable deposits (J. A. Barron, written communication, 1997; Barron and Isaacs, in press). Our studies concentrated on diatomites from a location in the vicinity of the economically mineable deposits which was topographically the lowest in all of the quarry, darkest in colour and presumably the least weathered. These beds dipped 45° to the north and constituted part of the southern limb of an east-west trending syncline.

Two stratigraphically continuous sections totalling ~59 m were cleared by bulldozers and scraped clean with sharpened hoes. We subdivided the sections into units based on the respective diatom or mud richness of the sediments (Fig. 2.2). The sections were measured and described, focusing on both laminated and non-laminated intervals. Samples were cut with a gas-powered concrete saw (30-cm diameter blade) producing blocks ranging in size from 10-15 cm by 20-50 cm; 23 blocks were collected. Three samples from a correlative interval on the northern limb of the syncline 850 m to the northwest were also collected to assess lamination-scale correlation; this section was topographically higher and more extensively weathered than our main traverse. In addition, reconnaissance samples collected throughout the quarry were reexamined for this study (K. Grimm, unpublished data, 1994; Chang 1995). All samples were wrapped for transport in foil, heavy-duty plastic wrap and bubble wrap.

Figure 2.1.   Map of study location: Celite Quarry, Santa Barbara County, California (modified from Grimm and Orange 1997).

BENCH 2

Columns: metres | Samples | Lithology | Units | Unit description

- 2-9, 2-8 (at ~16 m, samples analysed in detail)
- 2-7b (at ~15 m)
- 2-5 (at ~11 m)
- 2-4 (at ~8 m)
- 2-3, 2-2 (at ~6.5 m)

Unit 2D: HB couplets; abundant, closely-spaced bloom laminae in packets; SBs are common; muddy turbidite at 12.8-13.0 m with burrowing in HB laminae below

Unit 2C: diatom-rich, bloom-rich HB couplets

Unit 2B: massive mud layer: amalgamation of thin muddy turbidites; minimal bioturbation

Unit 2A: HB couplets

MAIN TRAVERSE

Columns: metres | Samples | Lithology | Unit | Unit descriptions

- M-BP* (at ~59 m)
- M-29 (at ~53 m)
- M-26 (at ~51 m)
- M-22 (at ~43 m)
- M-21* (at ~41 m)
- M-18 & 19 (at ~39 m)
- M-17 (at ~37 m)
- M-16 (at ~34 m)
- M-13 & 14 (at ~28 m)
- M-12 (at ~27 m)
- M-10 & 11 (at ~26 m)
- M-9* (at ~25 m)
- M-7 & 8 (at ~23 m)
- M-6 (at ~22 m)
- M-3 (at ~20 m)
- M-2 (at ~19 m)

Unit O: highly diatomaceous; abundant bloom laminae and mats; no thick muddy turbidites; 20 IMZ horizons, 8 slumped horizons containing bloom laminae

Unit N: mud-rich laminae; amalgamated burrowed beds at top

Unit M: similar to Unit G but muddier

Unit L: mud-dominated couplets; burrows at base; massive silty bed at top

Unit K: sub-equal HB laminae; burrowed bed at top of unit

Unit J: volcanic ash horizon

Unit I: closely-spaced diatom-rich laminae; abundant bloom beds; minor SBs

Unit H: similar to Unit G but muddier; few bloom laminae; burrowed bed at top of unit

Unit G: closely-spaced, razor-striped HB/MB couplets; minor SBs

Unit F: mottled burrowed bed

Unit E: MB/HB couplets; many bloom laminae; SBs; concretionary horizons at 27 m

Unit D: amalgamted burrowed beds; MB/HB couplets

Unit C: MB/HB couplets; razor/pin-striped laminae; minor burrowing; SBs

Unit B: mud-dominated MB couplets

Unit A: HB couplets; slumps at base of unit; bloom laminae and blebs abundant; SBs

Legend

- ▷ Samples collected, slabbed & x-rayed
- ★ correlative sample collected
- ▶ Samples analysed in detail for this study
- ~ Bioturbation
- Laminated diatomite with IMZ horizon
- Laminated diatomite
- Mud
- Mud with burrows
- Silt

HB=high bimodality; MB=moderate bimodality; SB=speckled bed; IMZ=intrastratal microfractured zone

Figure 2.2.   Stratigraphy of measured sections and sample locations.

7

In the laboratory, the blocks were unwrapped and slabbed perpendicular to bedding with a bandsaw to a thickness of 1 cm. Four slabs were cut from each block for the purposes of hand sample description, x-radiography, light microscopy, scanning electron microscopy, and geochemical analyses (Fig. 2.3).

2.3.1 Hand Sample Description

Microstratigraphic descriptions of slabbed and sanded hand samples focused on bimodality, thickness, mud-diatom domination, spacing and cyclicity. Non-laminated intervals include massive mud beds, bioturbated silty mud beds and speckled beds (Chapter 3).

2.3.2 X-radiography

X-radiography was performed at Vancouver Hospital, UBC Campus site, with a CGR 300-T mammography x-ray machine running at 26 keV for all samples; clay-rich samples were exposed at 50 mAs and diatom-rich samples at 32 mAs. X-radiography by mammography produces sharper, higher resolution images than conventional x-ray techniques because the collimated beam of the mammogram reduces parallax and obliquity between discrete laminae (Algeo et al 1994; Collins 1996; Grimm et al 1996; cf. Chang 1995). Saturation of x-ray film is inversely proportional to the bulk density of the sediments: diatomaceous sediments are porous and have a high x-ray transmissivity; thus, they appear light-coloured in x-ray contact prints whereas dense detrital sediments appear dark. Contact photographic prints were developed from the x-ray negatives and from the prints, five samples (2-8, 2-9, M-3, M-6 and M-BP; see Appendix 2) were chosen for more detailed description and analysis based on the superior image quality of their x-radiographs and diverse sedimentary features.

2.3.3 Optical Microscopy

Smear and strewn slides were used to identify microfossils, assess ecological assemblages, and states of frustule preservation from selected laminae. For smear slides, a minute volume of sediment from each lamina was extracted with a metal probe (Chang 1995). For strewn slides, a maximum of 1 cm^3 of sediment from each lamina was collected by separating the target lamina from surrounding
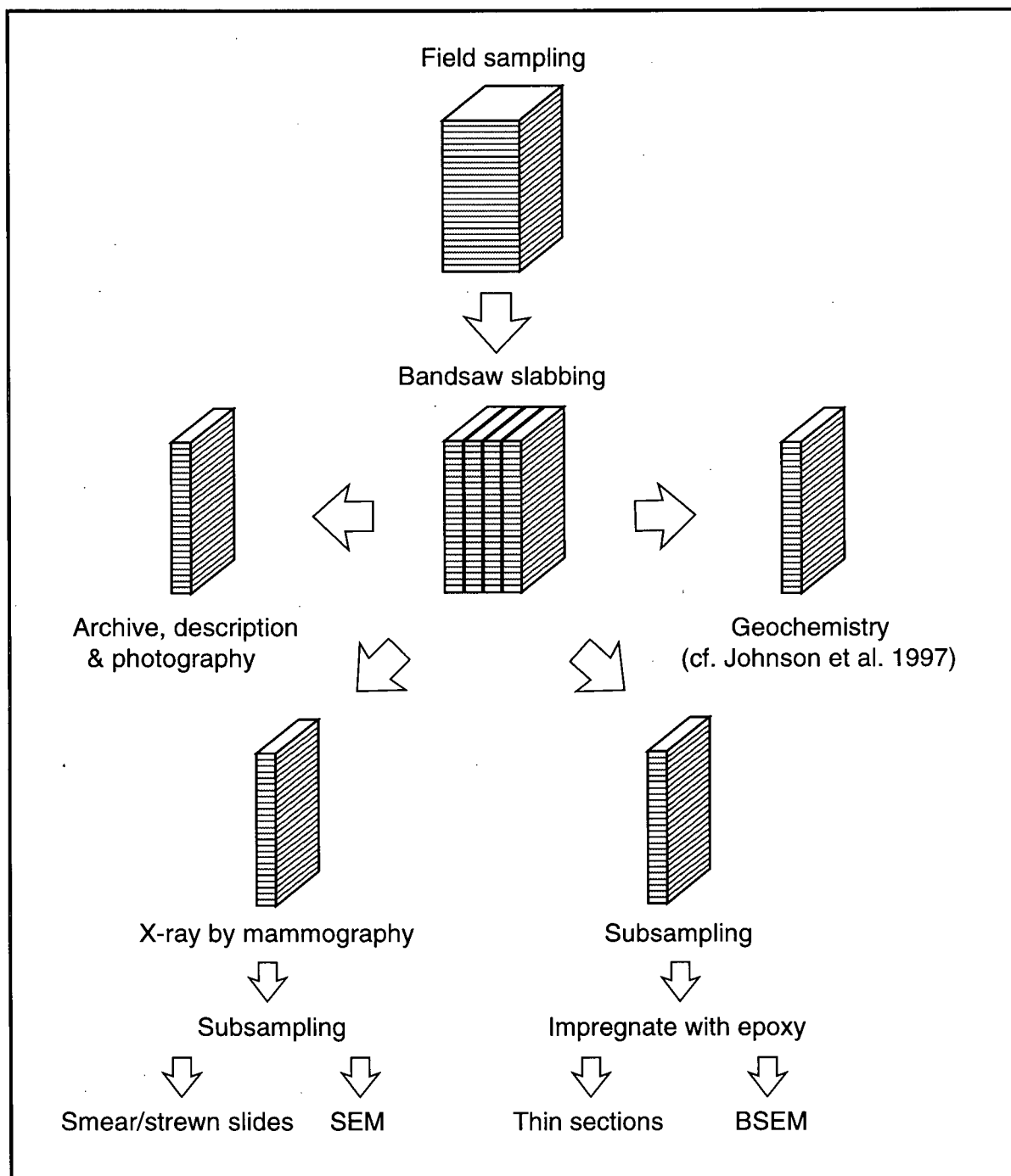
Figure 2.3. Methodology of analytical procedures (cf. Grimm 1992b).

sediments with a single-edge razor. The sediment was placed into a vial, diluted with distilled water and shaken to create a slurry. Approximately 5 mL of the slurry were pipetted from the vial and placed directly onto a cover slip. Smear and strewn slides were mounted with Hyrax epoxy.

Semi-quantitative counts were performed on a petrographic microscope at a magnification of 1000x by examining at least half of each slide; counting criteria are listed in Table 1. Preservation of diatom frustules and other microfossils was based on the degree of alteration (i.e. fragmentation and/or dissolution) of individual specimens (Table 1). Slides were examined in both plane-polarized light and crossed-polarized light. Cross-polarized light was used to highlight coccoliths which were not visible in plane-polarized light (Chang 1995). Full quantitative diatom counts were performed by Dr. Lisa D. White on selected smear slide samples (App. 6).

2.3.4   Scanning Electron Microscopy

High-magnification imaging was achieved through secondary electron microscopy and backscattered electron microscopy. Conventional secondary electron microscopy permits the imaging of specimen topography, giving a bedding-plane view of microfossil taxa content and their states of preservation. Centimetre-sized cubes were sectioned parallel to bedding and Au-Pd coated. Backscattered electron microanalysis of epoxy-impregnated samples produces cross-sectional images of sediments and allows for optimal examination of submillimetre fabrics which document intra- and interannual ocean-climate variability and changes in sedimentary processes (Bull and Kemp 1990; Kemp 1995; Pearce et al. 1995; Grimm et al 1996). Samples were sawed perpendicular to bedding into centimetre-sized cubes and rods, vacuum-impregnated with a low-viscosity epoxy (Struers brand Epofix) at 172 kPa, and left to set overnight. The surface to be imaged was then highly polished with fine Al_2O_3 abrasive on a cloth rotary lap and carbon-coated. Both secondary and backscattered electron microscopy were performed with a Philips XL-30 scanning electron microscope.

Table 2.1. Microfossil abundance and preservation criteria for semi-quantitative smear and strewn slide analyses.

Abundance

Abundant	≥2 specimens per field of view
Common	1 specimen per field of view
Few	1 specimen per vertical traverse
Rare	<1 specimen per vertical traverse
Barren	0 specimens in sample

Preservation

Good	lightly silicified and heavily robust specimens present, no alteration (i.e. fragmentation and/or dissolution)
Moderate	lightly silicified specimens present but altered
Poor	lightly silicified specimens absent or rare and altered; assemblage dominated by robust forms

2.4 General Sedimentology and Oceanographic Conditions

2.4.1 *Monterey Formation*

Organic-rich hemipelagic sediments of the Monterey Formation were deposited in either a series of fault-bounded basins similar to those along the modern California Borderland (Blake 1981; Hagadorn et al 1995), or on low-gradient slopes along an open continental margin (Isaacs et al. 1996). In either case, the Monterey Formation was deposited within an oxygen minimum zone (Garrison et al. 1981).

The Monterey Formation has been classically described as a tripartite sequence consisting of a lower calcareous facies dominated by coccolithophores, a middle transitional phosphatic facies, and an upper siliceous facies dominated by diatoms (Pisciotto and Garrison 1981). This perspective presumes that deposition of the Monterey Formation neatly preserves broad-scale paleoenvironmental changes at all locations (Isaacs et al. 1996). Recent reevaluation of this assessment illustrates that deposition of the Monterey Formation is much more complicated than previously documented, with facies deposition governed by a dynamic prograding margin and controlled by local water depths, bottom topography and sediment supply (Isaacs et al. 1996). More specifically, differential preservation of siliceous and calcareous components from one depositional site to another, along with varying degrees of phosphatization, may have been superimposed on major paleoceanographic trends (White et al. 1992). Owing to the localized differences, the tripartite sequence is not present in all areas (White et al. 1992).

Deposition of the upper siliceous facies of the Monterey Formation is generally attributed to intensified coastal upwelling. A series of middle Miocene cooling steps propagated by Antarctic ice sheet expansion from ~16-13 Ma (Ingle 1981; Barron and Baldauf 1989) resulted in a steep pole-to-equator thermal gradient, enhanced wind strengths and intensified coastal upwelling (Pisciotto and Garrison 1981; Ingle 1981; Barron and Baldauf 1989). Determination of the timing of initial siliceous deposition was based on the first appearance of glassy quartz and opal-CT cherts at the base of the siliceous facies (White 1989; White et al. 1992). Glassy quartz and opal-CT cherts are the diagenetic equivalents of detritus-poor, silica-rich diatomite (Pisciotto and Garrison 1981; Isaacs 1981). Initial deposition of the upper siliceous facies, as determined with cherts in on-shore sections, began at 14.8-

12

14.3 Ma in north-central California (Pt. Año Nuevo, 37°N; White et al 1992). Diatomaceous sedimentation in southern California (Lions Head, 35°N) began at 12.7 Ma. Siliceous sedimentation, determined in off-shore DSDP sections at Site 173 (40°N, off northern California), occurred at ~18 Ma and at ~12 Ma at Site 495 (12°N, off Central America). According to White et al. (1992), this north-south difference in age was probably due to the progressive southward intensification of the California Current.

The change in microfossil flora from coccolithophore to diatom-dominated sedimentation reflected increased nutrient delivery to surface waters via enhanced upwelling. Coastal upwelling along the California margin results from southward flowing winds parallel to the coast which drive the California Current (Huyer 1983). In modern oceans diatoms thrive in active upwelling areas such as the Peru-Chile margin and the Gulf of California (Soutar et al 1981; Baumgartner et al 1985; Sancetta et al 1992; Brodie and Kemp 1994). Off the California Borderland, increased northerly wind stresses during the spring and summer intensify the southward flowing California Current causing maximal upwelling and delivery of nutrient-rich waters to the surface (Sancetta et al 1992; Sautter and Sancetta 1992).

2.4.2   *Formation of Laminated Sediments*

When biogenic and detrital sediments accumulate in an area that is not conducive to erosion or bioturbation, laminated hemipelagic sediments are produced. Thus, heterogeneities in the texture and/or composition of sediment supply are required for the production of laminated diatomites whereas an absence of physical reworking or bioturbation permits their preservation (Grimm et al. 1996). A well-defined oxygen minimum zone, often situated beneath highly productive coastal upwelling regions, excludes bioturbating macrobenthos and is caused by the exhaustion of dissolved oxygen in the water as decaying organic matter settles through the water column (Gardner and Hemphill-Haley 1986). Fluctuations of the oxygen minimum zone over time may result from changing eustatic sea levels, or changes in biological oxygen demand via changes in primary productivity and export efficiency (Kennett et al. 1994). The sediment record reflects oxygen minimum zone fluctuations as evidenced by the quality of laminae and amount of bioturbation (Govean and Garrison 1981; Anderson et al. 1987; Gardner and Hemphill-Haley, 1986; Savrda 1995).

Laminated sediments may also be preserved in oxygenated environments. Laminated Neogene sediments involving thick mat laminae of the pennate diatom *Thalassiothrix longissima* and related species have been observed in the North Atlantic (Bodén and Backman 1996) and equatorial Pacific (Kemp and Baldauf 1993). Mats are buoyant, macroscopic diatom communities which photosynthesize and uptake nutrients (Villareal and Carpenter 1989; Villareal et al. 1993). The impenetrable meshwork of the *T. longissima* mats effectively produces preconsolidated laminae in the water column with high tensile strengths which, upon sedimentation, deter bioturbating bottom-dwelling organisms from obliterating primary sedimentary features (Bodén and Backman 1996).

2.4.3   Overview of the Monterey Formation at Lompoc

The upper siliceous facies of the Monterey Formation at Celite quarry consists of both laminated and non-laminated intervals. The majority of our section comprised millimetre-scale laminated diatomite. The most diatom-rich laminites in the quarry occur in economically mined intervals designated as DE-1 and DE-2 zones by Celite quarry (E. Morlan, personal communication, 1996). Hybrid fault/vein deformation structures termed intrastratal microfractured zones (Grimm and Orange 1997) are also abundant in this interval. Non-laminated intervals, representing episodic events that punctuate laminated sequences, include massive beds, bioturbated beds and speckled beds.

Massive beds are tan-coloured, decimeter-thick bands which are generally siltier than the surrounding laminated sediments. Most massive beds have a homogeneous texture although some show weak grading and contain intraclasts or convolute laminae. Multiple events may be amalgamated to form beds up to 50 cm in thickness. We attribute the deposition of these massive beds to muddy turbidites (Stow and Bowen 1980).

Bioturbated beds are markedly siltier than the surrounding laminated sediments, confirming the observations of Ozalas et al. (1994). Bioturbated beds are sharply based and commonly erosive, consisting of an upper massive and burrowed unit (primary stratum), and a lower unit of burrow-imprinted laminae (piped zone; Savrda 1995). Burrow-imprinted laminae are always associated with superjacent massive units that are abruptly overlain by undisturbed laminated sediments. Despite careful observation, no evidence for transitional fabrics (i.e. minimally burrowed or disturbed laminae)

14

between bioturbated beds and laminae overlying them were present, suggesting the abrupt termination of burrowing episodes. The only ichnogenus observed in our sections was *Thalassinoides* (cf. Föllmi and Grimm 1990; Savrda and Ozalas 1993; Grimm and Föllmi 1994).

Speckled beds are not siltier than surrounding laminated sediments, range in thickness from 3 mm to 10 cm and possess bedding-parallel fabrics. Speckled beds consist of sand- to pebble-sized diatom-rich aggregates, detritus-rich aggregates, and laminated intraclasts uniformly distributed throughout a matrix of mud and macerated biosilica (see Chapter 3). Speckled beds sharply overlie and are abruptly overlain by laminated sediments and are not crosscut by bioturbation. We attribute the formation of speckled beds to soft-sediment failure and erosive reworking of laminated diatomite within the oxygen minimum zone.

Stratigraphic oscillations between mud-rich intervals, diatom-rich intervals and non-laminated intervals may be influenced by external forces such as climate and sea level fluctuations (i.e. allocyclic mechanisms), and internal forces which include turbidity current lobe switching (i.e. autocyclic mechanisms).

Both laminated and non-laminated features were tracked across the quarry by comparing samples extracted from our main traverse in the south limb of the syncline to the weathered samples in the north. Non-laminated beds and laminae as thin as 0.5 mm were laterally continuous across the quarry with only minor localized differences (e.g. slump folding) between both ends of the syncline (Fig. 2.4). The distance between the two sampling sites was 850 m (T. Sumner, personal communication, 1997).

2.5   Classification of Lamination Styles

We introduce a new method for classifying lamination styles based on five main parameters: bimodality, thickness, domination, spacing and cyclicity (Fig. 2.5). This classification provides a convenient way for grouping sedimentary laminae that is useful for the description and subsequent interpretation of different lamina types.

15
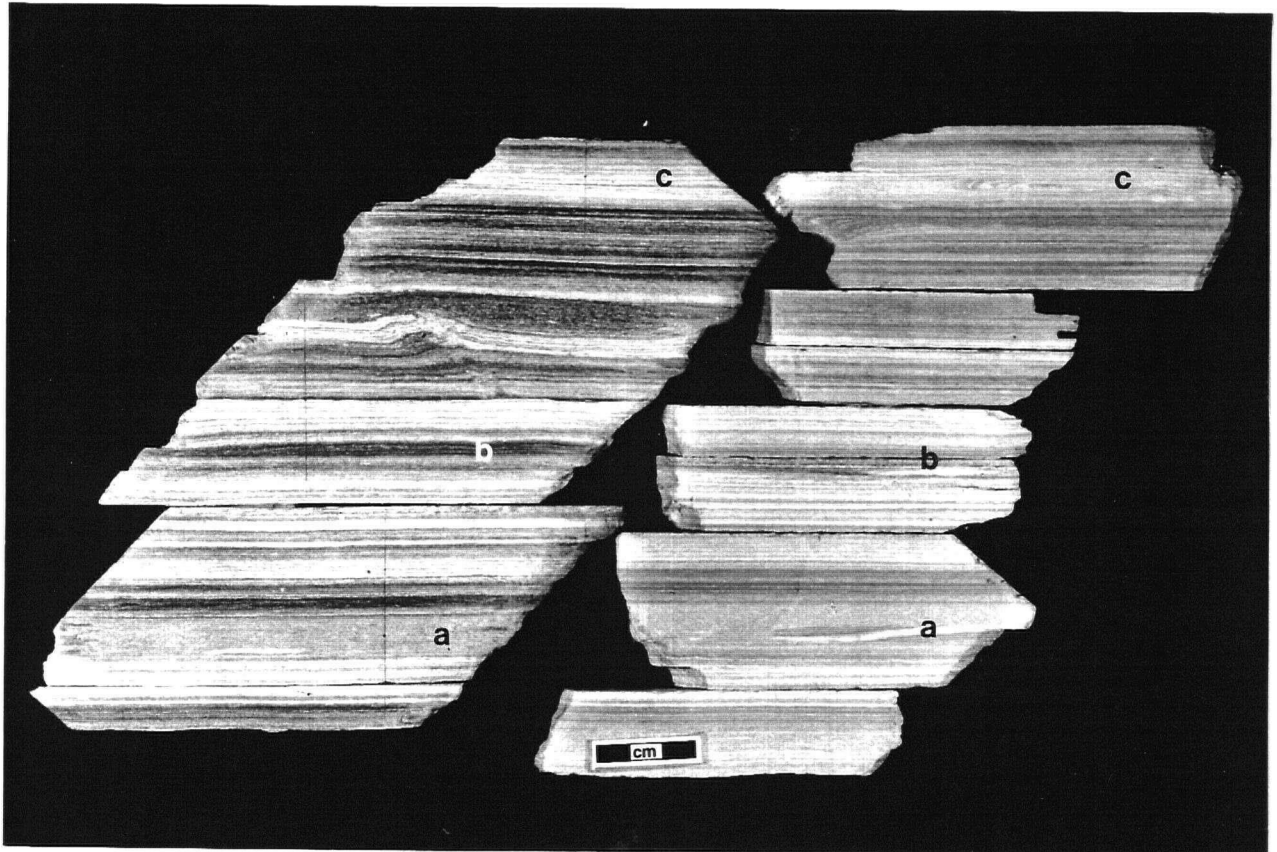
Figure 2.4. Sample M-BP: a comparison between unweathered (left) and weathered (right) slabs showing correlation of laminae and other sedimentary features across a distance of 850 m: (a-a) speckled beds (Chapter 3), (b-b) mud-rich couplets, (c-c) diatom-rich couplets. The only differences between the samples are localized slump folds.

2.5.1 Bimodality

Grimm et al. (1996) define bimodality as the relative difference in x-radiograph grey scale between adjacent laminae, reflecting the bulk density (i.e. grain size differences, packing and composition) of the sediments. This concept was expanded for application in the field and on slabbed samples by comparing the differences in colour of juxtaposed laminae of different compositions and textures (Fig. 2.6). Since detrital layers are darker and denser than light-coloured diatomaceous laminae, colour differences on hand samples parallel contrasts in x-radiograph grey scale; i.e. light-coloured diatom-rich laminae correlate to light shades on x-radiograph contact prints since porous diatom frustules are nearly x-ray transparent (App. 2). Adapting bimodality to field studies provides a quick, semi-quantitative assessment of sediment composition and bulk density.

In the field, couplets displaying a stark difference between white to light olive-grey diatomaceous laminae and dark olive mud laminae are termed *high bimodality* couplets. High bimodality couplets in x-radiographs show a large contrast in grey scale and thus bulk density (Figs. 2.5 and 2.6; App. 2). High bimodality sequences signify strong seasonality and high heterogeneity in sediment composition (Grimm et al. 1996). *Moderate bimodality* couplets possess a moderate colour difference between mud laminae and weakly diatomaceous laminae. *Low bimodality* couplets display little colour differences between mud laminae and poorly diatomaceous laminae which correspond to a low contrast in x-radiograph grey scale and subsequently weak seasonality (Grimm et al. 1996). We have not quantified differences between sample colour and x-radiograph grey scale, yet recognize that this can be readily accomplished via scanning and image analysis.

2.5.2 Thickness

Three thicknesses were ascribed for most laminae in our section (Figs. 2.5 and 2.6). We refer to laminae measuring <0.2 mm as *razor-striped* laminae. These laminae can be distinct, or indistinct and discontinuous. Razor-striped laminae in the upper portion of the x-radiograph contact print from sample 2-8 are well-defined (App. 2D). Laminae between 0.2-1.0 mm thick are considered *pin-striped* and are usually distinct. Sample M-BP shows striking, well-laminated pin stripes (Fig. 2.4). We term diffuse to distinct laminae with thicknesses of 1.0-1.5 mm as *chalk-striped* laminae. Sample M-6 displays both

distinct and diffuse chalk-striped laminae (App. 2B).

2.5.3   Domination

Couplet styles reflect intrannual variations in upwelling, coastal aridity and detrital input from continental sources. Couplets characterized by thick chalk-striped mud laminae and muddy turbidite layers are *mud-dominated*, and usually possess low bimodality where diatomaceous laminae are thin and/or indistinct (Figs. 2.5 and 2.6). Such a coupling is indicative of a relatively wetter climate where increased intensity of rainfall over short intervals of time delivers greater detrital runoff from the mainland (Soutar et al. 1981). *Diatom-dominated* couplets usually have high bimodality and are characterized by thick diatomaceous laminae (Fig. 2.6). *Subequal* couplets are characterized by equal proportions of generally pin-striped detrital and diatomaceous laminae.

2.5.4   Spacing

When referring to spacing, the mud laminae serves as the background (matrix) where diatomaceous laminae punctuate the matrix; thus, the distance between the diatomaceous laminae is judged, especially in mud-dominated chalk-striped sequences (Fig. 2.5). We term sequences with >10 laminae/cm as *closely spaced* where the laminae are often razor to pin-striped and moderately to well defined. Sequences encompassing 5-10 laminae/cm are *moderately spaced*, increasingly muddy and commonly pin to chalk-striped. Sequences containing <5 laminae/cm are *widely spaced* and are usually mud-rich with diffuse chalk-striped diatomaceous laminae (App. 2B).

2.5.5   Cyclicity

Cyclic deposition of laminae is dependent on short-term seasonal and long-term astronomical variables (e.g. Milankovich cycles; e.g. Pike and Kemp 1997). The laminae in our sections were observed to occur in couplets, packets, and bundles separated by non-laminated units (Fig. 2.6). *Couplets* are the basic building blocks of laminated sequences and, in the classic sense, are considered to be *varves* comprised of a winter-dominated component (detrital-rich lamina) and a summer-dominated component (diatom-rich lamina) which define the annual climatic cycle (Anderson 1986). Although we

1. BIMODALITY
a. High bimodality (HB):
   large contrast in grey scale/bulk density

b. Moderate bimodality (MB):
   moderate contrast in grey scale/bulk density

c. Low bimodality (LB):
   small contrast in grey scale/bulk density

2. THICKNESS
a. razor stripe (<0.2mm)
b. pin stripe (0.3-0.9mm)
c. chalk stripe (1-1.5mm)

3. DOMINATION:
a. mud-dominated (1.5:1 mud)

b. diatom-dominated (1.5:1 diatom)

c. subequal (1:1)

4. SPACING
a. closely-spaced: >10 laminae/cm

b. moderately-spaced: 5-10 laminae/cm

c. widely-spaced: <5 laminae/cm

5. CYCLICITY
a. couplet:
   a single pair of dark and light laminae
   (i.e. a "varve")

b. packet:
   a grouping of couplets

c. bundle:
   a grouping of packets

Figure 2.5. Classification of lamination styles.

Figure 2.6. Photographs of scraped outcrop surfaces depicting different lamination styles (cf. Fig. 2.5).

A) Razor- to pin-striped, low bimodality (white asterisk) to high bimodality (black asterisk) couplets. Coin is 2.4 cm.

B) Pin- to chalk-striped laminae comprising diatom-dominated (black asterisk) and mud-dominated (white asterisk) couplets, and macerated biosilica lamina (black arrow; see Fig. 2.13 and text for explanation). Three packets of couplets (a, b, c) are separated by thin muddy turbidites. Coin is 2.4 cm.

C) Four distinct, chalk-striped diatomaceous laminae; arrow denotes *Rouxia californica*-rich lamina. Coin is 1.8 cm.
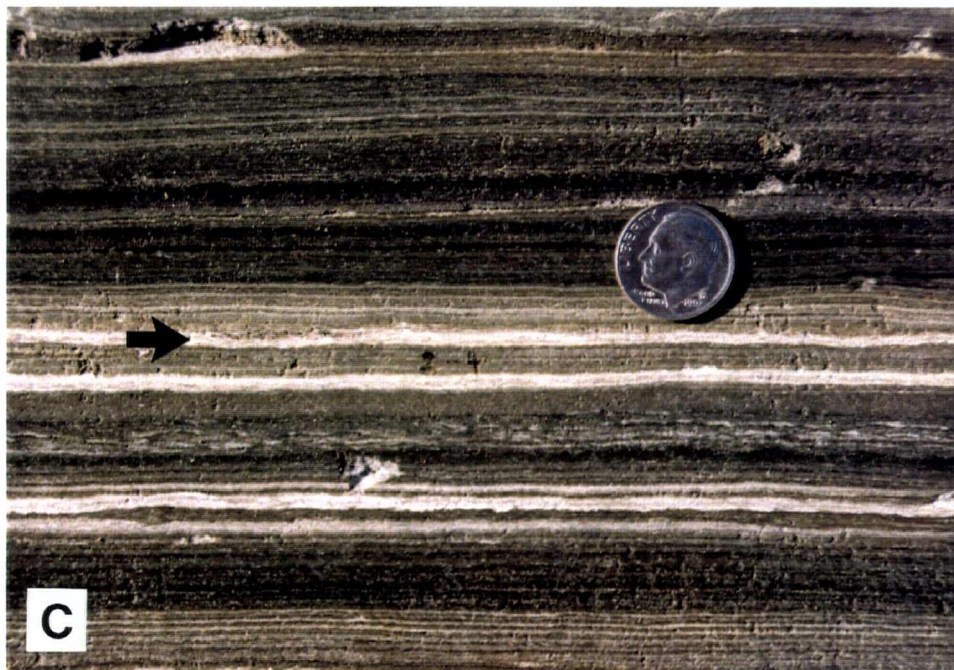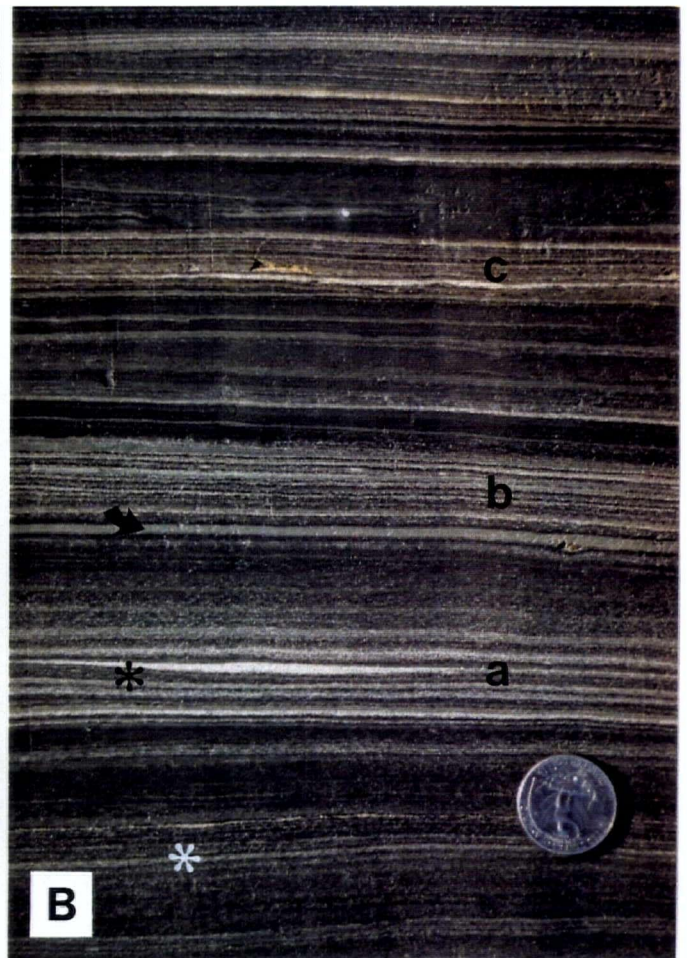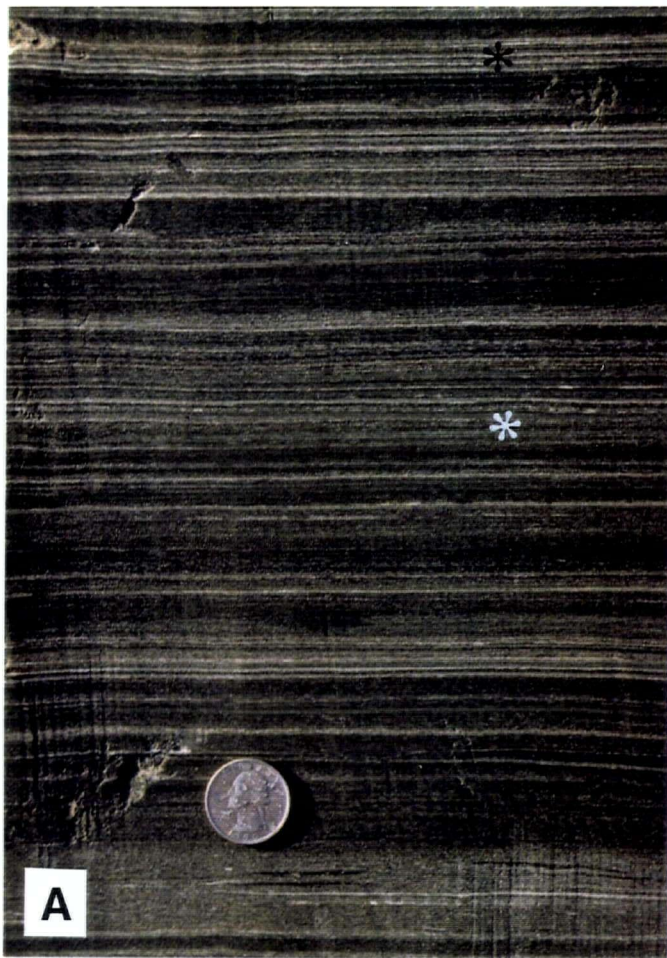
interpret that each individual couplet we observed represents a true varve, our assessments of individual laminae do not demand this. A *packet* is a centimetre-scale association of uninterrupted couplets that is synonymous with the first-order clastic-biogenic cycle defined by Pisciotto and Garrison (1981). A *bundle* (second-order clastic-biogenic cycle) consists of laminated packets alternating with mud-rich units on a centimetre to decimetre scale (Figs. 2.5 and 2.6B).

2.6   Description of Lamina Types

The following descriptions were based on a combination of hand sample observations, scanning electron microscopy and smear slide analyses from five selected samples. For the description of each lamina type, mesoscale descriptions will be discussed first, followed by microscale descriptions. Colour designations of laminae were borrowed from soil colour convention (Munsell Color Company 1971).

2.6.1   Detrital Laminae

These laminae are brown (5Y 2.5/2) to olive (2.5Y 6/2) razor, pin and chalk stripes of constant thicknesses. Detrital laminae are thicker and more abundant in mud-dominated intervals. The main constituents are detrital silt grains and clay, poorly preserved diatoms, and well-preserved robust taxa (Fig. 2.7). Using smear and strewn slide analyses (Apps. 4 and 6), the main diatom taxa identified are *Coscinodiscus* sp., benthics such as *Rhaphoneis miocenica*, *Arachnodiscus* sp. and *Navicula* sp.; the coastal neritic diatom *Actinoptychus* sp.; and resting spores of *Chaetoceros* sp., *Stephanopyxis turris* and *Leptocylindrus danicus*. Silicoflagellates are also present. These taxa are all heavily siliceous robust forms which preserve well. Lightly silicified diatoms, such as *Thalassiosira antiqua*, are also present but have been altered by dissolution and fragmentation.

2.6.2   Thin Biosiliceous Laminae

Thin biosiliceous laminae range in colour from white to olive grey (10YR 8/1 to 2.5Y 7/2) in high bimodality couplets, to increasingly darker colours towards low bimodality couplets; thickness

22

Figure 2.7. Microscopic components of detrital laminae.

A) Photomicrograph of a strewn slide from sample 2-8 (asterisk 1 in App. 2D). Note overall poor state of preservation except with robust *Rhaphoneis* pennate diatoms (R). Other components are detrital silt grains (sg), silicoflagellates (S) and *Thalassiothrix* (T). Scale=125 μm.

B) Benthic diatom *Arachnodiscus* (A) and a section of a girdle band (g). Scale=60 μm.

C and D) Backscattered electron micrographs of epoxy-impregnated samples from sample 2-8.

C) High bimodality couplet showing high contrast between detrital lamina with abundant silt grains (sg) on the left, and porous diatomaceous lamina on the right. Asterisk demarcates the boundary between the two laminae; white box indicates where high-magnification images in Figure 2.7D were collected.

D) Detailed photomosaic of area outlined in Figure 2.7C. The detrital lamina on the left of the image contains abundant angular silt grains (sg) and tubular sponge spicules (sp) which appear white due to their high density. Some diatom frustules are visible but most have been fragmented. The right side of the image is composed of diatom frustules, *Chaetoceros* resting spores (Ch) and setae which are porous and therefore appear dark.
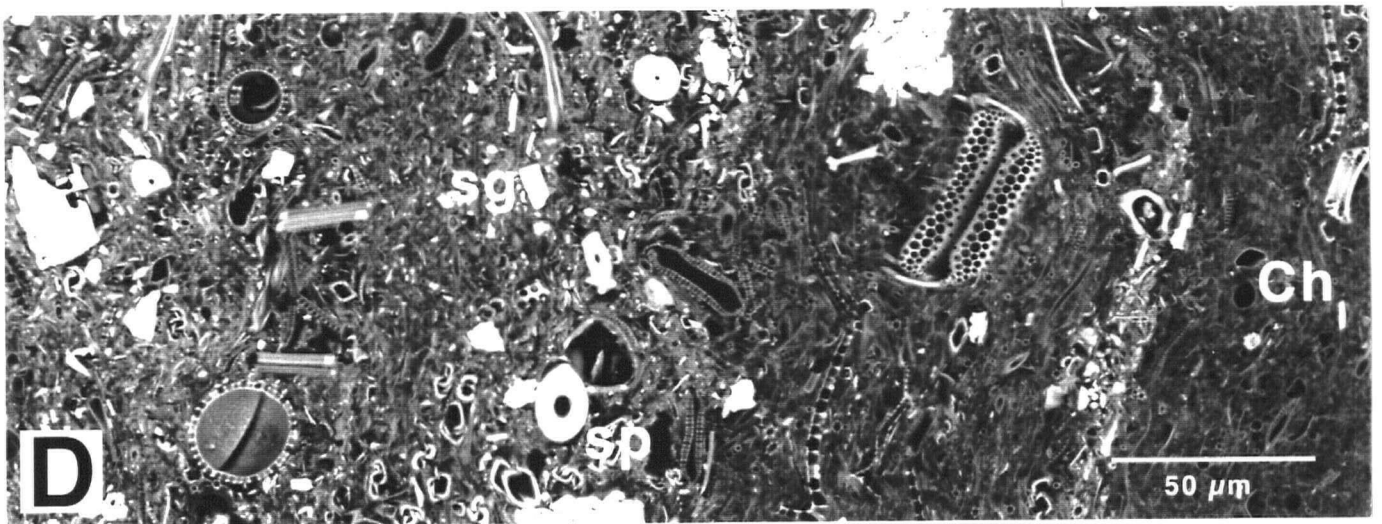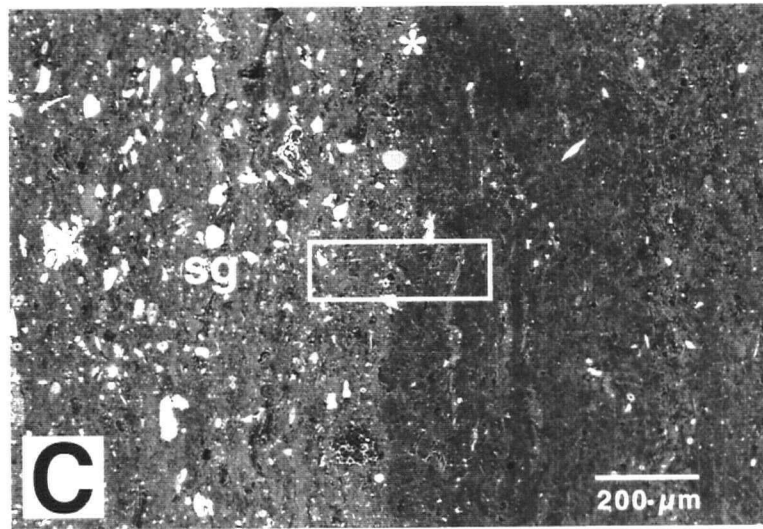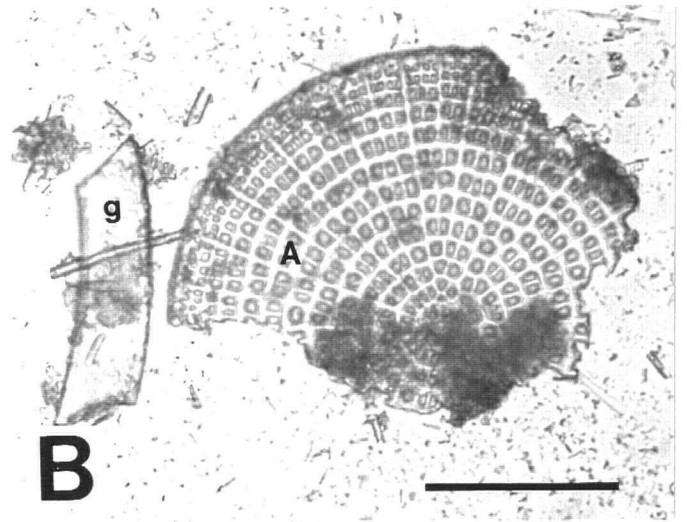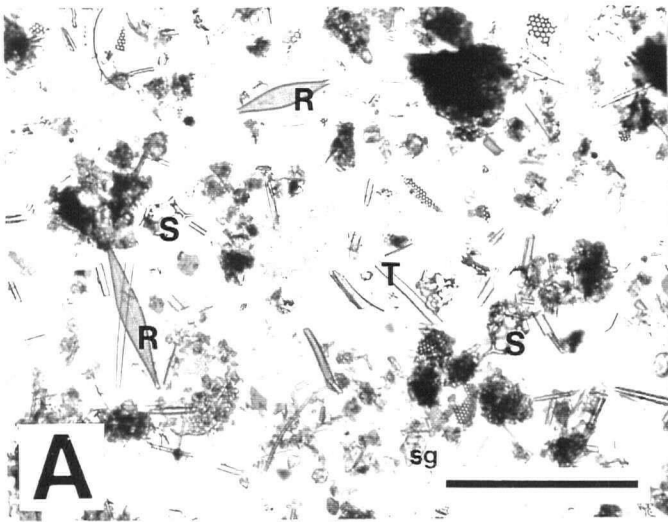
ranges from razor to pin stripes and diffuse chalk stripes (Fig. 2.6; App. 2). The taxonomic composition varies from high diversity mixed diatom assemblages to low diversity and monospecific diatom assemblages. Diatom assemblages in these laminae contain a combination of any taxa listed in Table 2 (also see App. 5). Some thin biosiliceous laminae are composed of monospecific assemblages containing diatoms such as *Coscinodiscus* (Fig. 2.8A and B). Low-diversity assemblages of the silicoflagellate *Dictyocha speculum* are also observed (Fig. 2.8C and D). *Dictyocha* assemblages are common in samples M-BP and 2-8 (App. 2D). Some pristine flocs of silicoflagellates have been observed within laminated sequences by backscattered electron microscopy. Preservation of frustules from diverse assemblage laminae is generally poor whereas monospecific diatom and silicoflagellate assemblages have moderate to good preservation.

2.6.3   *Thick Continuous Diatomaceous Laminae*

These laminae are conspicuously white coloured in the outcrop and slabbed samples (Fig. 2.6C). Thick continuous diatomaceous laminae are pin-striped to chalk-striped or thicker (up to 3 mm), distinct, and commonly occur in diatom-dominated high bimodality couplets. Scanning electron microscopy and smear slide analyses reveal that, of the taxa listed in Table 2 and Appendix 5, several genera produce thick continuous diatomaceous laminae. Monospecific and near-monospecific assemblages of *Coscinodiscus marginatus* and *Thalassiothrix longissima*, *Rouxia californica*, *Thalassiosira* sp., and *Chaetoceros* sp. resting spores are commonly observed (Fig. 2.9). *Chaetoceros* resting spores are also found in numerous flocs interspersed throughout laminated sequences (Fig. 2.9D). Thick continuous diatomaceous laminae containing *Denticulopsis hustedtii* and *Rhizosolenia* sp. are rare. In addition, a single thick coccolith lamina was observed (Fig. 3.6A). Both the *Denticulopsis* and coccolith laminae occurred adjacent to non-laminated intervals (specifically, speckled beds; Fig. 3.6); a larger sample set is required to determine if there is any genetic significance of this association.

2.6.4   *Thick Discontinuous Diatomaceous Laminae*

Thick discontinuous diatomaceous laminae are conspicuous features, being extremely white in the outcrop, and irregular or lensoid in profile. Upon closer inspection, some thick discontinuous

Table 2.2. Paleoecological analyses of diatomaceous laminae.

	Occurrence				Paleoecological Interpretation
A. Major diatom taxa*	High diversity laminae	Continuous low diversity laminae	Discontinuous low diversity laminae	Mono-specific floc	
Thalassiosira antiqua	Y	Y			cold-water diatom (1); ubiquitous bloom and non-bloom
Chaetoceros	Y	Y		Y	resting spore; self-sedimentation after bloom event
Thalassiothrix longissima	Y	Y	Y		cold-water, upwelling dominant (1); bloom/mat laminae former
Chaetoceros setae	Y	Y	Y	Y	broken off from vegetative cells and resting spores; mat forming
Nitzschia	Y				ubiquitous background primary productivity
Coscinodiscus marginatus	Y	Y		Y	cold-water diatom; ubiquitous bloom and non-bloom
Actinoptychus undulatus	Y				coastal neritic diatom (2); ubiquitous
Ethmodiscus	Y				large diatom, whole frustule never observed; background productivity
Rouxia californica	Y	Y			cold-water diatom (1); rare blooms; usually background productivity
Stephanopyxis turris	Y				resting spore
Rhaphoneis	Y				background productivity
Hemiaulus	Y				background productivity
Rhizosolenia styliformis	Y	Y			rare bloom former; only "stylus" portion observed
Denticulopsis hustedtii	Y	Y		Y	cold-water diatom (1); rare but strong bloom former
B. Minor diatom taxa					
Hemidiscus cuniformis	Y				background productivity
Asteromphalus	Y				background productivity
Actinocyclus	Y				background productivity
benthic flora	Y				background productivity
Leptocylindrus	Y				resting spore; rarely observed
C. Other microfossils					
Silicoflagellates	Y	Y		Y	occasional bloom former; usually background productivity
Radiolaria	Y				rare; background productivity
Coccoliths		Y		Y	rare bloom former; low nutrient, warm water settings (3)
D. Other morphologies					
sponge spicules	Y				common background debris
pollen	Y				rare background debris; derived from land
detrital silt grains	Y				occurs as background debris in variable amounts

*lists are presented in order of decreasing abundance, from semi-quantitative smear/strewn slide counts (Appendix 5)

References: (1) Barron and Keller 1983, (2) Pike and Kemp 1996, (3) Pisciotto and Garrison 1981

Figure 2.8. High magnification imaging of thin biosiliceous laminae.

A) Backscattered electron micrographs of two razor-striped *Coscinodiscus*-rich laminae (C_1 and C_2) within a moderate bimodality sequence from sample M-6 (black arrow 1 in App. 2B). Highly reflective angular silt grains (sg) are abundant in the mud-rich laminae and turbidites of this sample.

B) Higher magnification image of razor-striped *Coscinodiscus* laminae and silt grains seen in Figure 2.8A.

C) Secondary electron micrograph of a *Dictyocha speculum* assemblage from sample M-BP. The clean and pristine nature of the silicoflagellates indicates that they avoided grazing and rapidly sedimented.

D) Backscattered electron micrograph of a silicoflagellate (s) assemblage from sample 2-8 (asterisk 2 in App. 2D).
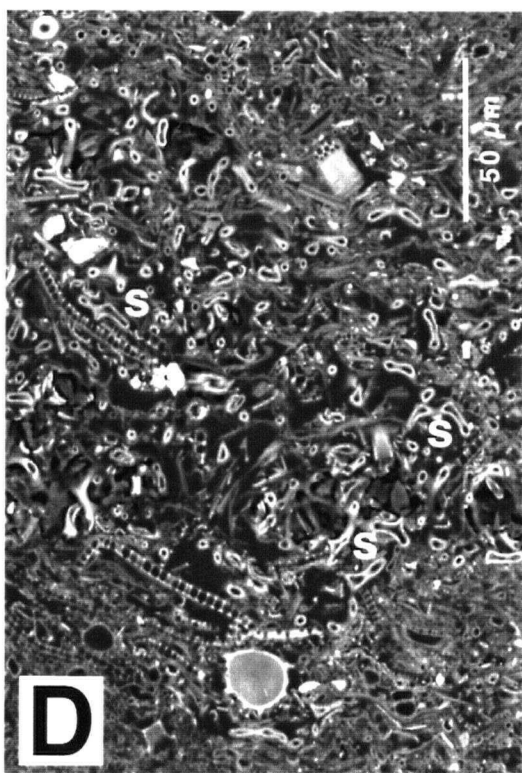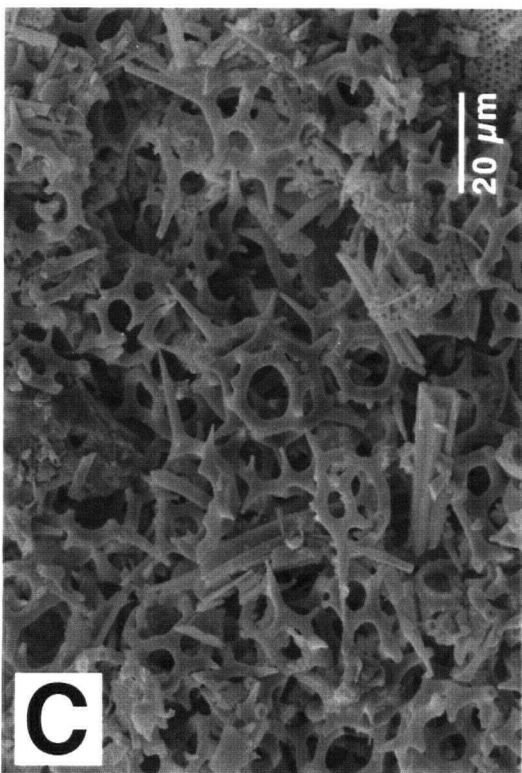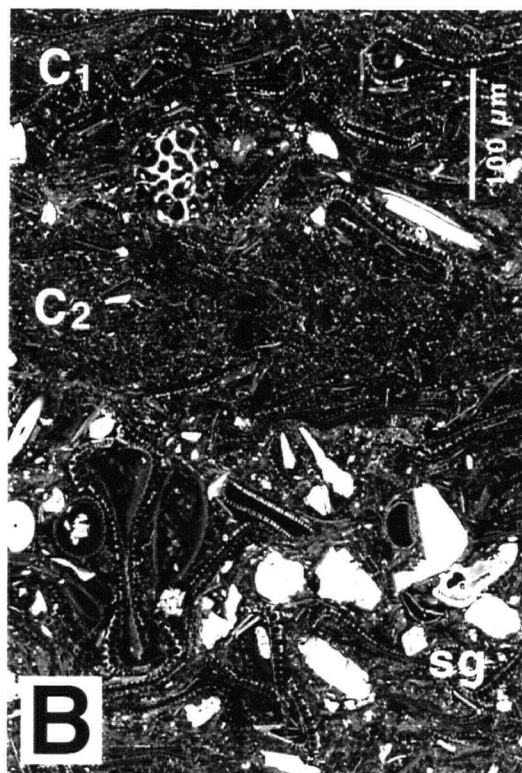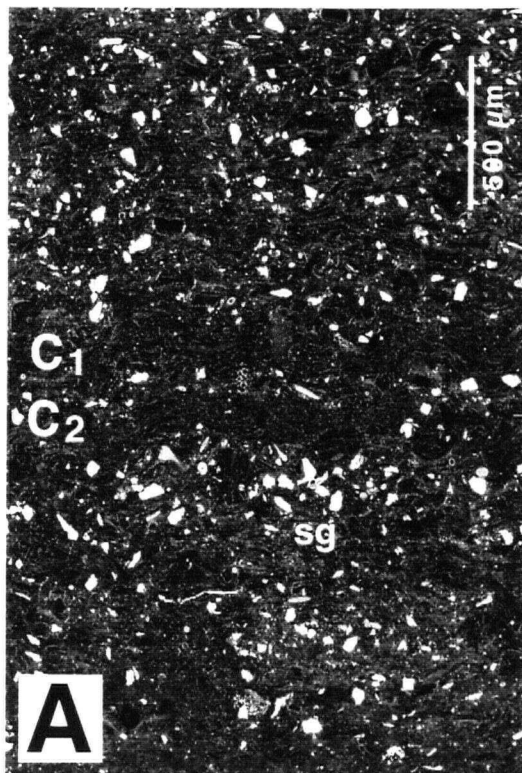
Figure 2.9. Images of thick continuous diatomaceous laminae.

A) Secondary electron micrograph of a *Coscinodiscus* lamina from sample M-6. This image was taken at the site marked by black arrow 2 in Appendix 2B.

B) Backscattered electron micrograph of a *Thalassiothrix* lamina from sample 2-8. Both cross-sectional (T) and longitudinal (T′) angles of *Thalassiothrix* frustules are visible.

C) Photomicrograph of a strewn slide rich in the pennate diatom *Rouxia californica* from sample M-29 which was extracted from an intrastratal microfractured zone. Note the clean, monospecific nature of the slide. Compare with detrital samples from Figure 2.7. Scale=60 μm.

D) Backscattered electron micrograph mosaic of a *Chaetoceros* resting spore floc from sample M-BP. Arrow denotes stratigraphic up direction.

30
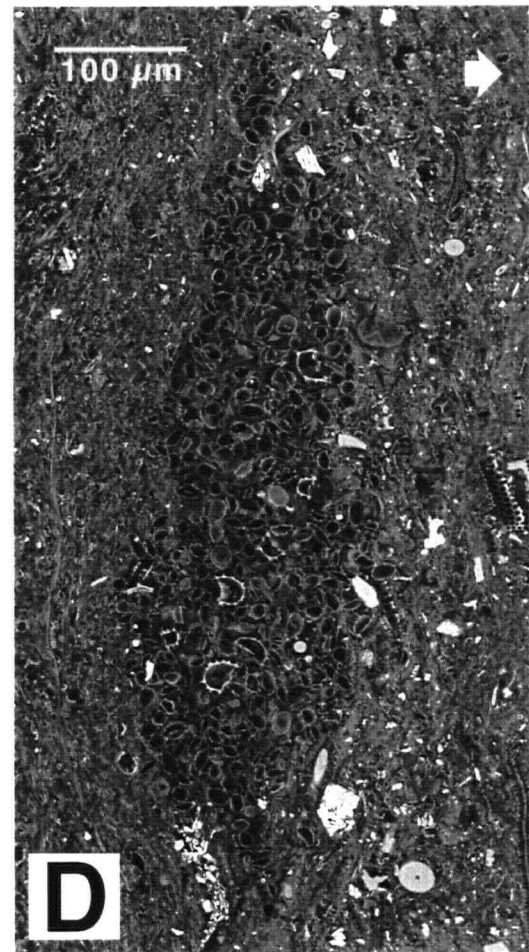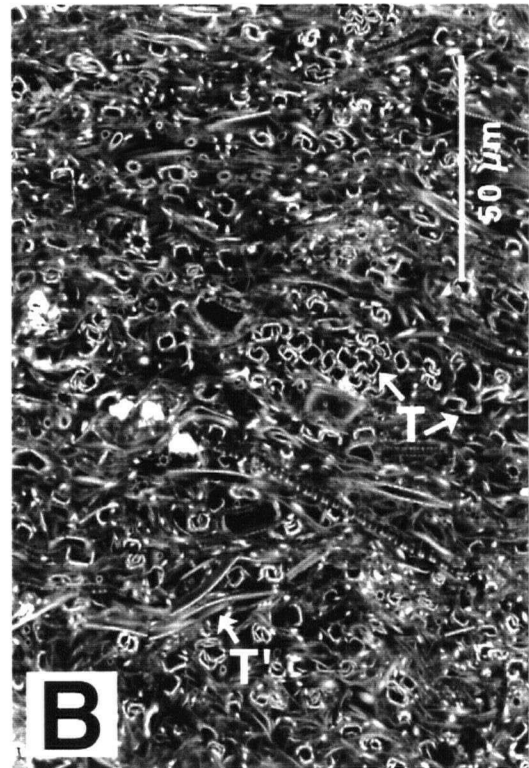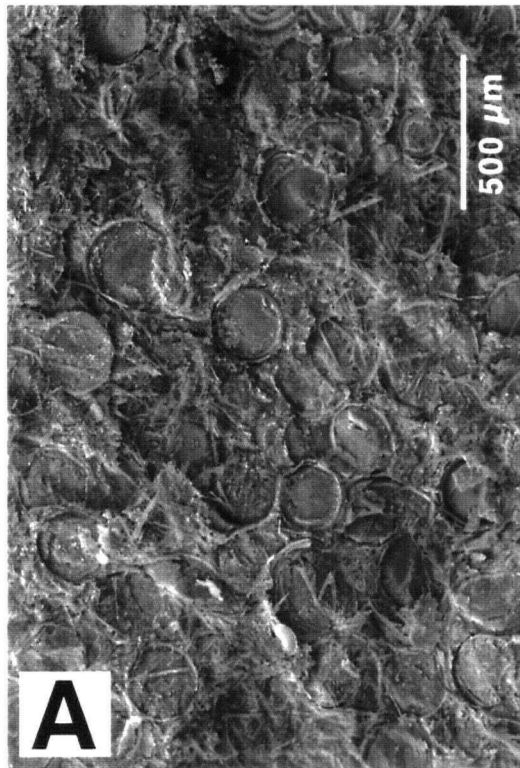
diatomaceous laminae are composed of centimetre-sized diatomaceous flocs that have been flattened by compaction, producing an overall clotted texture (Fig. 2.10). The thickest and most extensive example of this lamina type was observed in the upper section of Unit 2D in the Bench 2 section (Figs. 2.2 and 2.10A); this lens-shaped lamina is 15 cm long and 5 mm thick and surrounded by subequal to mud-dominated pin-striped laminae. All other thick discontinuous diatomaceous laminae are less extensive and are located within the diatomaceous-rich DE-1 and DE-2 zones associated with intrastratal microfractured zones (Fig. 2.10B).

Microscopic analyses of the thick discontinuous diatomaceous laminae reveal low diversity microfossil assemblages. The extensive lens from sample 2-8 (App. 2D and Fig. 2.10A) is composed completely of *Chaetoceros* resting spore and vegetative cell *setae* with minor components of *Chaetoceros cinctus*, *C. debilis*, *C. diadema*, and *C. vanheurkerii* resting spore bodies, *Thalassiothrix longissima*, and other diatoms (Fig. 2.11). Preservation of the setae and other minor microfossils is excellent. Smear slide and secondary electron microanalysis of a thick discontinuous diatomaceous lamina from one of the intrastratal microfractured zone samples (M-29) and a bloom floc from sample 2-9 reveal a very clean, monospecific assemblage of *T. longissima* (Fig. 2.12). Preservation of the frustules is excellent and no other diatom taxa are present.

2.6.5   Macerated Biosilica Laminae

These laminae occur at irregular intervals throughout our section, are commonly light olive-grey (2.5 Y 7/2) to light brown (10YR 7/1), and range in thickness from 1-7 mm. The upper and lower contacts are sharp, and there is no grading or fabric (arrow in Fig. 2.6B). The majority of these laminae appear to occur within diatomaceous-rich intervals. In the outcrop these laminae appeared to be composed of detrital silt because of the brown colour; however, observations from optical and electron microscopy reveal that these laminae are composed entirely of fragmented, hashed and compacted biosilica (Fig. 2.13A). The compact nature was evident during sample preparation for secondary electron imaging where there was difficulty in separating macerated biosilica laminae from superjacent laminae without damaging the surface to be imaged. Backscattered electron images confirm that this lamina type is not detrital in composition because of the scarcity of reflective silt grains (Fig. 2.13B; cf. Fig. 2.8A and

31
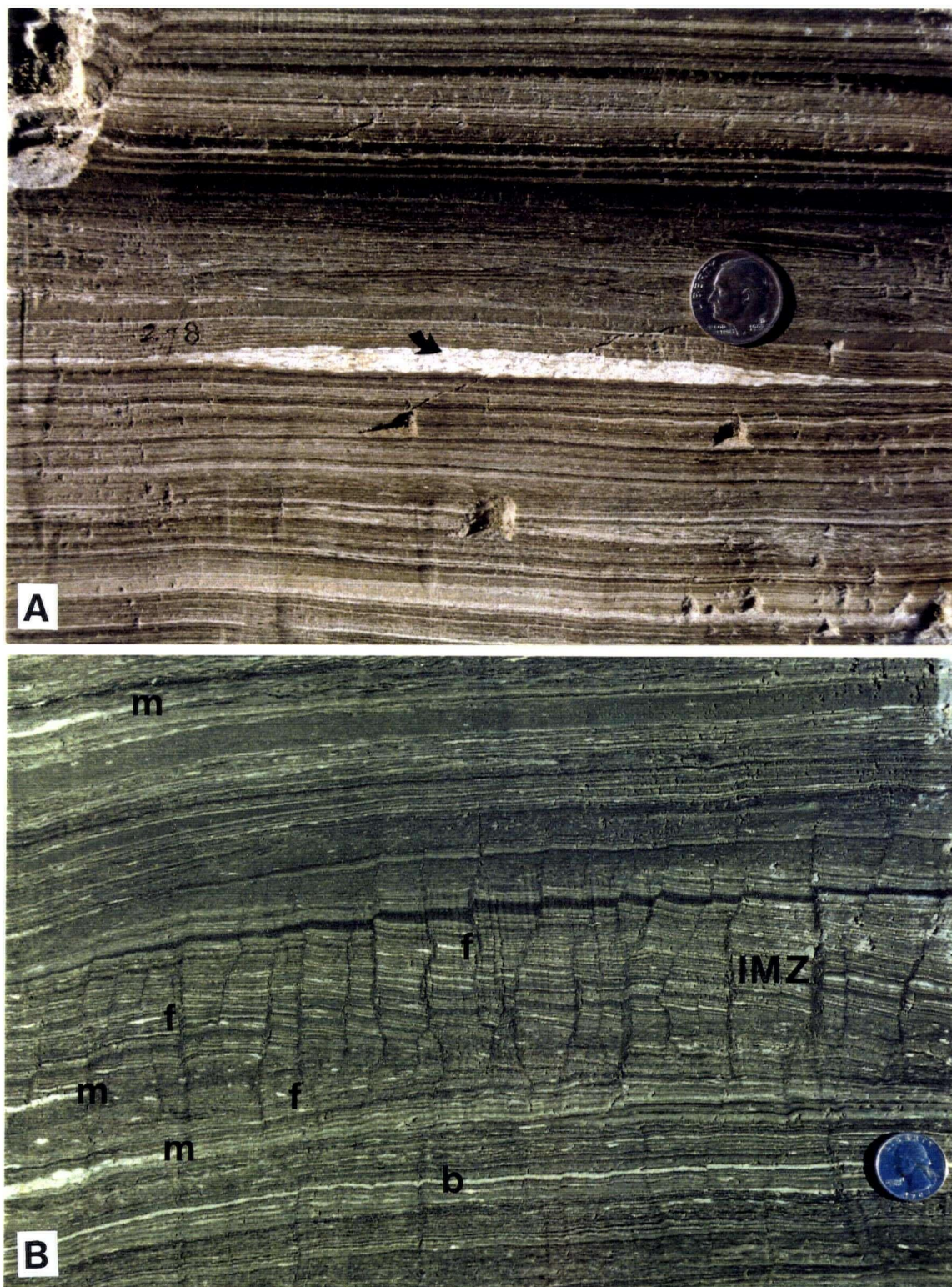
Figure 2.10. Thick discontinuous diatomaceous laminae. **A)** Outcrop photograph of a thick, lensoid *Chaetoceros* setae lamina from sample 2-8 in the Bench 2 section. The lens appears to be composed of amalgamated flocs; length of the lens is ~15 cm with a thickness of 5 mm. Coin is 1.8 cm. Arrow denotes where high-magnification images were collected (cf. Fig. 2.11). **B)** Outcrop photograph of an intrastratal microfractured zone (IMZ) with three mat laminae (m) and a bloom lamina (b). Coin is 2.4 cm. Note the numerous diatomaceous flocs (f) throughout this photograph. *T. longissima*-rich mat laminae in IMZ horizons occur in Celite DE-1 and DE-2 zones which are mined economically. See text for details.
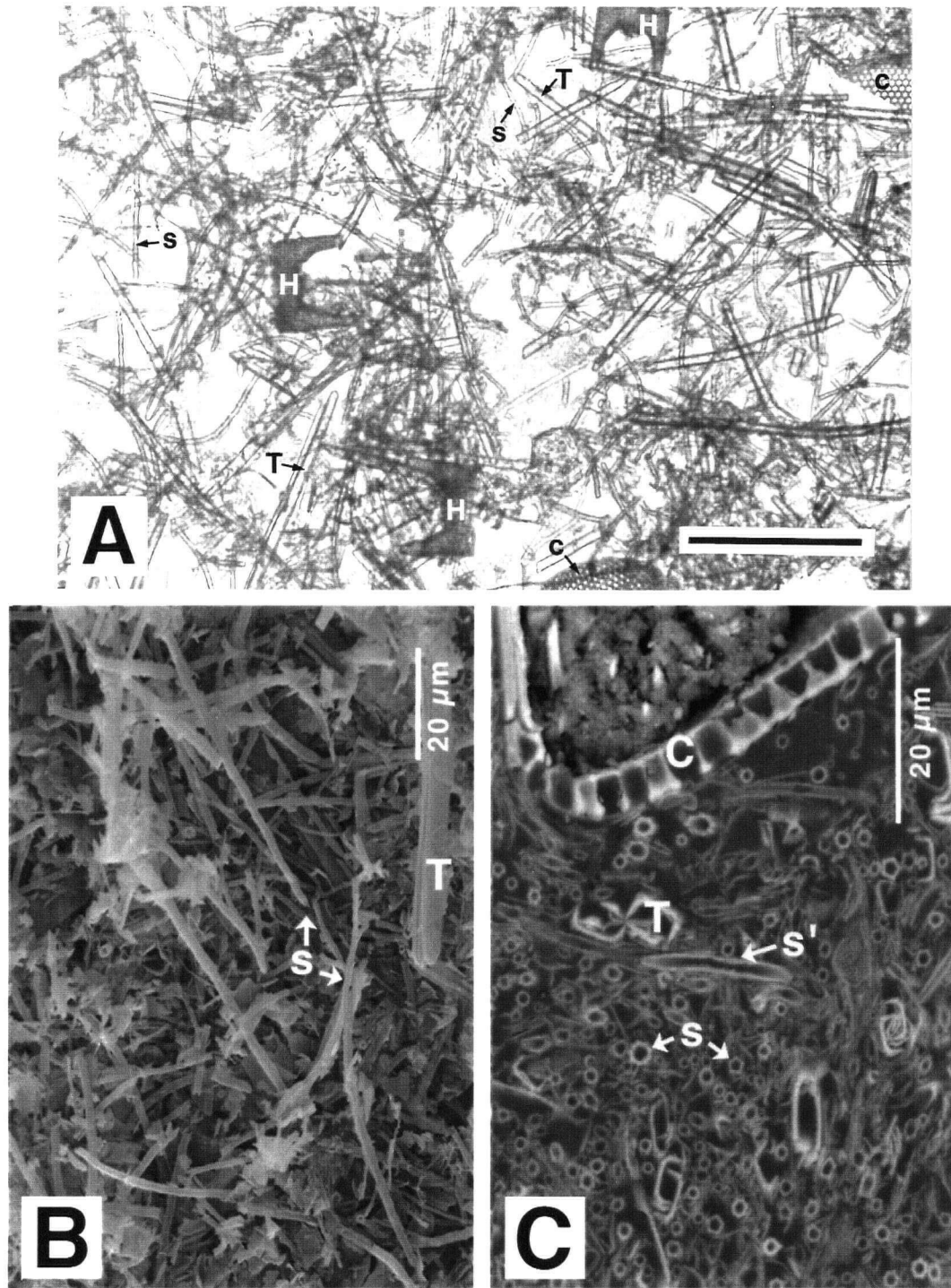
Figure 2.11. High-magnification images of *Chaetoceros* setae lamina from sample 2-8 (hollow arrows in App. 2D; black arrow in Fig. 10A). **A)** Photomicrograph of a strewn slide. Setae (s) are the knobby and curved forms whereas *Thalassiothrix* (T) are smooth, hyaline and straight. Some centric diatoms (c) and three *Hemiaulus* (H) valves are present as well. Scale=60 μm. **B)** Secondary electron micrograph of *Chaetoceros* setae (s) and a *Thalassiothrix* frustule (T). **C)** Backscattered electron micrograph of *Chaetoceros* setae—cross-sectional (s) and longitudinal (s′)—*Thalassiothrix* (T), and a large *Coscinodiscus* valve (C). The setae were derived from either vegetative cells or resting spores.

33
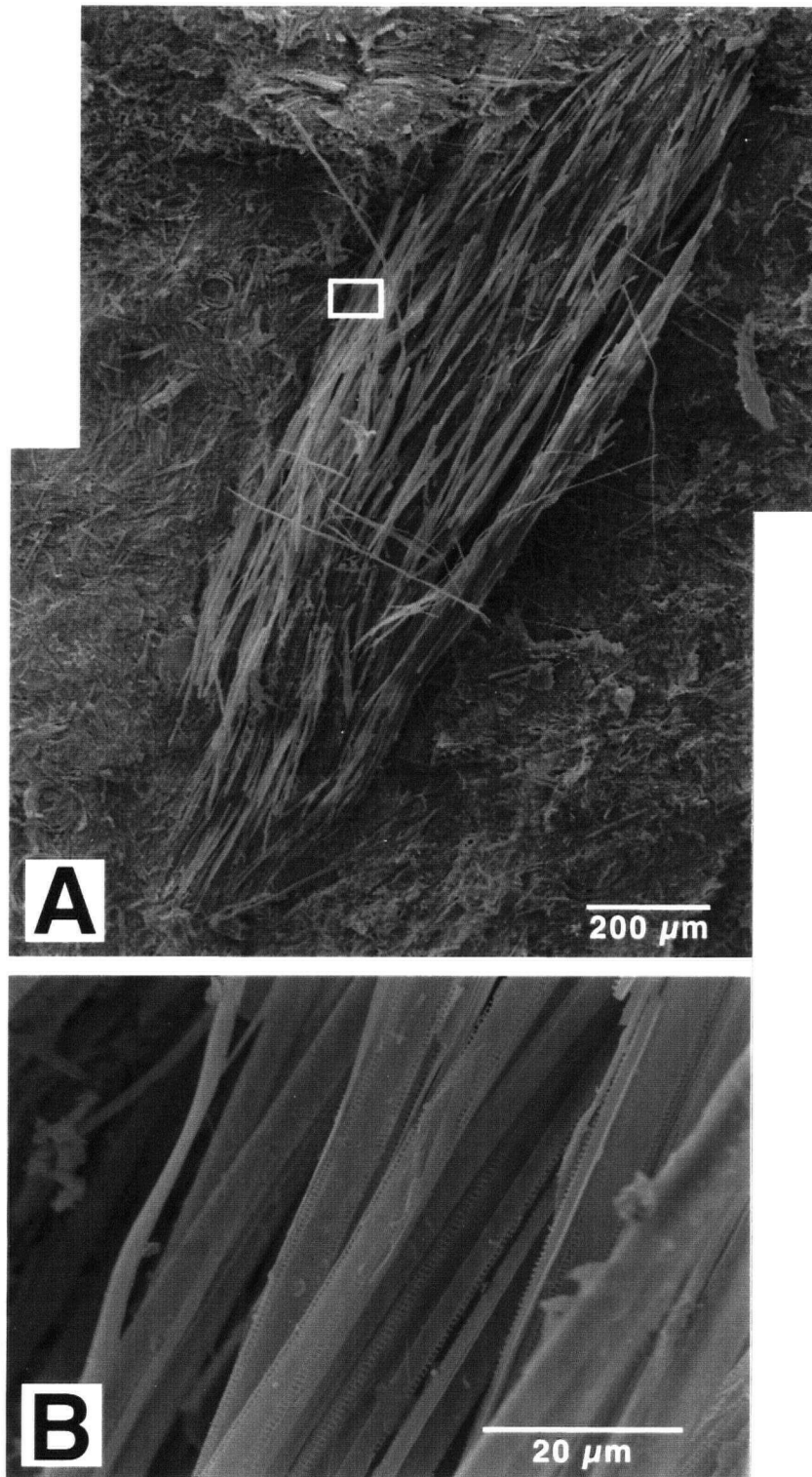
Figure 2.12. Secondary electron micrographs of a *Thalassiothrix* raft from a bloom floc in sample 2-9. **A)** Photomosaic of raft. Note the hairlike and tangled nature of the frustules. White box indicates where detailed image in Figure 2.12B was taken. **B)** Magnified image of left side of raft showing clean, unaltered condition of the frustules. Rafts such as these may be the building blocks of thick discontinuous *T. longissima* laminae such as those observed in the intrastratal microfractured zones (cf. Fig. 2.10B).
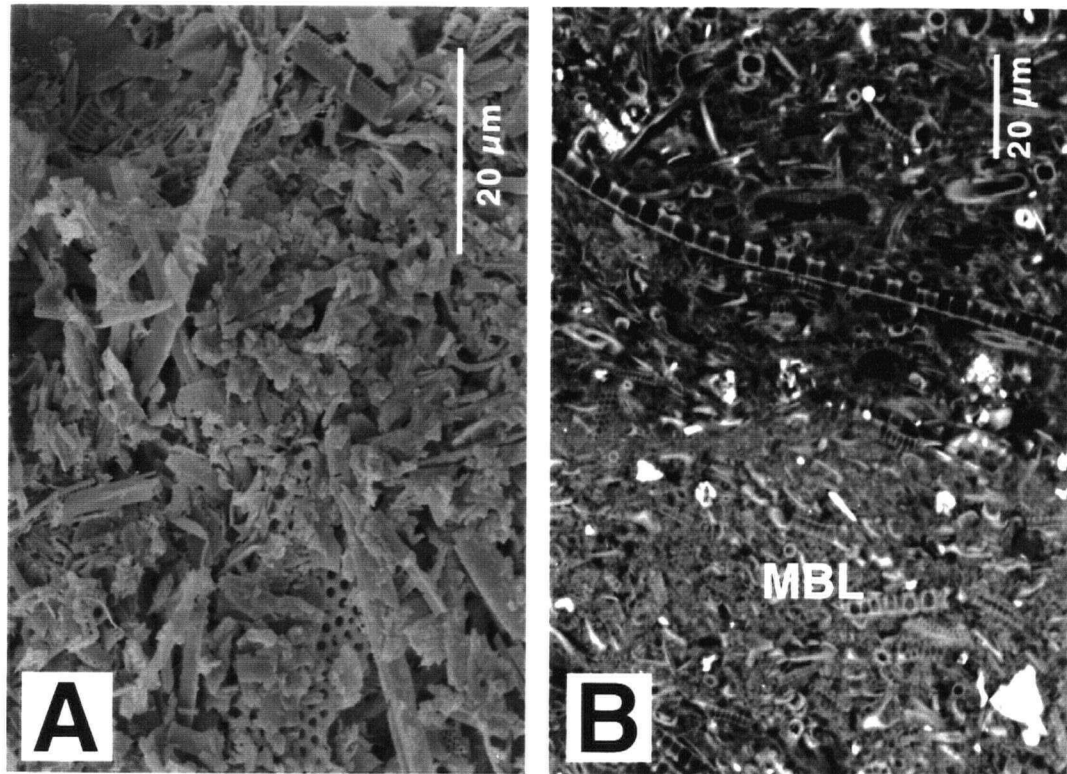
Figure 2.13. Macerated biosilica laminae (cf. Fig. 2.6B). **A)** Secondary electron micrograph of highly fragmented and hashed nature of diatom frustules. Morphotaxa are diverse. **B)** Backscattered electron micrograph of a moderate bimodality couplet. Compare compact macerated biosilica lamina (MBL) at the bottom of the image with porous diatomaceous lamina at the top. The scarcity of reflective silt grains in MBL confirms that this lamina is not detrital in origin (cf. Fig. 2.8A and B).

B). The highly fragmented state of the frustules prevents positive identification of diatom taxa; however, there appears to be a diverse assemblage of biotic components with distinctive morphologies; we will collectively term these components "morphotaxa" (Grimm 1992a).

2.7 Interpreting Laminae: Sedimentology, Ecology, Biological Processes and Paleoenvironment

Laminated diatomites from the Lompoc quarry consist of couplets from mud-dominated and diatom-dominated intervals. Stratigraphic oscillations between mud-dominated intervals and diatom-dominated intervals may be influenced by two forces: allocyclic mechanisms and autocyclic mechanisms. A combination of both mechanisms may have operated to give rise to cyclic deposition.

Laminated diatomaceous sediments are event-stratified since they preserve discrete sedimentary events in a relatively continuous series. Where subseasonal-scale events, such as diatom blooms are preserved, a high-resolution record of paleoenvironment and diatom paleoecology is available for study (Kemp 1995; Grimm et al. 1996, 1997). Relative thickness of diatomaceous laminae as a part of either low, moderate or high bimodality couplets depends on the relative amount of terrigenous influx and episodicity (i.e. intensity and duration) of continental rainfall (Soutar and Crill 1977). Low and moderate bimodality couplets represent low heterogeneities in sediment flux which are most likely attributable to weak seasonality (i.e. a year with a mild winter and damp summer). These intervals, often containing increased silt contents and diatoms that are fractured from intense grazing by zooplankton (Sancetta 1989; Grimm et al. 1996; Pike and Kemp 1996a), suggest deposition during periods of decreased wind speeds and suppressed upwelling (Sancetta et al. 1992). Samples M-6 and M-3 display mud-dominated, low to moderate bimodality couplets (App. 2A and B). Conversely, high bimodality couplets represent high sediment heterogeneity which signifies a high seasonality (i.e. a year with a wet winter and arid summer; Grimm et al. 1996). A wet winter would produce dark and silt-rich detrital laminae whereas an arid, productive summer would deliver minimal detritus to the basins and give rise to abundant diatom blooms. Distinctive dark and light couplets are seen in samples M-BP (Fig. 2.4), 2-8 (App. 2D) and 2-9 (App. 2E).

Many of the couplets we observed probably represent true, annually deposited varves which

record subannual climatic and oceanographic signatures (cf. Anderson 1986). However, we possess insufficient data to test whether couplets from the Monterey diatomites are true varves. Nevertheless, varve determination is not essential for interpreting origins of lamina types. In the following discussion, we interpret the sedimentological, ecological and environmental characteristics of individual lamina types.

2.7.1   Origins of Detrital Laminae

Detrital grains were derived from the continent and fringing shelves and delivered to the offshore basins and slopes by diverse mechanisms. In modern marginal basins, the main delivery agent is fluvial: fine terrigenous sediments from the California Borderland are transported offshore during the rainy winter season from small steep coastal drainages (Gorsline et al. 1984). Mud and silt are transported across the continental shelf and down the slope by turbid layer flows (Stow and Bowen 1978; Gorsline et al. 1984). Suspended sediments may travel further out onto the shelf via nepheloid plumes discharged by rivers (Gorsline 1984), where the sediments can be scavenged from the water column by rapidly sinking organic aggregates (Honjo 1982; Grimm et al. 1997). Eolian transport of detritus from continental deserts and the reworking of shelves during severe storms may also contribute to formation of detrital laminae (Pike and Kemp 1996a).

The thickness of detrital laminae can be correlated with the intensity and duration (i.e. episodicity) of continental rainfall; thicker detrital laminae and muddy turbidites have been generally observed to form as a result of increased episodicity of rainfall and flooding (Soutar and Crill 1977; Soutar et al 1981; Gorsline et al 1984). Muddy, low to moderate bimodality sequences within in our section, such as those exemplified in samples M-3 and M-6, may signify periods of wetter climate in which high amounts of continental rainfall and flooding washed out terrigenous debris, masking diatomaceous laminae which may have been prominent had detrital influx not increased. According to Gorsline et al. (1984), major flood years are followed by a period of slope instability and slumping resulting in the deposition of muddy turbidites as seen in sample M-6.

Diatoms in detrital laminae were heavily silicified forms such as resting spores of various species (*Chaetoceros* sp., *Leptocylindrus danicus*, *Stephanopyxis turris*), benthic taxa and coastal neritic taxa

37

like *Actinoptychus* and *Arachnodiscus* (Cleve-Euler, 1968); *Arachnodiscus* was not observed in any diatomaceous laminae. The generally higher degree of fragmentation and poor preservation of diatom frustules would most likely be due to zooplankton grazing, dissolution and/or the reworking of previously deposited sediments. Since diatom frustules washed off from the shelf may be kept in suspension by surface plumes held by gyres and eddies for days to weeks (Gorsline et al 1984; Thornton 1984), they are subject to extensive periods of alteration (Gorsline et al 1984; Sancetta 1989). In principle, finely silicified frustules and those with a great surface area (e.g. *Thalassiosira* and *Ethmodiscus* respectively) should suffer greater dissolution in waters depleted in dissolved silica than compact and heavily silicified forms (e.g. resting spores, *Rhaphoneis*; Sancetta 1989; White and Alexandrovich 1992).

2.7.2   Origins of Thin Biosiliceous Laminae

We interpret thin biosiliceous laminae with a high diversity and generally highly fragmented diatom assemblage to form during intervals of lower primary productivity, probably in the winter and early spring (Sautter and Sancetta 1992; Kemp 1995); thus, we term these laminae *background diatomaceous laminae*. The diverse diatom assemblages signify weak upwelling and low nutrient levels that were enough to support a diverse diatom community but not as abundant enough to produce a bloom. The poor degree of preservation of diatoms indicates efficient nutrient recycling and grazing by zooplankton that take advantage of the phytoplankton food source (Pike and Kemp 1996a; Grimm et al. 1997). Also, low dissolved silica content resulting from insufficient primary productivity causes diatom frustules to dissolve (Fig. 2.14 and App. 7A; White and Alexandrovich 1992). The occurrence of monospecific assemblages of *Coscinodiscus marginatus* in some laminae suggests possible differential preservation between lightly and heavily silicified diatom taxa where the robust frustules of *C. marginatus* allowed them to preserve better than weakly silicified taxa (White and Alexandrovich 1992).

2.7.3   Origins of Thick Continuous Diatomaceous Laminae

Most thick, chalk-striped laminae are composed of pristine monospecific to near-monospecific assemblages of *Coscinodiscus*, *Denticulopsis*, and other diatoms (Fig. 2.9). We attribute the formation of
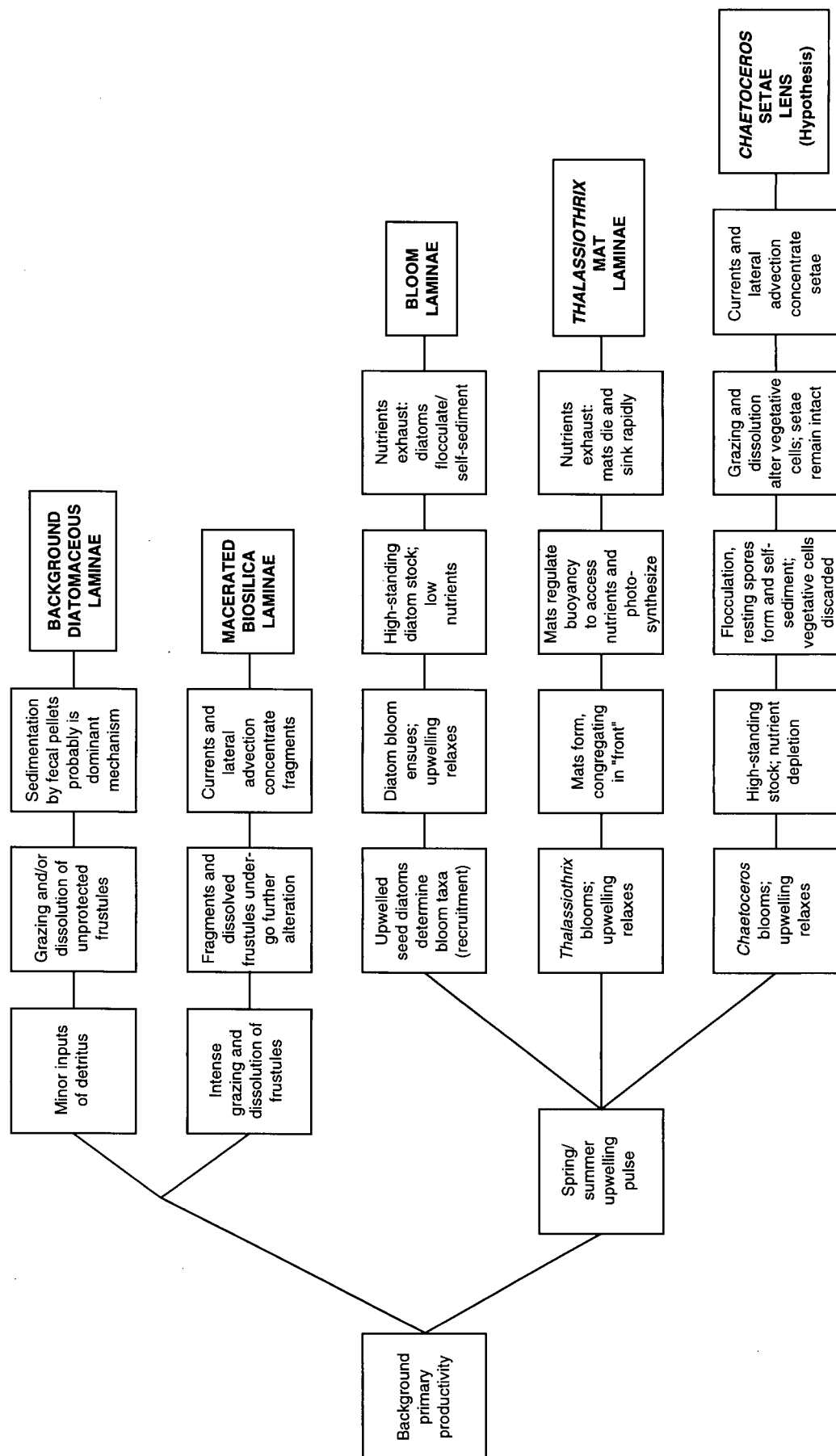
Figure 2.14. Summary of the ecology and environment of the formation of diatomaceous laminae (see App. 7).

thick continuous diatomaceous laminae to optimal blooming, efficient sedimentation, and minimal dissolution and fragmentation probably during spring and summer (Sancetta 1989; Kemp 1995; Pike and Kemp 1996a); thus, we call these laminae *bloom laminae* (App. 7C). As upwelling strength increased in conjunction with improvement of environmental conditions (increases in irradiance caused by decreases in cloud cover coinciding with surface water stratification resulting from decreased local wind stresses), the result was an adequate supply of both nutrients and light to support high rates of primary production (Sancetta and Calvert 1988; Sautter and Sancetta 1992; Sancetta et al. 1992). Improved biological productivity added increased dissolved silica, preventing lightly silicified diatoms from dissolving (cf. White and Alexandrovich 1992).

Bloom assemblages varying from lamina to lamina were likely due to the different growth processes of each diatom group and their seeding strategies in response to certain oceanographic conditions (Table 2; Fig. 2.14; Smetacek 1985; Pitcher 1990). For example, *Coscinodiscus marginatus, Denticulopsis* sp. and *T. longissima* are considered to be cold-water diatoms which bloom in response to the injection of nutrients and cold waters to the surface by strong upwelling. These diatoms flourished off coastal California during the middle Miocene cooling event for two reasons: (1) as thermal gradients and northerly wind stresses intensified, increased upwelling resulted with delivery of abundant nutrients to the surface, and (2) when cold subarctic waters progressively penetrated down to the Californian margin during the Miocene cooling steps, cold-water diatoms displaced warm-water flora (Barron and Keller 1983; White et al. 1992). *Rhizosolenia sp., Rouxia californica* and *Thalassiosira antiqua* also have an affinity for cold water (Table 2; Barron and Keller 1983).

Grimm et al. (1997) define self-sedimentation as the post-bloom phenomenon whereby diatoms produce sticky gels, flocculate and sink rapidly in large masses (cf. Alldredge and Gottschalk 1989). Reasons for why diatoms self-sediment include the evasion of intense post-bloom zooplankton grazing, and optimal recruitment of resting spores and utilization of spatially and temporally discontinuous nutrient sources during subsequent upwelling events (Grimm et al. 1997). The self-sedimentation phenomenon is likely responsible for the occurrence of distinctly thick bloom laminae of *Denticulopsis*, *Chaetoceros* resting spores and other taxa (cf. fig. 3A and B in Grimm et al. 1996). *Chaetoceros* sp. grow rapidly at the onset of spring upwelling (Barron 1983; Barron and Keller 1983; Sautter and Sancetta

1992) and then form resting spores at the end of the bloom when nutrients are exhausted, irradiance decreases and vertical mixing of the surface waters begins in the late summer (Hargraves and French 1983; Sautter and Sancetta 1992; Grimm et al. 1997). Discrete *Chaetoceros* flocs, as seen in sample M-BP (Fig. 2.9D), may have been manufactured in the water column and sedimented directly, or may have eroded from a previously deposited bloom lamina and/or macroaggregate (Chapter 3). Efficient export via self-sedimentation allows diatoms to bypass dissolution and trophic recycling by zooplankton grazing, permitting the preservation of unaltered frustules. This phenomenon is clearly recorded in the Monterey Formation laminites, and has strong implications for biogeochemical cycles. The efficient flux of diatom blooms delivers opal and labile organic carbon from the surface waters directly to the sediments (Villareal et al. 1993; Grimm et al. 1996, 1997) thereby enriching the carbon and opal content of such sediments that accumulate directly beneath highly productive waters (Archer et al. 1993; Kemp and Baldauf 1993).

2.7.4 Origins of Thick Discontinuous Diatomaceous Laminae

Two types of thick discontinuous diatomaceous laminae fall within this category: those consisting of pristine monospecific and near-monospecific assemblages of the pennate diatom *Thalassiothrix longissima*, and those composed of tangled, unaltered *Chaetoceros* setae. We will discuss each separately.

T. longissima laminae possess a crinkled appearance, and contain pristine elongate and intertwined frustules which make these laminae similar to *T. longissima*-rich laminae described by Kemp and Baldauf (1993; their fig. 3b) and Bodén and Backman (1996). Thus, we interpret thick discontinuous *T. longissima* laminae to be *mat laminae*.

What causes mat laminae of *T. longissima* to form? A combination of oceanographic conditions and frustule morphology aids in laminae formation. First, *T. longissima* are mat-forming diatoms. They have been used as an indicator of vigorous upwelling and high primary productivity (Barron and Keller 1983; Kemp et al. 1995), and have been observed to congregate in great abundances. Second, *T. longissima* frustules have the ability to interlock and mesh. *T. longissima* is characterized by its long, hairlike frustules which measure between 1.5-5.0 μm wide and up to 4 mm long (Fig. 2.12). The

meshwork produced by interlocking frustules results in a mat lamina that is able to withstand bioturbation; rapid sinking of mats from surface waters to the seafloor aids in production of thick sequences of mat laminae (Pike and Kemp 1997). The thick mat laminae described from the equatorial Pacific and North Atlantic are composed of numerous mats superimposed on one another (Kemp and Baldauf 1993; Bodén and Backman 1996). It appears that mass volumes of *T. longissima* mats flourished in response to elevated nutrient levels from enhanced upwelling events, formed discrete flocs and mats in the surface waters by a combination of interlocking and exudation of sticky gels (Kemp 1995; Grimm et al. 1996), and were rapidly delivered to the seafloor thus self-sedimenting themselves (Alldredge and Gottschalk 1989; Grimm et al. 1996; Grimm et al. 1997).

In modern oceans, *T. longissima* still forms mats (Kemp and Baldauf 1993) but rhizosolenid mats are more common (Villareal and Carpenter 1989). We can use rhizosolenid mat morphology and physiology as an analogue to the Miocene *T. longissima* mats. *Rhizosolenia* is an elongate diatom with intertwining capability and can form mats up to 30 cm in diameter in well-stratified waters (Villareal and Carpenter 1989). *Rhizosolenia* mats are able to regulate their buoyancy by migrating down to the nitrogen-enriched nutricline and then returning to the surface to photosynthesize (Villareal et al 1993; Yoder et al. 1994; Pike and Kemp 1997). The affinity for nitrogen (i.e. depletion and subsequent replenishment) by individual diatom cells within mats and the need to photosynthesize at the surface may be the cause for buoyancy regulation (Villareal and Carpenter 1989; Villareal et a. 1993). Rhizosolenid mats have been observed in great abundances following the 1992 El Niño event as normal cold-water conditions (anti-El Niño or La Niña) returned to the Equatorial Pacific (Kemp et al. 1995). As cold water subducted beneath residual warm water, a sharp front was developed in which mats congregated beneath surface waters on the warm side of the front (Yoder et al. 1994). *T. longissima* mats during the Miocene may have behaved similarly under La Niña conditions. Nutrient depletion, breakdown of the stratified water column, excessive mat size, aged cells and physiological loss of buoyancy causes rhizosolenid mats to sink out of the surface waters intact (Sancetta et al. 1991), and similar factors may have caused the sedimentation of *T. longissima* mats (Fig. 2.14 and App. 7D).

T. longissima mat laminae were most abundant in the Celite-designated DE-1 and DE-2 zones. The presence of these mat laminae, along with numerous bloom laminae and bloom flocs (Fig. 2.10B),

made DE-1 and DE-2 zones the most silica-rich in Celite quarry (Celite Corporation, unpublished data). The elevated silica content in these zones likely influenced the physical properties of the laminated diatomites in these zones; subsequent sediment disruption led to the formation of abundant intrastratal microfractured zones (cf. Grimm and Orange 1997; Chapter 3).

Thick discontinuous diatomaceous laminae containing abundances of well preserved *Chaetoceros* setae are difficult to interpret when both vegetative cell and resting spore setae were observed but vegetative cells were absent. For large volumes of setae to be generated, a bloom of *Chaetoceros* vegetative cells and the formation of resting spores must occur. *Chaetoceros* responds rapidly to elevated nutrient levels and produce resting spores *en masse* when nutrients are exhausted at the end of a bloom (Round et al. 1990). Near-monospecific setae laminae have been described by Pike and Kemp (1996) in laminated Holocene sediments from the Gulf of California. Bull and Kemp (1995) described flocs of *Chaetoceros radicans* setae measuring up to 1 mm in length in diatom ooze laminae of Late Holocene to Quaternary laminated sediments from the Santa Barbara Basin. Bull and Kemp noted that some setae were still attached to resting spores and that the origin of the setae flocs was not by fecal pellet packaging. The preservation of *Chaetoceros* setae with the absence of vegetative cells can be attributed to the fact that setae were more robust than the weakly silicified vegetative cells and therefore survived grazing and dissolution. It may also be that zooplankton grazed exclusively on the vegetative cells and discarded the setae which fell out from the surface waters, concentrated via convective currents, tangled, and rapidly sedimented to the seafloor (Fig. 2.14 and App. 7E; Alldredge and Gottschalk 1989; Bull and Kemp 1995).

2.7.5 Origins of Macerated Biosilica Laminae

Macerated biosilica laminae consisting of diverse morphotaxa occur within diatom-rich intervals. Macerated biosilica laminae constitute some moderate to high bimodality couplets, apparently taking the place of background diatomaceous or bloom laminae in these couplets. If macerated biosilica laminae are similar in microfossil content to high diversity background diatomaceous laminae, then similar interpretations regarding ecology, oceanography and climatology can be postulated, although above average intensity of zooplankton grazing (Sancetta 1989) must have occurred for every diatom

43

component to be fragmented (Fig. 2.14 and App. 7B). Zooplankton grazing alone, however, cannot account for large volumes of macerated biosilica which sometimes comprise laminae up to 7 mm thick. A possible combination of grazing, dissolution and physical reworking during vertical flux and/or lateral transport (Sancetta 1989; White and Alexandrovich 1992) could produce large amounts of concentrated macerated biosilica.

2.7.6   *Significance of Monospecific Silicoflagellate and Coccolith Assemblages*

Pristine *Dictyocha* silicoflagellate assemblages occurred as thin laminae and discrete flocs, such as those found in samples M-BP and 2-8 (Fig. 2.8C and D). Sautter and Sancetta (1992) noted that maximal silicoflagellate blooms in the modern San Pedro Basin, off the California Bight, occurred during the winter when diatom abundances were low, upwelling was sluggish and pelagic waters intruded into coastal areas. Silicoflagellate abundances decreased in the early spring when conditions were favorable for diatom proliferation (Sautter and Sancetta, 1992). Silicoflagellate-rich laminae and flocs were only recently discovered the sediment record (cf. Grimm et al. 1996; 1997). In modern oceans, silicoflagellates are a common component in the phytoplankton community but a minor participant in sediments which explains the lack of conspicuously thick, monospecific silicoflagellate laminae from ancient and modern sediments. The pristine nature of silicoflagellates suggests that they might have also undergone self-sedimentation (Grimm et al. 1996).

The occurrence of the one prominent coccolith lamina, sandwiched between detritus-rich speckled beds from a reconnaissance sample (cf. Fig. 3.6A), may also represent formation via blooming and self-sedimentation. The occurrence of this coccolith bloom lamina within otherwise siliceous-rich sediments represents a unique and short-lived environmental condition. Coccolithophores thrive in warm, low-nutrient waters when upwelling is weak to non-existent and displace diatom communities in these conditions (Pisciotto and Garrison 1981). The deposition of the coccolith lamina may have occurred during an El Niño or related condition which affected the California Current by causing a deepening of the thermocline, increases in sea surface temperature, cessation of coastal upwelling and low nutrient delivery to the photic zone (Barber and Chavez 1983; Lange et al. 1987; Lange et al. 1990). However, even if upwelling was not entirely extinguished, the intrusion of warm water into coastal regions

during El Niño events can produce nutrient-poor surface waters causing the demise of diatom stocks and the dominance of coccolithophores (Soutar et al. 1981; Barber and Chavez 1983; Baumgartner et al. 1985). Coccolithophores have been observed to produce sticky gels and bind themselves to suspended lithogenic particles thus suggesting a capacity for self-sedimentation (Honjo 1982; Grimm et al. 1997).

2.8   Conclusions

Field descriptions and sampling, description of slabbed samples, x-radiography, light microscopy, and scanning electron microscopy were completed. Lamination styles were classified in a new scheme outlined above and summarized in Figure 2.5. Individual laminae were described, and biologically mediated sedimentological processes and diatom paleoecology at subannual resolution in the Miocene were assessed. The major findings are summarized below:

(1) Diatomaceous sediments at Celite with detritus-rich and diatom-rich intervals are attributed to allocyclic and autocyclic mechanisms.

(2) Non-laminated intervals include massive silty mud beds, bioturbated silty mud beds, and speckled beds. These non-laminated intervals are all sharply based and abruptly overlain by undisturbed laminated sediments.

(3) Lamination styles were classified on the basis of bimodality, thickness, mud-diatom domination, spacing, and cyclicity (Fig. 2.5).

(4) Detrital laminae are composed of clay, detrital silt grains and clay, macerated biosilica, and a diverse assemblage of diatom groups including robust resting spores and coastal neritic taxa such as *Actinoptychus* and *Arachnodiscus*. We interpret that deposition occurred when increased rainfall or large storms delivered detritus from the continents to the seafloor during the autumn and winter .

(5) Thin biosiliceous laminae are generally ≤1 mm thick and consist of a variety of diatom taxa. We interpret that these laminae were produced by background primary production during the non-bloom winter season. Fragmentation of frustules was due to zooplankton grazing; dissolution ensued due to the low dissolved silica content. Pristine assemblages of the silicoflagellate *Dictyocha speculum*

were also observed.

(6) Thick continuous diatomaceous laminae contain monospecific to near-monospecific assemblages of diatom species such as *Coscinodiscus marginatus* and *Rouxia californica*. These laminae are attributed to blooms produced during the spring when environmental conditions (high nutrients and irradiance) optimal for diatom proliferation were present.

(7) Thick discontinuous diatomaceous laminae are subdivided into *T. longissima* mat laminae and *Chaetoceros* setae laminae. The presence of *T. longissima* mats signifies a stratified water column or vigorous upwelling and high primary productivity during possible La Niña (anti-El Niño cooling) events. These mats may be analogous to thick mat laminae discovered in oxygenated waters of the equatorial Pacific (Kemp and Baldauf 1993) and North Atlantic (Bodén and Backman 1996). Like rhizosolenid mats in modern oceans, *T. longissima* mats may have also photosynthesized at the surface in warm water fronts and migrated down to deeper waters to retrieve nitrogen. The mats rapidly sank when nutrients were exhausted. *Chaetoceros* setae laminae were composed of unfragmented setae derived from vegetative cells and resting spores; these laminae are problematic to interpret. Understanding the sedimentology of *Chaetoceros* setae laminae requires further study of modern-day *Chaetoceros* ecology.

(8) Macerated biosilica laminae are composed of completely fragmented biosilica which resulted from either extreme zooplankton grazing, dissolution and/or reworking of diatom frustules.

In conclusion, the recognition of different lamina types and the classification of couplet types and lamination styles permits the characterization of sedimentological, biological and ecological processes operating at subannual time scales. This has important implications for interpreting and refining the paleoenvironment in which hemipelagic diatomaceous sediments accumulate beneath highly productive coastal upwelling regions. Future studies complementing lamination-scale assessment of the Monterey Formation laminated sediments and analogous deposits should include lamination-scale geochemical analyses (e.g. Johnson et al. 1997) and development of a detailed time-series.

CHAPTER 3

SPECKLED BEDS IN THE MIOCENE MONTEREY FORMATION, CALIFORNIA, USA: DISTINCTIVE GRAVITY FLOW DEPOSITS IN FINELY LAMINATED DIATOMACEOUS SEDIMENTS

3.1   Abstract

Distinctive and sharply based non-laminated intervals we term "speckled beds" are abundant in finely laminated diatomites of the Monterey Formation at Lompoc, California. Speckled beds are non-uniformly distributed in a 59-m measured section, do not exceed 10 cm in thickness, and have sharp basal and upper contacts. Speckled beds are characterized by well-sorted, sand- to pebble-sized diatom-rich and detritus-rich aggregates, and laminated intraclasts, uniformly distributed in a fine-grained matrix of detrital mud and macerated biosilica. Aggregates are generally disc-shaped, range in length from <1 mm to 1 cm and are oriented parallel to bedding. We employed hand sample description, light microscopy and scanning electron microanalysis to interpret the composition and origin of speckled beds.

The unique physical properties of diatomaceous sediments provide cohesive substrates that are prerequisite for the formation of speckled beds. We interpret that speckled beds are end-products of slope destabilization and mass movement processes within the oxygen minimum zone. The presence of convolute laminae, intrastratal microfractured zones, and slumped laminae throughout the quarry attest to syndepositional deformation of laminated sediments on a subaqueous slope. The absence of grain size grading in speckled bed fabrics suggests that depositional gravity flows were highly viscous, suggesting deposition via high-density turbidity currents.

The recognition of speckled beds clarifies the origin of these distinctive yet problematic deposits and differentiates them from bioturbated intervals and other gravity-flow deposits. The fabric of speckled beds indicates provenance from an oxygen minimum zone, illustrating that cohesive substrates commonly develop in diatomaceous sediments in the absence of a hiatus. The recognition of speckled beds as recorders of slope failure events complements studies of similar deposits utilized in

paleoseismic studies of Holocene diatomaceous laminites at Saanich Inlet, British Columbia (Ocean Drilling Program Sites 1033 and 1034).

3.2   Introduction

Non-laminated beds associated with laminated diatomaceous sediments are prominent recorders of episodic and interruptive events derived from numerous geological and oceanographic processes. These processes include gravity flow deposition (Stow and Bowen 1980; Blais 1995; Blais-Stevens et al. in press), flood suspensate fallout (Behl 1995), oxygenation events and bioturbation (Savrda and Ozalas 1993; Grimm and Föllmi 1994). To fully comprehend the high-resolution records for which laminated sediments are increasingly sought, and to correctly assess their paleoenvironmental significance, a thorough understanding of the processes by which different types of non-laminated intervals are produced is necessary.

The potential of laminated diatomaceous sediments as high-resolution recorders of sedimentary processes, paleoclimate and paleoceanography has long been known and utilized (Savrda and Ozalas 1993; Kemp 1995; Grimm et al. 1996; Grimm et al. 1997). Past studies of the Monterey Formation and modern analogs focused on laminated diatomaceous sequences (e.g. Soutar et al. 1981; Chang 1995; Chang et al., in preparation) where the origin and composition of laminae and their climatic variability and significance had been assessed (Hülsemann and Emery 1961; Soutar and Crill 1977; Schrader et al. 1980; Baumgartner et al. 1985; Schimmelmann et al. 1992). More recent work regarding non-laminated intervals in diatomaceous laminites from various hemipelagic formations include studies on sandy turbidites (Behl 1995), turbidites with burrows attributed to redeposited tracemakers (Föllmi and Grimm 1990; Grimm and Föllmi 1994), grey layers (Soutar et al. 1981; Behl 1995), and bioturbated and oxygenated-event beds (Govean and Garrison 1981; Ozalas 1993; Savrda and Ozalas 1993).

Speckled beds are common in the Monterey Formation but the texture and composition of these non-laminated fabrics have not been previously documented in detail. In this paper, we describe speckled beds and discuss their origin as end-member products of slope failure, transport and

48

redeposition of laminated diatomaceous sediments from an oxygen minimum zone; this perspective provides insight into the physical properties of these organic-rich sediments (Grimm and Orange 1997). Speckled beds preserve evidence of highly cohesive diatomaceous substrates that has important implications for interpreting probable firmground horizons within the Monterey Formation and other hemipelagites. Speckled beds are unusual and puzzling fabrics that reflect unique sedimentary processes with significant values for reconstructing the paleogeography and paleoenvironment of other hemipelagic sequences deposited within or downslope from an oxygen minimum zone, thus contributing to the recognition of upwelling-influenced sediments in other areas.

3.3   Materials and Methods

Field studies at the Celite diatomite quarry in Lompoc, Santa Barbara County, southern California (Fig. 3.1) focused on excavation, description, photography and sampling. A thick section of laminated diatomite measuring 218 m is exposed at Celite quarry, ranging in age from 8.2 Ma at the base of the exposure to 7.3 Ma at the top of the economically mineable deposits (Late Miocene; J. A. Barron, written communication, 1997). Studies centred on diatomites in a location which was topographically the lowest in the quarry as these deposits were the darkest in colour and presumably the least weathered; the beds dipped 45° to the north and constituted part of the southern limb of an east-west trending syncline.

Two stratigraphically continuous sections totalling ~59 m in length were cleared by bulldozers and scraped clean with sharpened hoes. Each section was measured, described in detail and photographed. Descriptions focused on bimodality (cf. Grimm et al. 1996), thickness, mud-diatom domination, spacing, and cyclicity (Chapter 2). Bioturbated beds, muddy turbidites, speckled beds and deformational features (cf. Grimm and Orange 1997) were also examined.

Sample blocks ranging in size from 10-15 cm by 20-50 cm were cut with a gas-powered masonry saw (30-cm blade) and manually excavated. The samples were wrapped for transport in foil, heavy-duty plastic wrap and bubble wrap. A total of 23 blocks were collected. Three samples from a correlative
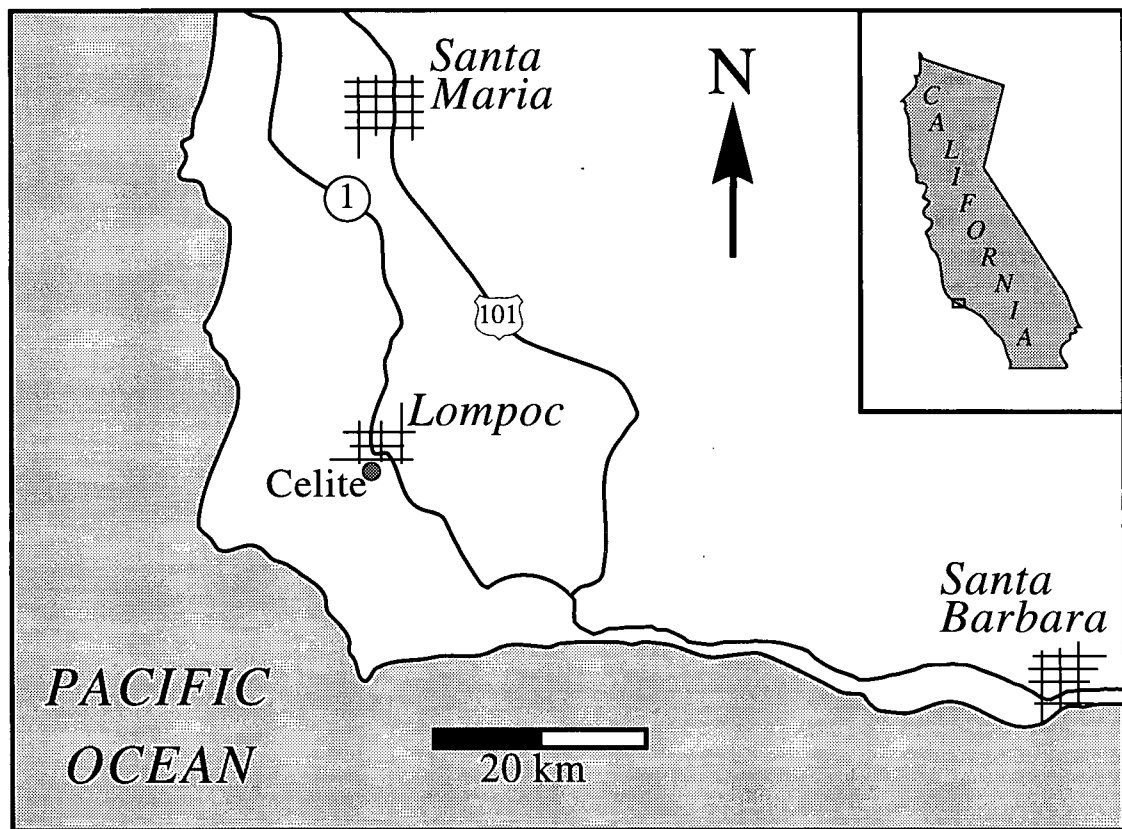
Figure 3.1.   Map of study location (modified from Grimm and Orange 1997).

interval on the northern limb of the syncline were also collected to assess lamination-scale correlation; this section was topographically higher and thus more weathered than our main traverse. In addition, reconnaissance samples collected throughout the quarry (Chang 1995) were reexamined for this study.

In the laboratory, sample blocks were cut perpendicular to bedding into cm-thick slabs with a bandsaw; several slabs were produced from each block for various laboratory analyses (Fig. 3.2).

3.3.1   Hand Sample Description

Lamination-scale descriptions on hand samples centred on bimodality, thickness, mud-diatom domination, spacing, cyclicity, slump features, turbidites, bioturbation and speckled beds. Contacts between laminated and non-laminated intervals were also observed. Slabs selected for photography were sanded and sprayed with WD-40 to enhance fine-scale features (cf. Savrda et al. 1985).

3.3.2   X-radiography

X-radiography was used to acquire detailed, high-resolution images of the samples. X-radiography was performed at Vancouver Hospital, UBC Campus site, with a CGR 300-T mammography x-ray machine running at 26 keV for all samples; clay-rich samples were exposed at 50 mAs and diatom-rich samples at 32 mAs. X-radiography by mammography produces sharper, higher resolution images than conventional x-ray techniques because the collimated beam of the mammogram reduces parallax and obliquity between discrete laminae (Algeo et al 1994; Collins 1996; Grimm et al 1996; cf. Chang 1995). Saturation of x-ray film is inversely proportional to the bulk density of the samples: diatomaceous sediments are porous and have a high x-ray transmissivity; thus they appear light-coloured in the x-ray contact prints whereas dense detrital sediments appear dark. Contact photographic prints were developed from the x-ray negatives and, from the prints, five samples were selected for further laboratory analysis based on the superior image quality of their x-radiographs and diverse sedimentary features (Fig. 2.2; App. 2).

3.3.3   Light Microscopy

Thin sections were produced for mesoscale examinations of cross-sectional speckled bed fabrics.

Field sampling

Bandsaw slabbing

Archive, description
& photography

Geochemistry
(cf. Johnson et al. 1997)

X-ray by mammography

Subsampling

Subsampling

Impregnate with epoxy

Smear/strewn slides   SEM

Thin sections   BSEM
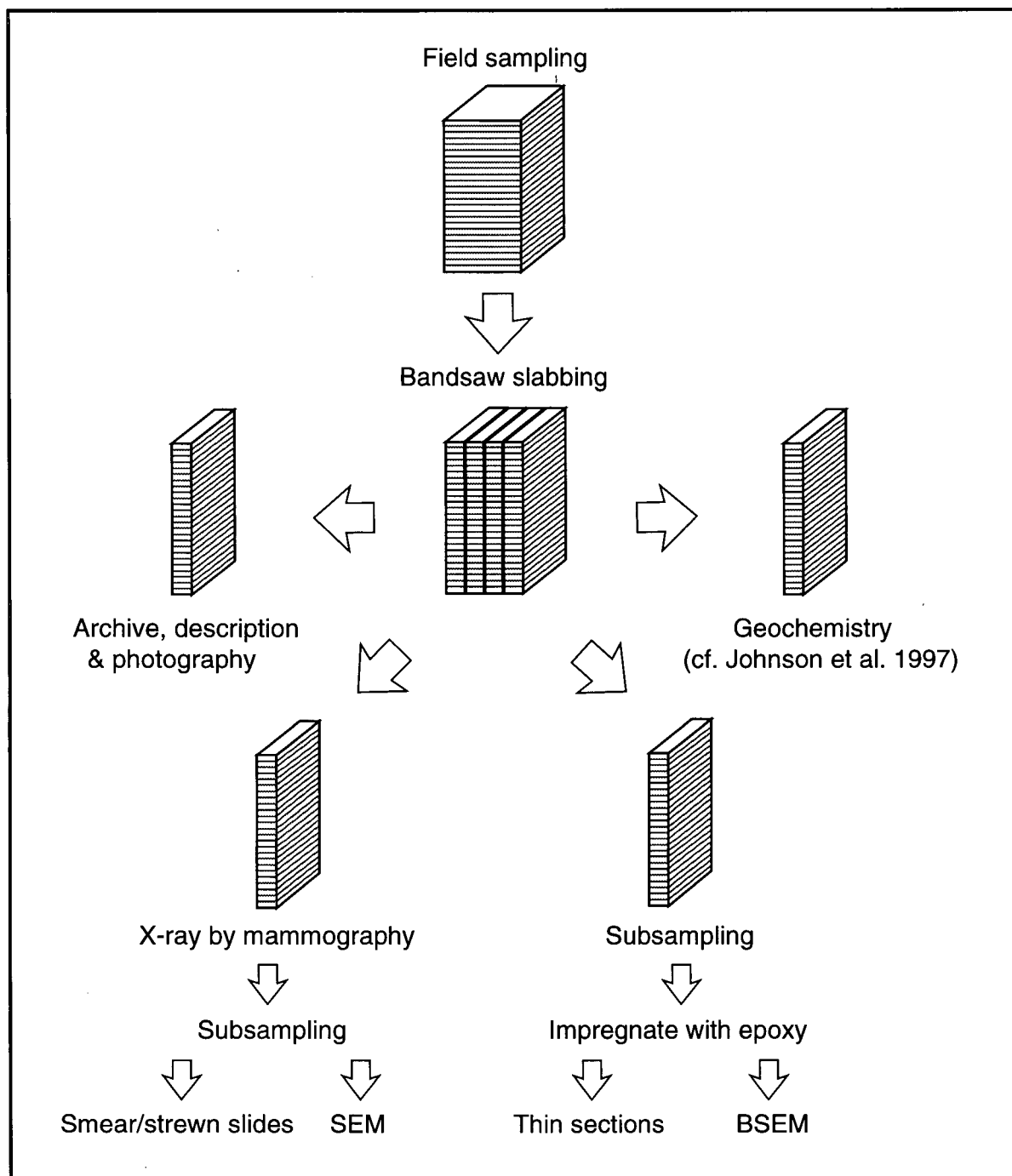
Figure 3.2.   Flowchart of sampling procedures.

Conventional smear and strewn slides were utilized for taxonomic identification of microfossils. Details of smear and strewn slide preparation were discussed in Chapter 2.

3.3.4   *Scanning Electron Microscopy*

High-magnification imaging and identification of submillimetre features was achieved with the use of scanning electron microscopy in the secondary and backscattered electron modes. Secondary electron microscopy permits the imaging of sample topography and the examination of various microfossil taxa and the state of their preservation. Samples were prepared by sectioning cm-sized cubes parallel to bedding and coating the surface to be imaged with Au-Pd. Backscattered electron microanalysis of epoxy-impregnated samples produces cross-sectional images of sediments and allows for the optimal high-magnification examination of submillimetre fabrics which document changes in sedimentary processes (Kemp 1995; Pearce et al. 1995; Grimm et al 1996). Samples were sawed perpendicular to bedding into cm-sized cubes and rods, vacuum-impregnated with a low-viscosity epoxy (Struers brand Epofix) at 172 kPa, and left to set overnight. The surface to be imaged was then highly polished with fine Al_2O_3 abrasive on a cloth rotary lap and carbon-coated. Both secondary and backscattered electron imaging were performed on a Philips XL-30 scanning electron microscope.

3.4   General Sedimentology

3.4.1   *Monterey Formation*

The Monterey Formation is an organic-rich hemipelagic deposit which accumulated in anaerobic conditions in either a series of fault-bounded basins similar to the modern California Borderland basins (Blake 1981; Hagadorn et al 1995), or on low-gradient slopes along an open continental margin (Isaacs et al. 1996). The Monterey Formation has been classically regarded as a tripartite sequence consisting of a lower calcareous facies dominated by coccolithophores, a middle transitional phosphatic facies, and an upper siliceous facies dominated by diatoms (Pisciotto and Garrison 1981). Recent work by Isaacs et al. (1996), however, show that deposition of the Monterey Formation was governed by a dynamic

prograding margin with deposition of facies controlled by local water depths and bottom topography. Owing to the localized differences in depositional environments, the tripartite sequence is not present in all areas (White et al. 1992).

Biosiliceous sedimentation commenced when upwelling strength was enhanced after the onset of Miocene global cooling at ~16 Ma (Pisciotto and Garrison 1981; Ingle 1981; White et al. 1992). Intense coastal upwelling delivers an abundance of nutrients to the surface waters where diatoms proliferate, and produces a well-defined oxygen minimum zone as decaying organic matter settles through the water column. The modern depth of the oxygen minimum zone off the coast of California is 250-1000 m but these depths and the intensity of the oxygen minimum zone have fluctuated through time (Ingle 1981; Gardner and Hemphill-Haley 1986).

Sediments occurring in anaerobic environments are generally well-laminated because the low oxygen content of the water (<0.1 mL/L) excludes bioturbating macrobenthos that would rework sedimentary laminae (Savrda et al. 1984; Savrda and Bottjer 1987). In the siliceous member of the Monterey Formation, the diversity of trace fossils is low with *Chondrites*, *Planolites* and *Thalassinoides* being the main ichnogenera (Govean and Garrison 1981; Savrda and Bottjer 1987; Savrda and Ozalas 1993).

Slope instability in Monterey diatomites is evidenced by convolute laminae, slump folding, intrastratal microfractured zones (hybrid fault/vein structures; Grimm and Orange 1997), and slumped laminae. Experiments by Schwarz (1982) and Prior and Coleman (1984) showed that the slope angle need not be large to cause slope failure and fluid flow; a shallow slope angle of 0.5-3° was sufficient for gravitational forces to destabilize slope sediments.

In sum, we concur with White et al. (1992), Isaacs et al. (1996) and other investigators that the upper siliceous member of the Monterey Formation was deposited in anaerobic conditions on gentle slopes under a region of intense coastal upwelling.

3.4.2   *Properties of Laminated Diatomaceous Sediments*

The unique physical properties of diatomaceous sediments are an important precursor for the formation of speckled beds. In general, hemipelagic laminated diatomaceous sediments consist of two

main phases—diatom-dominated laminae and detrital-dominated laminae—which deposit within the oxygen minimum zone beneath highly productive coastal upwelling zones. Diatom-rich laminae result from the mass flocculation and sedimentation of diatom frustules after a spring and summer bloom events (Soutar et al. 1981; Alldredge and Gottschalk 1989; Grimm et al. 1996). Biological processes, including the exudation of sticky gels, facilitate diatom aggregation resulting in rapidly exported large masses of unfragmented biosilica from the surface waters to the sediments (Alldredge and Gottschalk 1989; Grimm et al. 1997). Detritus-rich laminae are produced from fluvial runoff during higher rates of continental rainfall during fall and winter (Soutar and Crill 1977). The main constituents are terrigenous clays and silts and robust diatom species (Chapter 2).

The preservation of organic matter within hemipelagites accumulating under highly productive coastal upwelling zones dramatically alters the strength of the sediments. When compared to sediments of lower organic matter content, organic-rich (>5% organic carbon) hemipelagites possess extremely low wet bulk densities, high water contents, high liquid and plastic limits, high natural shear strengths, and high sensitivity (Keller 1983). Each of these parameters is discussed briefly below.

Wet bulk density is the wet weight per unit volume of a sediment and is inversely proportional to organic matter content (Keller 1983). It has been shown in Peruvian margin sediments that as total organic content increases, wet bulk density progressively decreases (Busch and Keller 1981; Keller 1983; Hill and Marsters 1990). Conversely, water content has been observed to be proportional to organic matter content; organic-rich hemipelagites possess a high water content due to the adsorptive ability of porous diatom tests, clays and other microscopic components (Reimers 1982; Lee et al. 1990).

Liquid and plastic limits are measures of the ability of a sediment particle to adsorb water and mark the lower boundaries of water contents whereby a sediment behaves as a liquid or a plastic, respectively (Keller 1983). Busch and Keller (1981) determined that increased water content and organic matter elevated both the liquid and plastic limits of Peruvian hemipelagites, allowing them to remain as a coherent mass, when undisturbed, where organic-poor sediments with the same water content would fluidize. This ability of organic-rich sediments to exist as a coherent and cohesive mass, i.e. possessing high natural undisturbed shear strengths, is derived from a combination of sticky gels exuded by diatoms (Alldredge and Gottschalk 1989), bacterial mucilaginous sheaths (Reimers 1982),

55

gels formed within pore waters during burial diagenesis (Lee et al. 1990; Hill and Marsters 1990) and interlocking diatom frustules (Lee et al. 1990) which act to bind sedimentary particles together. These factors permit the development of cohesive "firmgrounds" without the necessity for a depositional hiatus (cf. Ozalas et al. 1994).

The difference between the undisturbed and disturbed shear strengths of organic-rich hemipelagites has been determined by Keller (1983) to be large. Sediment sensitivity, the ratio of natural undisturbed shear strength to disturbed or remolded shear strength, is used to quantify the susceptibility of sediments to failure. Busch and Keller (1981) and Keller (1983) showed that the shear strength of cohesive and coherent laminated sediments in undisturbed conditions was greatly reduced when the sediment was disturbed; thus organic-rich sediments possess high sensitivity ratios. Rapid sediment loading, cyclic loading by internal waves and seismic activity may trigger sediment failure (Keller 1983).

3.4.3   Laminated Intervals at Celite

Laminated intervals are characterized by mm-scale alternations of dark detritus-rich laminae with light-colored diatomaceous laminae (Chang 1995). We classified laminae and couplets on the basis of bimodality, thickness, spacing, mud- versus diatom-domination, and cyclicity (Figs. 2.5 and 3.3). Bimodality is based on the bulk density contrast of juxtaposed laminae of differing compositions and textures as determined by examining x-radiograph grey scale (Grimm et al. 1996). High bimodality couplets show a high contrast between diatomaceous and detrital-rich laminae whereas low bimodality couplets display a low bulk density difference. Mud-dominated intervals usually contain low bimodality couplets; and diatom-rich, high bimodality intervals are generally bloom-dominated (Grimm et al. 1996).

In Chapter 2, we classified five main lamina types based on composition, texture and structure. Dark detrital laminae are composed mainly of detrital silt grains and robust diatom species (A. Chang, unpublished data, 1994). Thin biosiliceous laminae (<0.2-1.0 mm) contain high-diversity diatom assemblages; silicoflagellate-rich laminae are sometimes observed. Thick continuous diatomaceous laminae attributed to blooms are dominated by monospecific assemblages of *Coscinodiscus, Rouxia,*

Figure 3.3. Outcrop photographs representing different lamination styles.

A) Razor-striped low bimodality (white asterisk) to high bimodality (black asterisk) couplets (cf. Grimm et al. 1996; Chapter 2). Coin is 2.4 cm.

B) Pin- to chalk-striped laminae displaying diatom-dominated couplets (black asterisk) and mud-dominated couplets (white asterisk). Coin is 2.4 cm.

C) Four distinct bloom laminae. Coin is 1.8 cm.
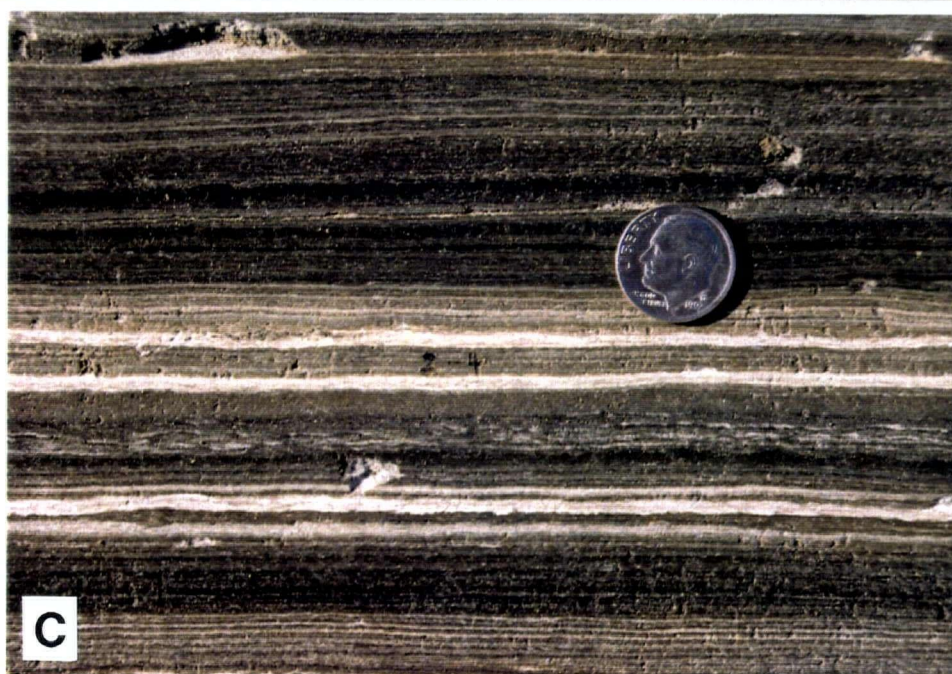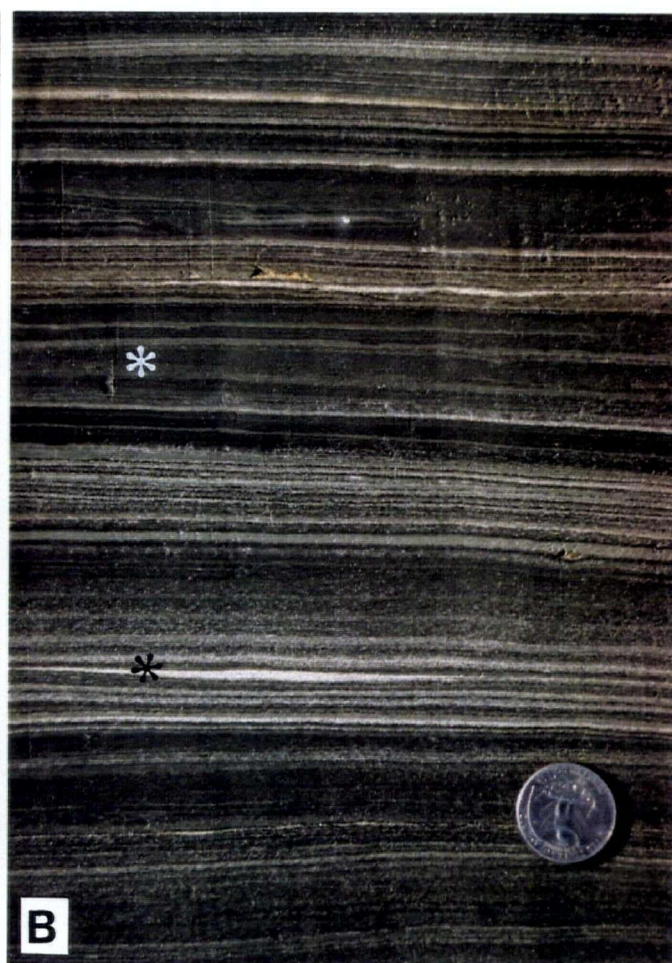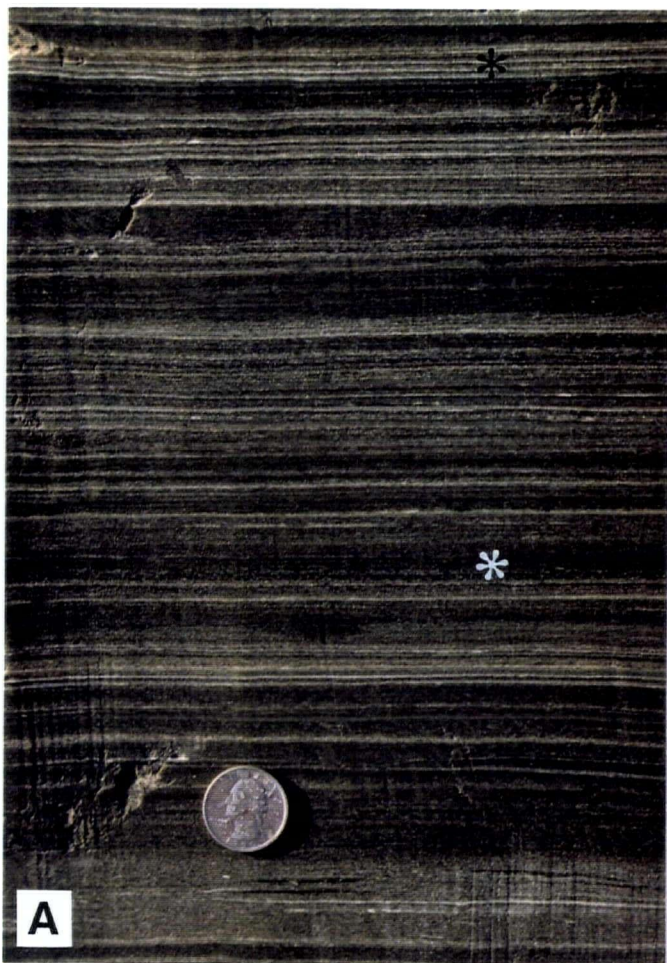
Chaetoceras, *Thalassiothrix* and *Denticulopsis* (Chang 1995; Chapter 2). Thick discontinuous diatomaceous laminae (2-5 mm) consist of monospecific or near-monospecific assemblages of *Thalassiothrix* and *Chaetoceros* setae. Macerated biosilica laminae range in thickness from 1-7 mm and consist entirely of macerated frustules from a variety of taxa.

3.4.4   Non-laminated Intervals

Three types of non-laminated intervals were observed intercalated with laminated diatomaceous sequences: massive beds, bioturbated beds and speckled beds. All of these intervals have sharp bases and sharp tops and are abruptly overlain by undisturbed, thinly laminated diatomite.

Massive beds are tan-colored, decimeter-thick bands which are generally siltier than the surrounding laminated sediments; these beds are laterally continuous with no discernible changes in thickness (Fig. 3.4A; cf. fig. 2A in Grimm and Orange 1997). Most massive beds have a homogeneous texture but some massive intervals show weak grading and contain intraclasts or convolute laminae. Multiple events may be amalgamated to form beds up to 50 cm in thickness. We interpret that massive beds are deposited by muddy turbidites (Stow and Bowen 1980).

Bioturbated beds are also consistently siltier than the surrounding laminated sediments confirming the observations of Ozalas et al. (1994). Bioturbated beds are sharply based and are commonly erosive. As described in Savrda (1995), bioturbated beds consist of an upper massive and burrowed unit (primary stratum), and a lower unit of burrow-imprinted laminae (Fig. 3.4B). The primary stratum is identical to the mud infill of the burrows, confirming their derivation from primary strata (Savrda and Ozalas 1993). Burrow-imprinted laminae are always associated with a superjacent massive unit; we did not observe burrows in the absence of a primary stratum. Each burrowed primary stratum is abruptly overlain by undisturbed laminated sediments; despite careful observation, no evidence for transitional fabrics (i.e. minimally burrowed or disturbed laminae) between bioturbated beds and laminae overlying them are present, suggesting the abrupt termination of burrowing episodes. The only ichnogenus observed in our sections was *Thalassinoides* (cf. Föllmi and Grimm 1990; Savrda and Ozalas 1993; Grimm and Föllmi 1994).

Speckled beds are distinct from massive and bioturbated beds and are the focus of the discussion
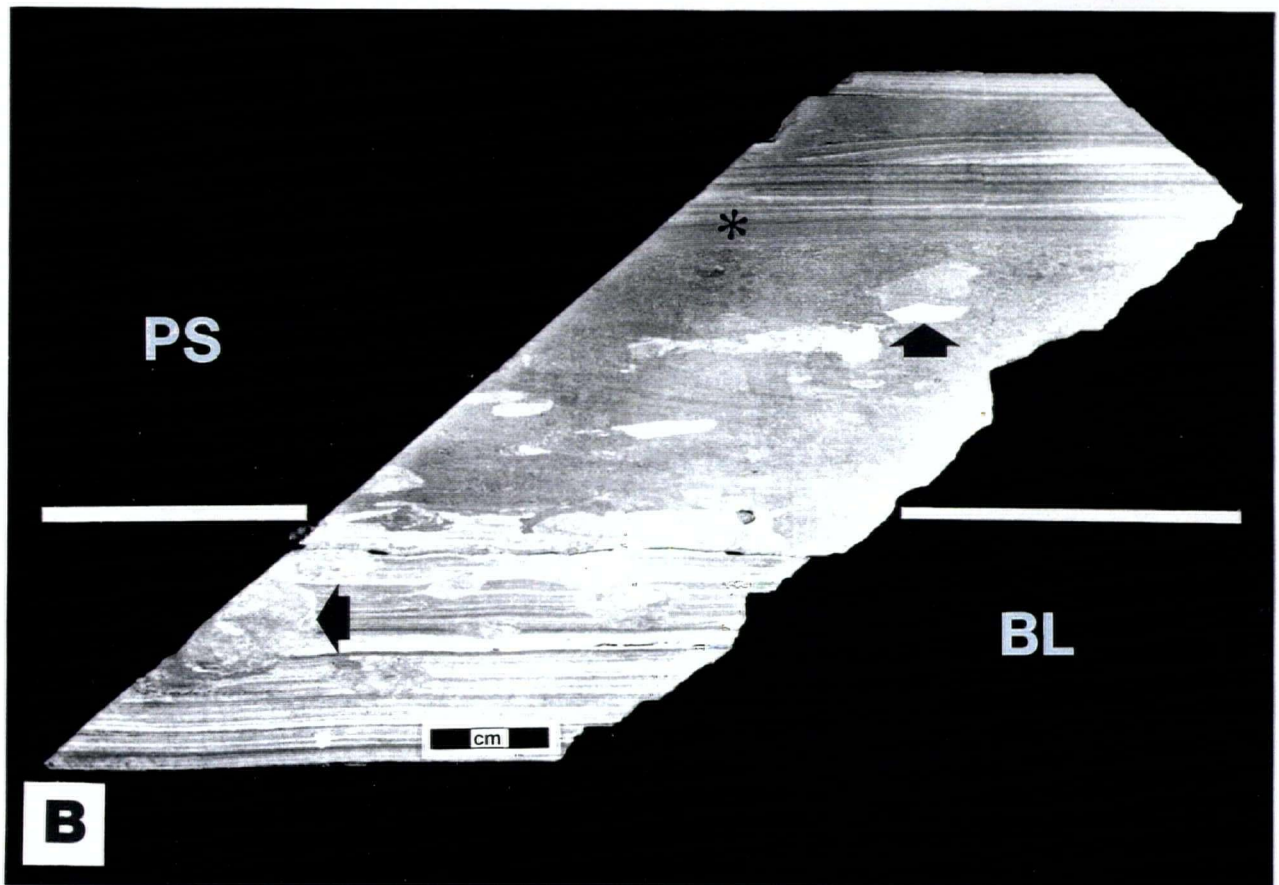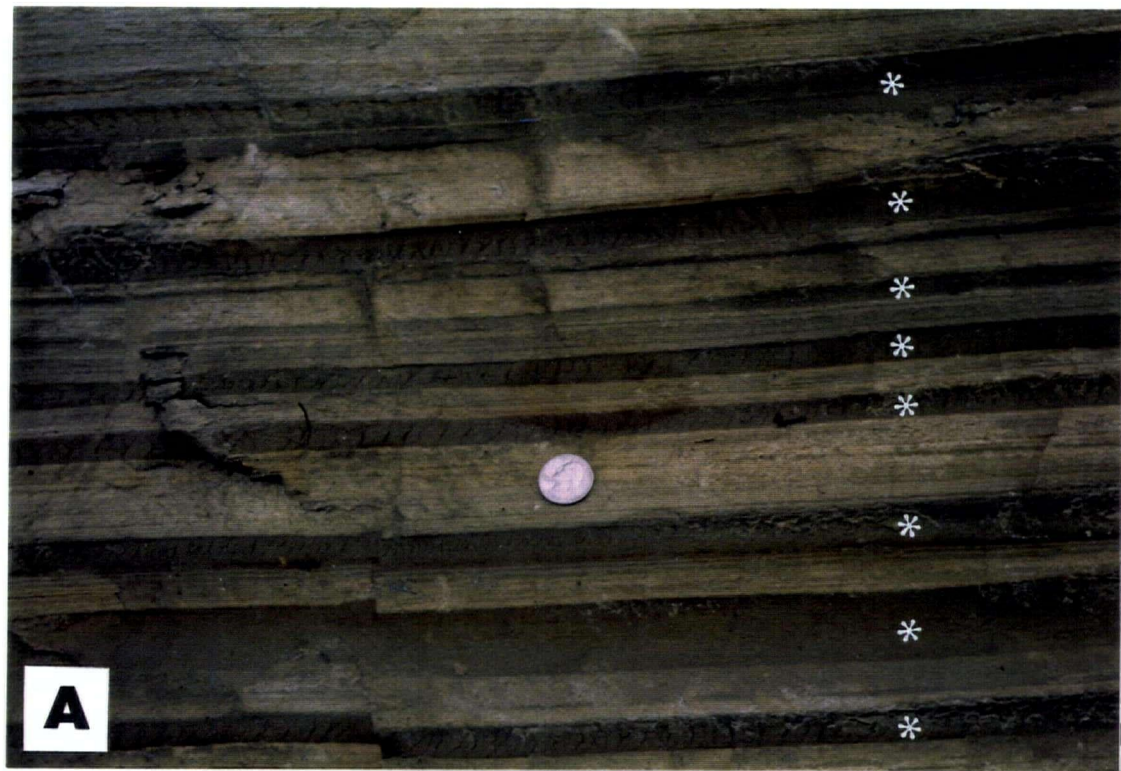
Fig. 3.4. Non-laminated intervals. **A)** Outcrop photograph of massive muddy turbidites (asterisks). Coin is 2.4 cm. **B)** Slabbed and sanded sample of bioturbated bed showing burrowed primary stratum (PS) in the upper two-thirds of the sample and burrow-imprinted laminae (BL) in the lower third of the sample. Arrows point to burrows of the ichnogenus *Thalassinoides*. Asterisk marks top of bioturbated bed.

below.

3.5   A Description of Speckled Beds

Speckled beds are recognized by their distinctive speckled appearance. Speckled beds are common and non-uniformly distributed throughout the 59-m section, occurring in both mud-rich and diatom-rich laminated sequences (Chang et al. 1997). Speckled beds have sharp bases, abrupt upper contacts, range in thickness from 3 mm to 10 cm, are not siltier than surrounding laminated sediments, and are neither burrowed nor situated immediately adjacent to bioturbated strata.

3.5.1   Mesoscale Observations

Mesoscale features were observed on slabbed and sanded surfaces of hand samples. The speckled appearance of speckled beds is derived from discrete detrital and diatomaceous aggregates distributed uniformly in a matrix of mud and diatom hash. There are three size classes of aggregates: 1) *speckles*: < 1 mm—coarse sand size and smaller; 2) *blebs*: 1 mm to 3 mm—very coarse sand to granule; and 3) *lozenges*: 3 mm to 10 mm—granule to small pebble size. In vertical section, the aggregates appear lenticular in shape with rounded or tapered terminations and are flattened parallel to bedding. In plan view, larger diatom-rich blebs and lozenges have an irregularly circular to ovoidal form; thus, three-dimensionally, blebs and lozenges are disc-shaped. Generally, the distribution of detrital and diatomaceous aggregates throughout the matrix of individual speckled beds is uniform with no size or shape grading of aggregates. We have classified four main types of speckled bed based on the overall texture and the size of the aggregates (Fig. 3.5).

Unimodal speckled beds are composed exclusively of well-sorted speckles and blebs (Figs. 3.5A and 3.6A). There is no compositional or textural patchiness or grading as the speckles are very uniformly distributed. The proportions of diatom-rich to detritus-rich blebs are generally equal. There is a noticeable difference between fine-grained unimodal speckled beds and coarse-grained unimodal speckled beds. Fine-grained speckled beds (Fig. 3.6A, arrow 1) are macroscopically smooth in

61

Figure 3.5. Slabbed samples depicting the four types of speckled beds.

A) *Unimodal*. Speckles and blebs are well sorted and uniformly distributed. In this slab from sample M-3, a brief laminated interval separates the lower diatom-dominated (Di) speckled bed from the upper detritus-dominated (De) speckled bed.

B) *Bimodal*. Diatomaceous blebs and lozenges are distributed uniformly throughout a unimodal matrix. In this overall diatom-rich slab from sample 2-9, several diatomaceous lozenges are visible (arrows). These lozenges are composed mainly of *Chaetoceros* setae (cf Fig. 3.9). Compare with x-radiograph (App. 2E).

C) *Amalgamated*. Distinguished by successive sharp to faint transitions between different speckled bed fabrics; in this sample, detrital-rich (De) and diatom-rich (Di) fabrics alternate. Asterisks demarcate boundaries. Numerous *Denticulopsis*-rich blebs and wisps within the diatom-rich fabrics may have derived from erosion of the thick *Denticulopsis* bloom (b).

D) *Speckled bed with laminated intraclasts*. The matrix of these speckled beds are generally unimodal but some are bimodal. Pebble-sized laminated intraclasts (LI) are common, showing discordant internal laminae.

63
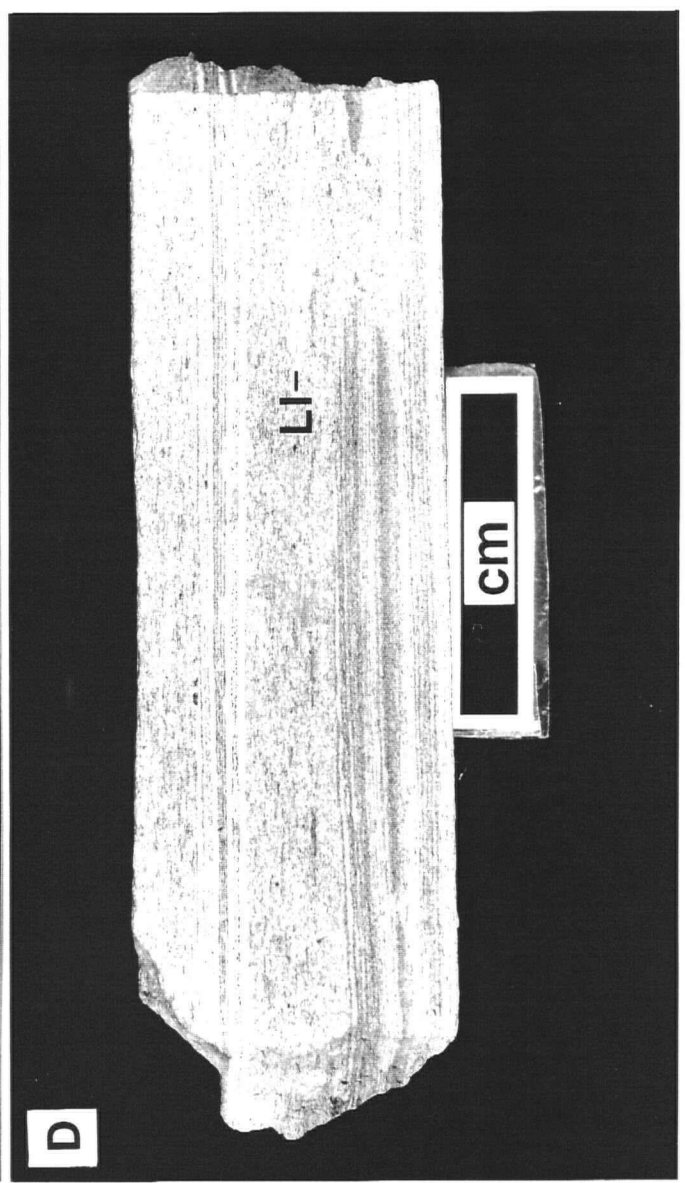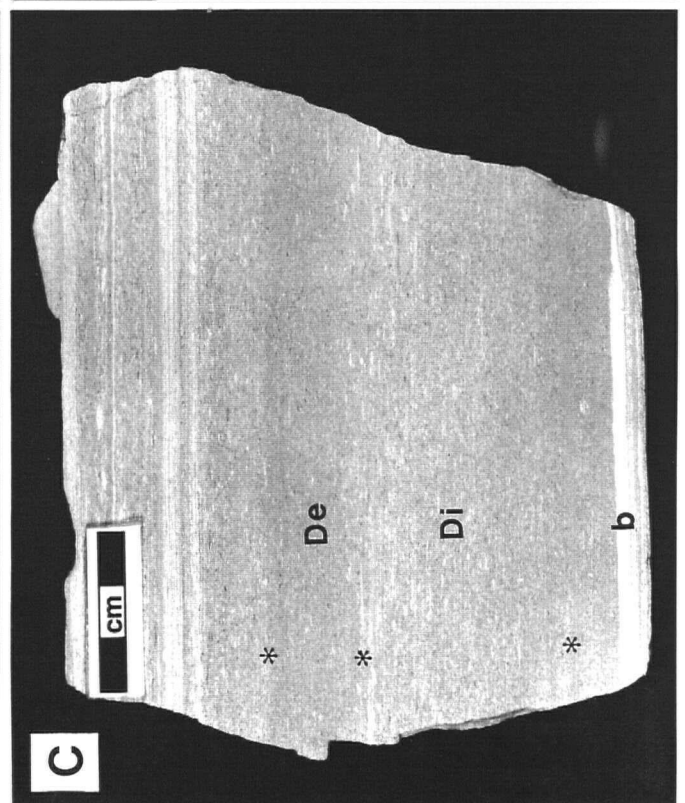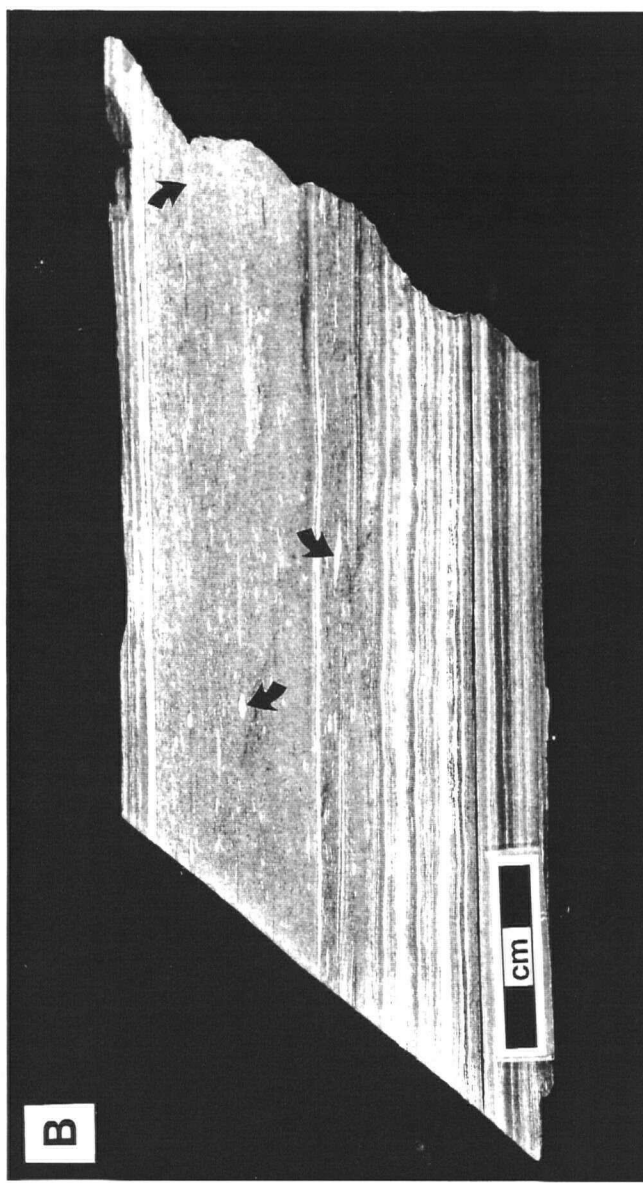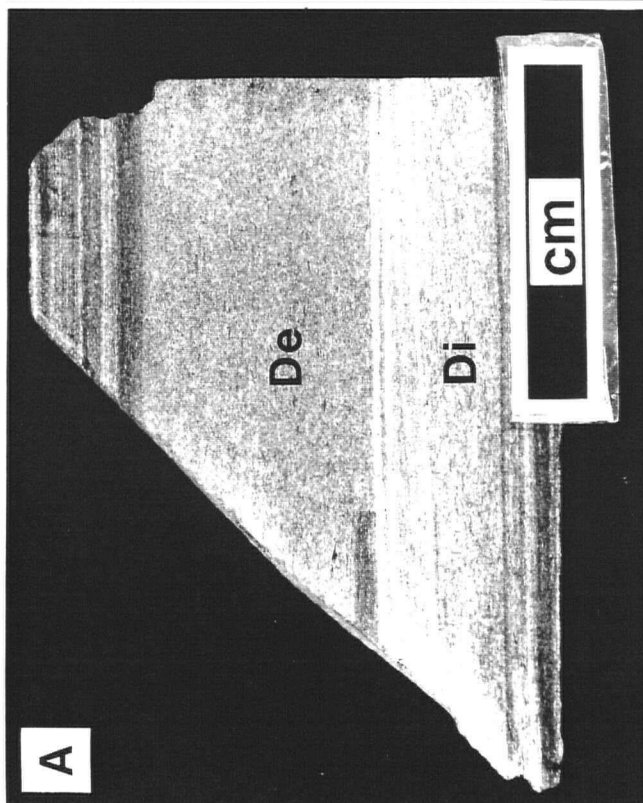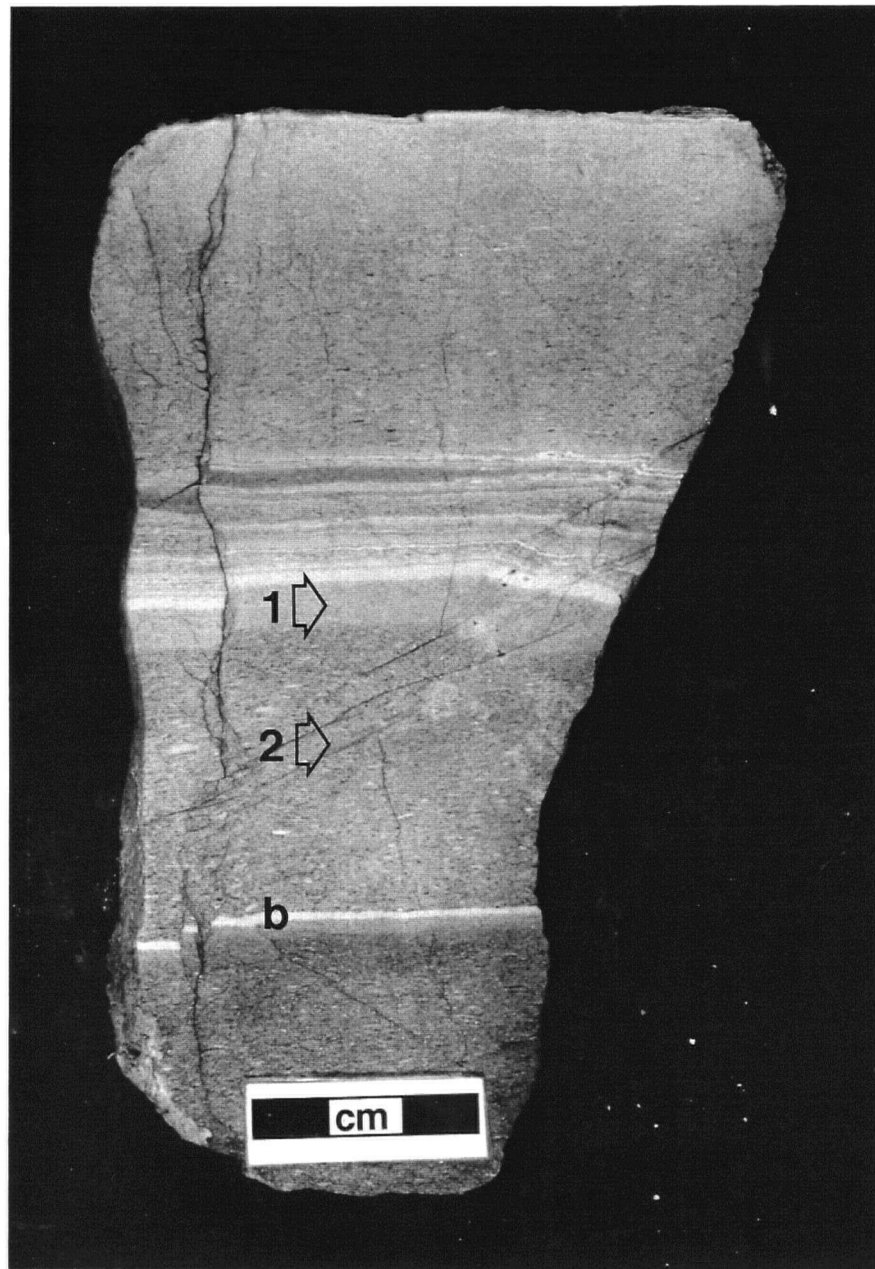
Figure 3.6. Slabbed and sanded samples of amalgamated speckled beds from reconnaissance samples.

A) An overall detritus-rich sample which gradually becomes less detrital toward the top of the sample. The fine-grained unimodal speckled bed indicated by arrow 1 is composed mainly of macerated biosilica and has minimal speckles (cf. Fig. 3.8A). The coarse unimodal speckled bed indicated by arrow 2 contains abundant benthic foraminifera and detrital aggregates (cf. Fig. 3.8B and C). Bloom lamina (b) contains abundant coccolithophores.
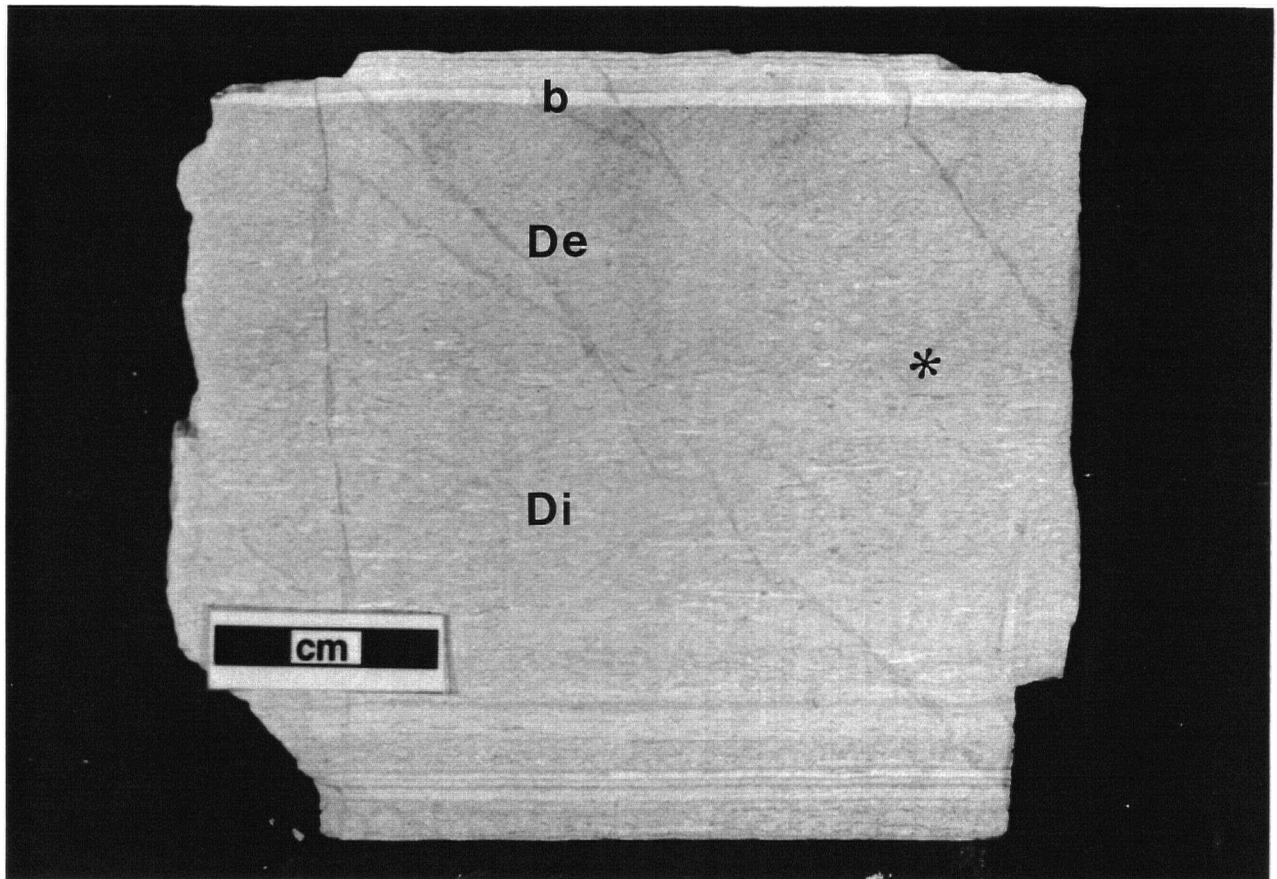
Figure 3.6 (continued). Slabbed and sanded samples of amalgamated speckled beds from reconnaissance samples.

B) Similar to the sample depicted in Figure 3.5C, this sample shows alternations of detrital-rich (De) and diatom-rich (Di) fabrics with *Denticulopsis*-rich wisps. Asterisk demarcates boundaries. A 2-mm thick *Denticulopsis* bloom (b) caps the amalgamated speckled bed sequence.

appearance as the speckles are scarce or on the silt to fine-sand scale. Coarse-grained unimodal speckled beds (fine-sand to coarse sand; Fig. 3.5A; arrow 2 in Fig. 3.6A) are more common and form the matrix to all other speckled bed types. Unimodal speckled beds range from 3 mm to 4 cm in thickness.

The matrix of *bimodal* speckled beds is composed of coarse-grained unimodal speckled bed sediments (Fig. 3.5B). Set in the matrix are large white diatomaceous blebs and lozenges ranging in thickness from 1 mm to 2 mm and lengths of 2 mm to 10 mm. Some wispy lozenges are flat and elongate. Conspicuous blebs and lozenges comprise up to 10% of the entire fabric and are distributed uniformly throughout the unimodal host matrix. Detritus-rich lozenges are rare to non-existent whereas detrital blebs and wisps are more common. Bimodal speckled beds range from 1 to 5 cm in thickness.

Amalgamated speckled bed s display transitions from one texture of speckled bed to another with each texture being no more than 4 cm thick (Figs. 3.5C and 3.6). The contacts between each speckled bed texture are faint to sharp and are parallel to bedding. The maximum thickness of amalgamated speckled beds is ~10 cm.

The matrix for *speckled beds with laminated intraclasts* may be either unimodal or bimodal, although the unimodal matrix is the more common (Fig. 3.5D). This type of speckled bed has not been observed with an amalgamated matrix. The length of laminated intraclasts ranges from 1 cm to over 10 cm where their long axes are oriented parallel to bedding; the internal laminae of the clasts may be discordant with bedding. The thickness of these speckled beds ranges from 1 cm to 5 cm.

3.5.2   Microscale Observations

Microscale observations were made on thin sections, smear and strewn slides, and by scanning electron microscopy. In thin section and backscattered electron microscopy, submillimetre features which are not visible in hand sample become evident (Fig. 3.7A). Silt to fine-sand-sized speckles of variable composition are observed to stand on their own or to comprise larger speckles (Fig. 3.7A). Other submillimetre features include the alignment of large diatom frustules: isolated diatom valves are generally aligned parallel with bedding whereas diatoms incorporated into diatom-rich blebs are not aligned (Fig. 3.7B-D). In either case, diatom valves remain uncrushed or are flattened into a bow-tie shape (cf. Fig. 3.7B). The porous nature of the diatom frustules gives rise to the darker backscattered

Figure 3.7. Backscattered secondary electron micrographs of epoxy-impregnated sediment showing submillimeter features. Stratigraphic up direction is towards the top of each image.

A) Three speckles of differing composition from a unimodal speckled bed. The dark speckle at the top (S1) is composed of unfragmented diatoms, the bright speckle at the bottom (S2) is comprised of diatom hash and detritus, and the speckle at centre is of an intermediate composition. White arrow indicates where high magnification image in Figure 3.7B was taken.

B) High magnification image of the speckle S2 from Figure 3.7A showing reflective detrital silt grains and finely hashed diatoms. Two intact but flattened *Coscinodiscus* (C) frustules, aligned parallel to bedding, are visible.

C) Diatomaceous bleb from a bimodal speckled bed. The tapered ends of the bleb are out of view. Arrows indicate upper and lower contacts of the bleb.

D) Magnified view of the centre of the diatomaceous bleb from Figure 3.7C showing unfragmented *Coscinodiscus* frustules.
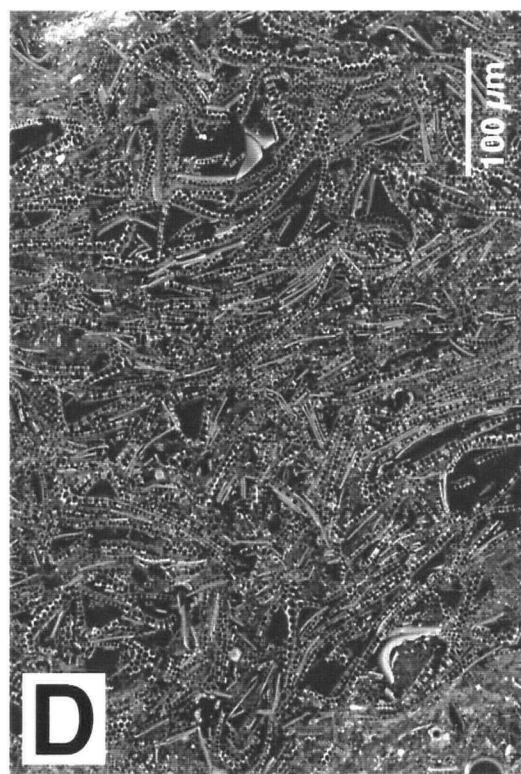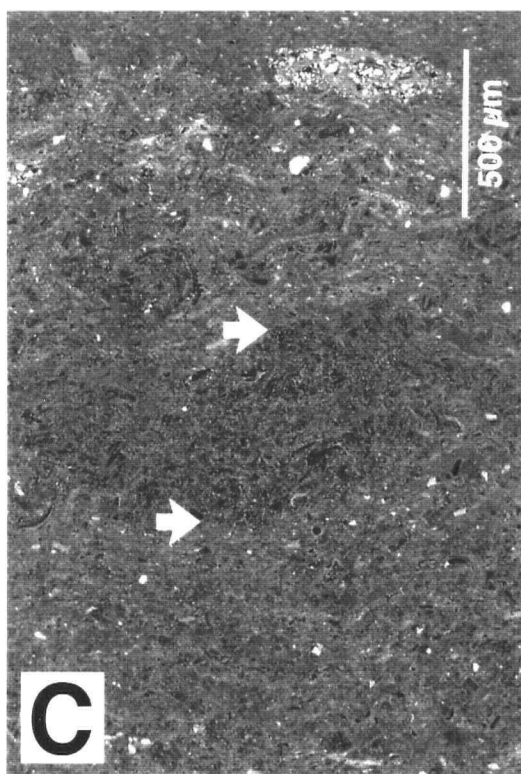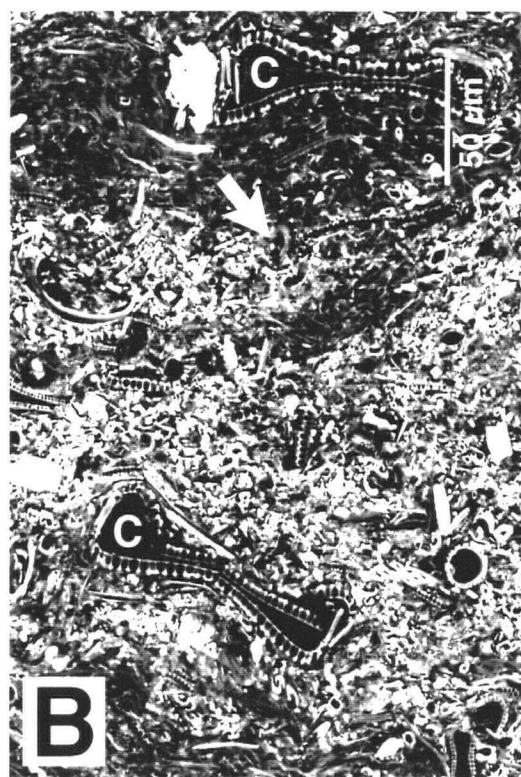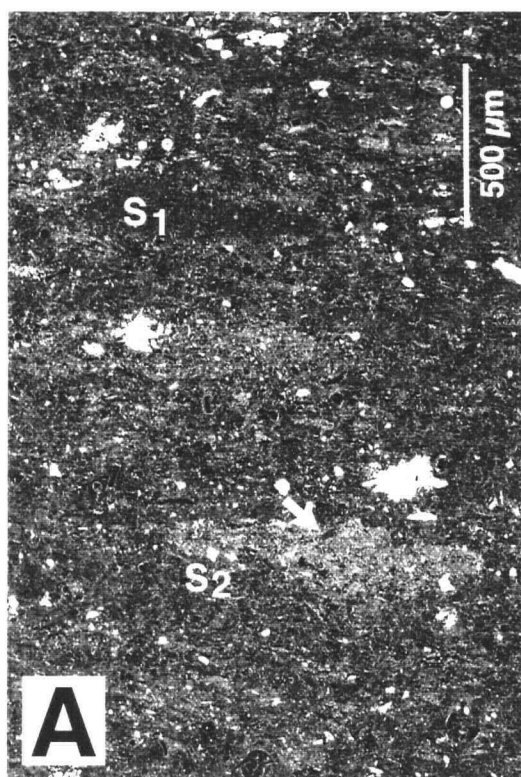
electron image. The matrix supporting speckles and blebs is composed mainly of fragmented macerated biosilica with a subordinate detrital component.

The smoothness of the fine unimodal speckled bed indicated by arrow 1 on an amalgamated speckled bed sample in Fig. 3.6A becomes evident with high-magnification imaging. There are essentially very few speckles and the matrix is a uniform, well-sorted diatom hash (Fig. 3.8A). In the coarse unimodal speckled bed from the same sample (arrow 2 in Fig. 3.6A), speckles and blebs of various compositions, detrital aggregates and benthic foraminifera are visible (Fig. 3.8B and C). Detrital aggregates are not associated with nearby silty laminae and are believed to be the discarded remnants of agglutinated benthic foraminifera (cf. Pike and Kemp 1996b). Off central California, modern benthic foraminifera such as *Bolivina* and *Uvigerina* have been observed to live in dysaerobic (<0.3 mL/L) conditions at the core of the oxygen minimum zone (Mullins et al. 1985; Vercoutere et al. 1987).

Backscattered and secondary electron imaging of bimodal speckled beds and diatom-rich intervals of amalgamated speckled beds yielded intriguing results. Diatom-rich blebs and lozenges were found to consist of low-diversity and monospecific diatom assemblages with moderate to excellent states of preservation. The pristine monospecific diatoms in most lozenges and blebs contrast strikingly with the macerated biosilica and detrital silt grains of the surrounding matrix. The main taxa comprising these blebs and lozenges are *Coscinodiscus* (Fig. 3.7C and D), *Chaetoceros* setae (Fig. 3.9), *Chaetoceros* sp. (Fig. 3.10A), *Thalassiothrix* (Fig. 3.10B), and *Denticulopsis* (Fig. 3.10C).

In summary, speckled beds are ubiquitous in the quarry, are not associated with bioturbation, and are texturally distinct from other types of non-laminated intervals. Speckles and small blebs may be either diatomaceous or detrital whereas larger blebs and lozenges are chiefly composed of monospecific diatoms. The three aggregate types, including the presence of laminated intraclasts, result from the reworking (erosion and transport) of laminated sediments and show that their provenance is from within an oxygen minimum zone.
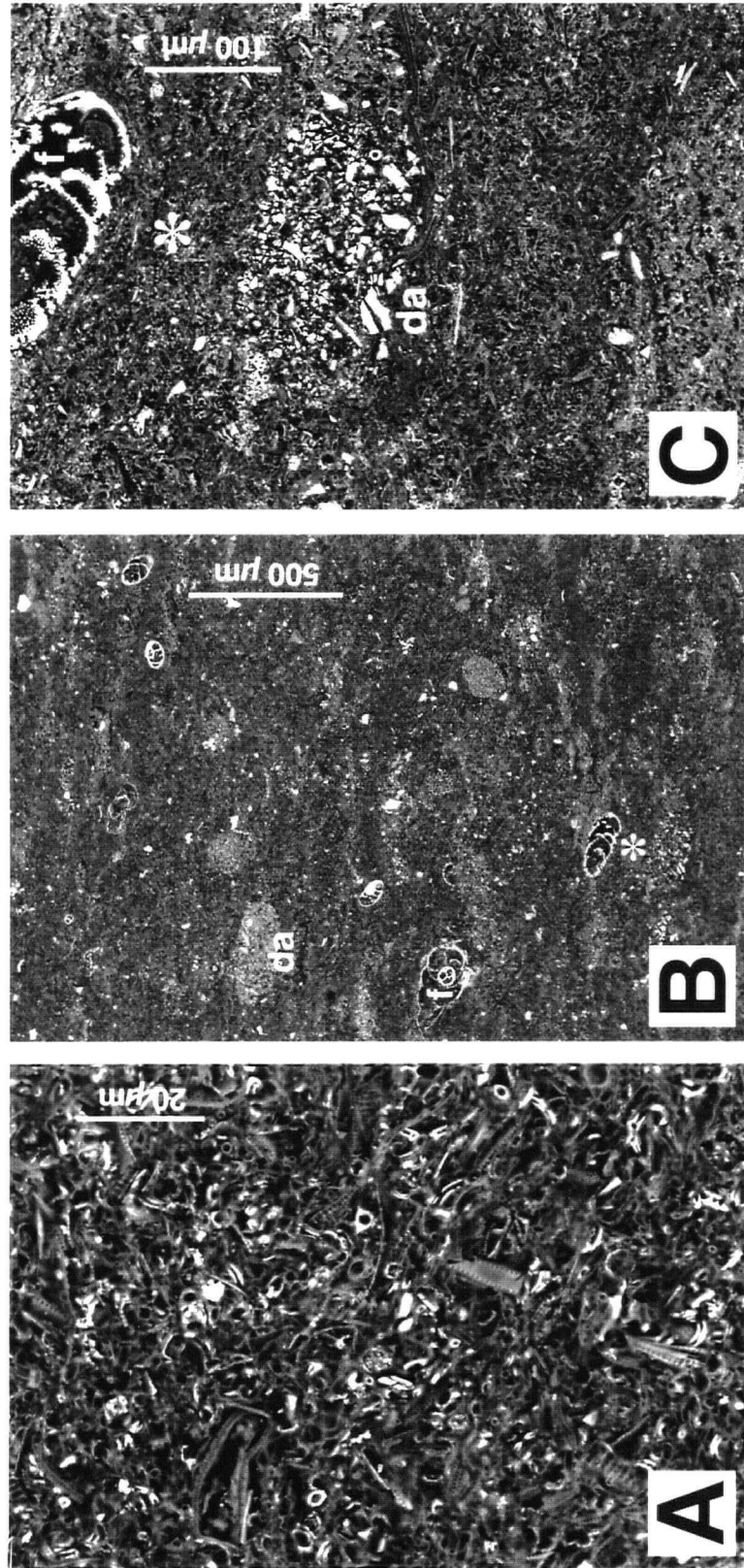
Figure 3.8. Backscattered electron images from fine and coarse unimodal speckled beds. A) High magnification image of fine unimodal speckled bed at arrow 1 in Figure 3.6A showing finely hashed frustules and very little detrital content. Speckles are minimal resulting in the macroscopically structureless fabric seen in Figure 3.6A. B and C) High magnification images of coarse unimodal speckled bed fabric at arrow 2 in Figure 3.6A with speckles of variable composition resulting in a blotchy appearance. Agglutinating foraminiferan (f) and detrital aggregates (da) are prominent in this interval. Asterisk in Figure 3.8B shows where image in Figure 3.8C was collected.

70

Figure 3.9. Backscattered electron micrographs of a diatomaceous lozenge from a bimodal speckled bed.

A) Photomosaic of the lozenge; length=11 mm. Note the scarcity of silt grains (white specks) within the lozenge as compared with the matrix. Labelled asterisks mark the sites of high-magnification imaging (Fig. 3.9B-D).

B) Lower boundary (arrows) of lozenge showing sharp contact between the lozenge, consisting of *Chaetoceros* setae (s) with minor constituents of *Thalassiothrix* and silicoflagellates (Si); and the surrounding matrix, composed of detrital silt grains (sg), sponge spicules (sp) and macerated biosilica.

C) Centre of lozenge showing unfragmented tubular setae (s), a *Chaetoceros* resting spore (Crs), *Thalassiothrix* (T) and silicoflagellates (Si).

D) Upper boundary of lozenge at arrows. Si=silicoflagellate, T=*Thalassiothrix*.

71

72
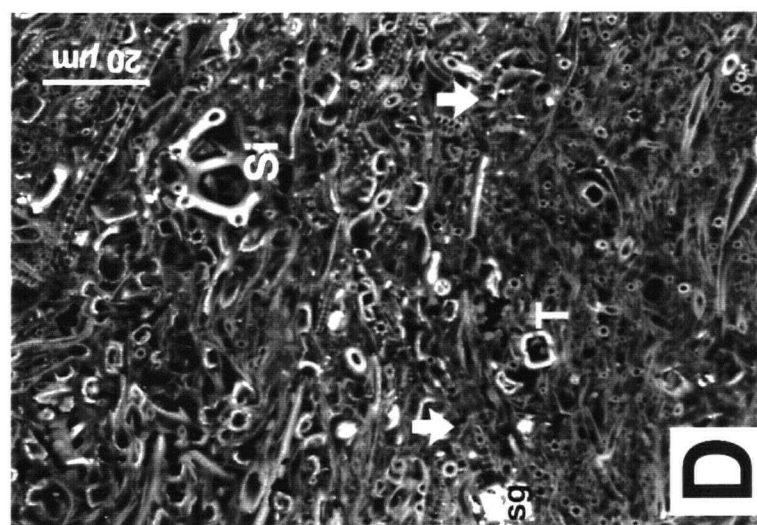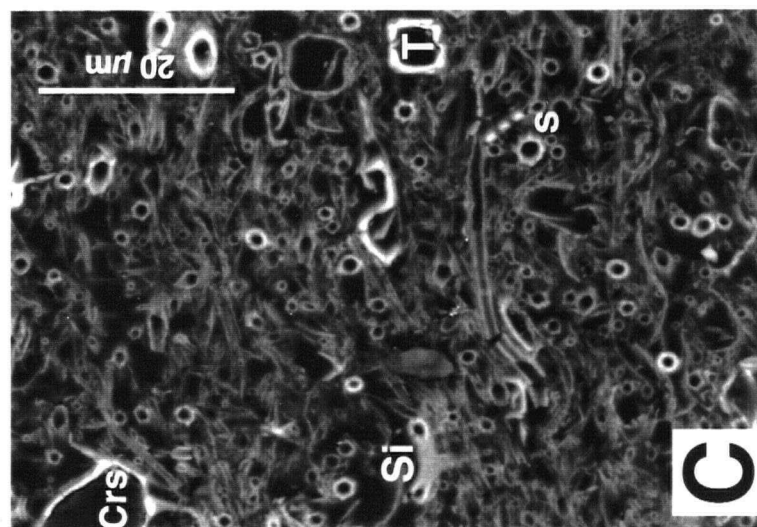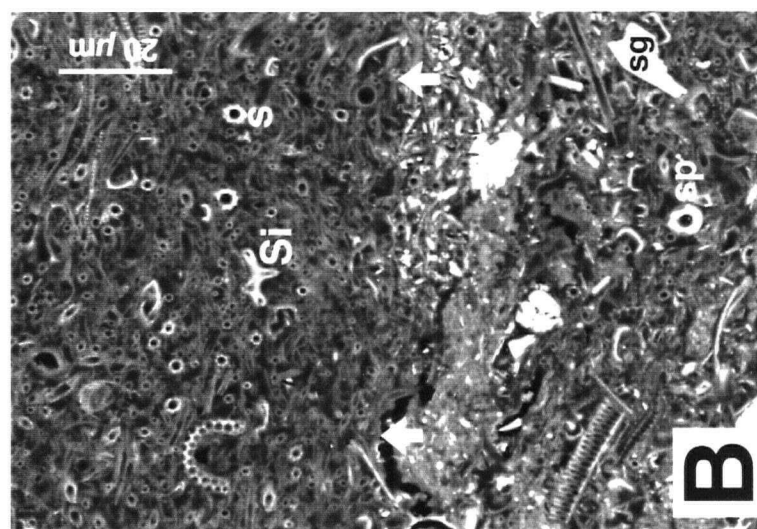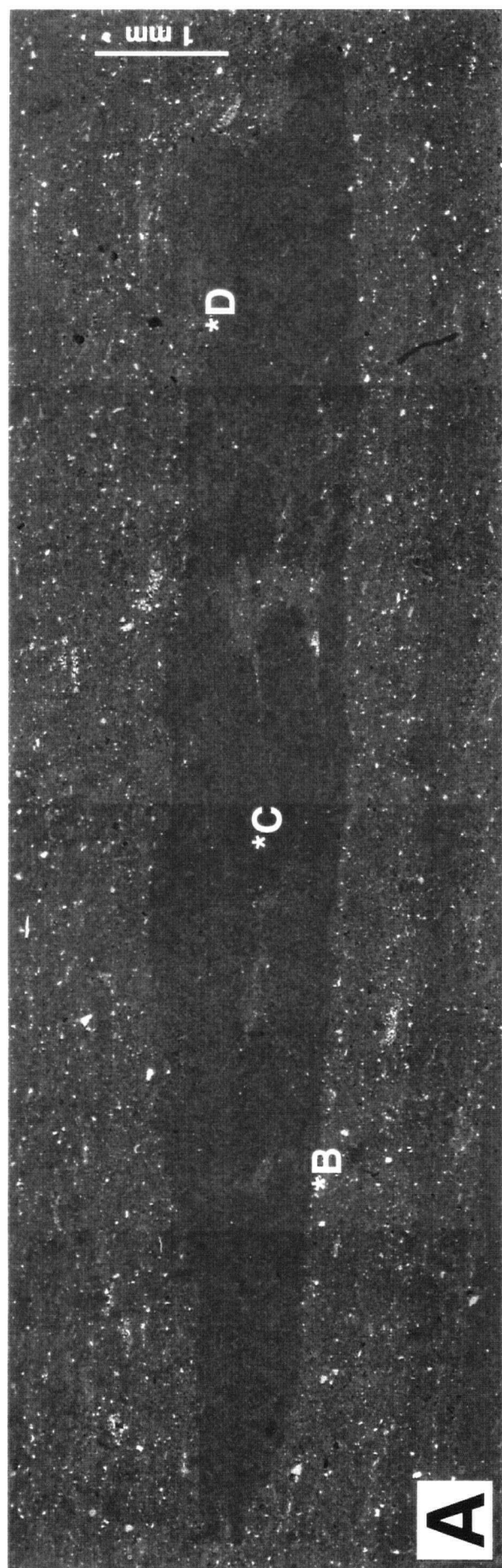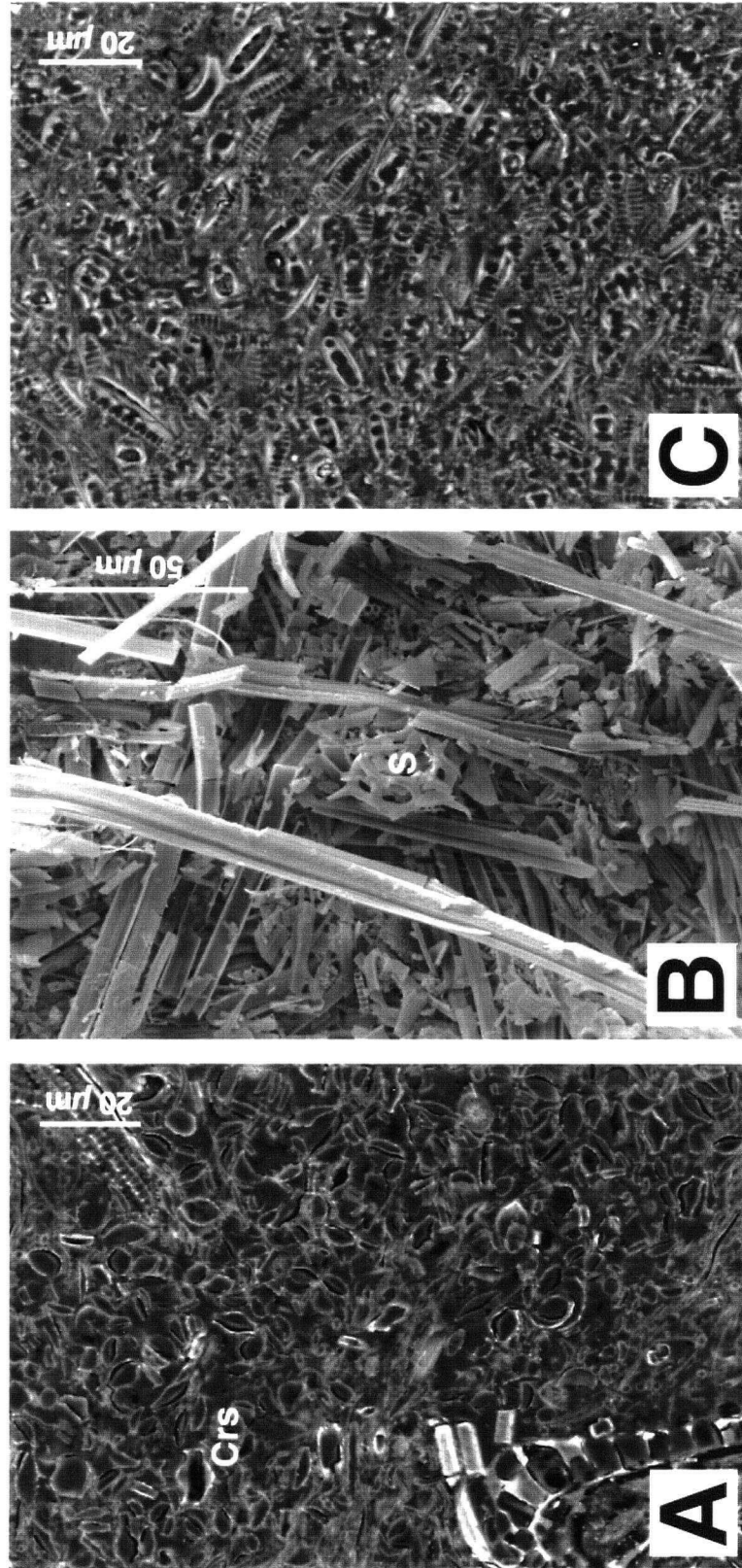
Figure 3. 10. Monospecific blebs and lozenges from bimodal speckled beds and diatom-rich intervals of amalgamated speckled beds. **A)** Backscattered electron micrograph of *Chaetoceros* sp. resting spores (Crs) from a bimodal speckled bed. **B)** Secondary electron micrograph of *Thalassiothrix* frustules with a silicoflagellate (s) from a bimodal speckled bed. **C)** Backscattered electron micrograph of *Denticulopsis* from an amalgamated speckled bed. The degree of preservation of frustules in monospecific blebs and lozenges is generally good to excellent.

3.6   Interpretations of the Origins of Speckled Bed Fabrics

The composition and texture of speckled beds differs from those of bioturbated intervals. For instance, pelletal fabrics associated with bioturbated zones from Monterey diatomites, as described by Savrda and Ozalas (1993; their fig. 3), may initially resemble speckled beds. However, Ozalas et al. (1994) determined the pelletal fabrics consisted of fecal pellets produced by an unidentified organism. Although pelletal fabrics lacked distinct burrows just as speckled beds do, they were commonly observed superjacent to burrowed primary strata where the contact between the primary stratum and the pelletal fabric was gradational. Pelletal fabrics were interpreted to have been deposited during the termination of oxygenation events of dysaerobic waters (Savrda and Ozalas 1993; Ozalas et al. 1994).

The different textures of each type of speckled bed reflect slightly different source material and modes of deposition. The uniform size of speckles and blebs in unimodal speckled beds may have derived from the disruption of laminated sequences which contained equal proportions of mud-rich and diatom-rich laminae (i.e. subequal couplets; Chapter 2). In bimodal speckled beds, large diatomaceous blebs and lozenges were likely derived from the erosion of diatom-rich sequences containing thick diatomaceous laminae. For example, *Denticulopsis* lozenges from the amalgamated speckled beds depicted in Figures 3.5C and 3.6B reside within speckled bed fabrics that are bounded above and below by 2-mm thick *Denticulopsis* bloom laminae. The disruption of diatomaceous laminae composed of *Chaetoceros* setae and *Thalassiothrix* may give rise to anomalously large lozenges, as seen in Figure 3.9. The interlocking meshwork of elongate morphologies such as that of *Chaetoceros* setae and *Thalassiothrix*, in conjunction with biologically exuded phytoplankton gelatins and diagenetically produced gels (Alldredge and Gottschalk 1989; Hill and Marsters 1990; Grimm et al. 1997), likely imparted additional strength, permitting their abundance in larger blebs and lozenges (Bodén and Backman 1996; Lee et al. 1990; Chapter 2) and the preservation of pristine diatom assemblages after transport.

The formation of the overall textures of amalgamated speckled beds and speckled beds with laminated intraclasts differs from unimodal and bimodal speckled beds. Amalgamated speckled beds, comprising alternating beds of different speckled bed fabrics, represent some of the thickest speckled bed sequences observed (up to 10 cm); however, each bed within the amalgamation is no more than 4

74

cm which falls in the range of thicknesses of isolated speckled beds. This suggests that each bed may represent individual depositional events. Pebble-sized laminated intraclasts incorporated into speckled bed matrices may have originated from the erosion and entrainment of laminae from the uppermost sediment column. Regardless of which type of speckled bed is involved, all speckled beds are produced under special circumstances which are described fully below.

3.7   Formation of Speckled Beds: Gravity Flow Hypothesis and Discussion

To produce speckled beds, three prerequisites must be satisfied: 1) the presence of *cohesive* laminated diatomaceous sediments preserved within the oxygen minimum zone, 2) deposition of these laminated sediments on a *slope*, and 3) initiation of slope failure and/or erosional entrainment *within* the oxygen minimum zone. It is imperative that slope failure occurs within the oxygen minimum zone since laminated intraclasts and diatomaceous lozenges are derived from the erosion of laminated sequences. Slope failure occurring above or below the oxygen minimum zone would contain sand and silt intraclasts. Conversely, slope failure within the oxygen minimum zone with deposition downslope from the oxygen minimum zone would result in the formation of speckled beds within non-laminated sediments (Fig. 3.11).

The abundance of deformation structures observed in the quarry indicates that a shallow incline (0.5-3.0°; Schwarz 1982; Prior and Coleman 1984) was present during the deposition of laminated diatomites, and that slope instability and sediment failure was widespread and common. We infer that an initial disturbance triggered slumping and gliding, resulted in the disaggregation of laminae and led to the generation of a bottom-hugging gravity flow (Stow and Bowen 1980; Gorsline 1984). The gravity flow hypothesis consists of four stages: initiation, transport, deposition and burial (Fig. 3.12).

Initiation.—Triggering of slope destabilization may occur by seismic activity or by cyclic loading induced by storm-generated internal waves. In addition, sediment overloading, gravitational forces acting on oversteepened slopes, increases in pore fluid pressures, or loss of sediment strength can also cause mass failure (Middleton and Hampton 1976; Keller 1983; Prior and Coleman 1984; Blais 1995;
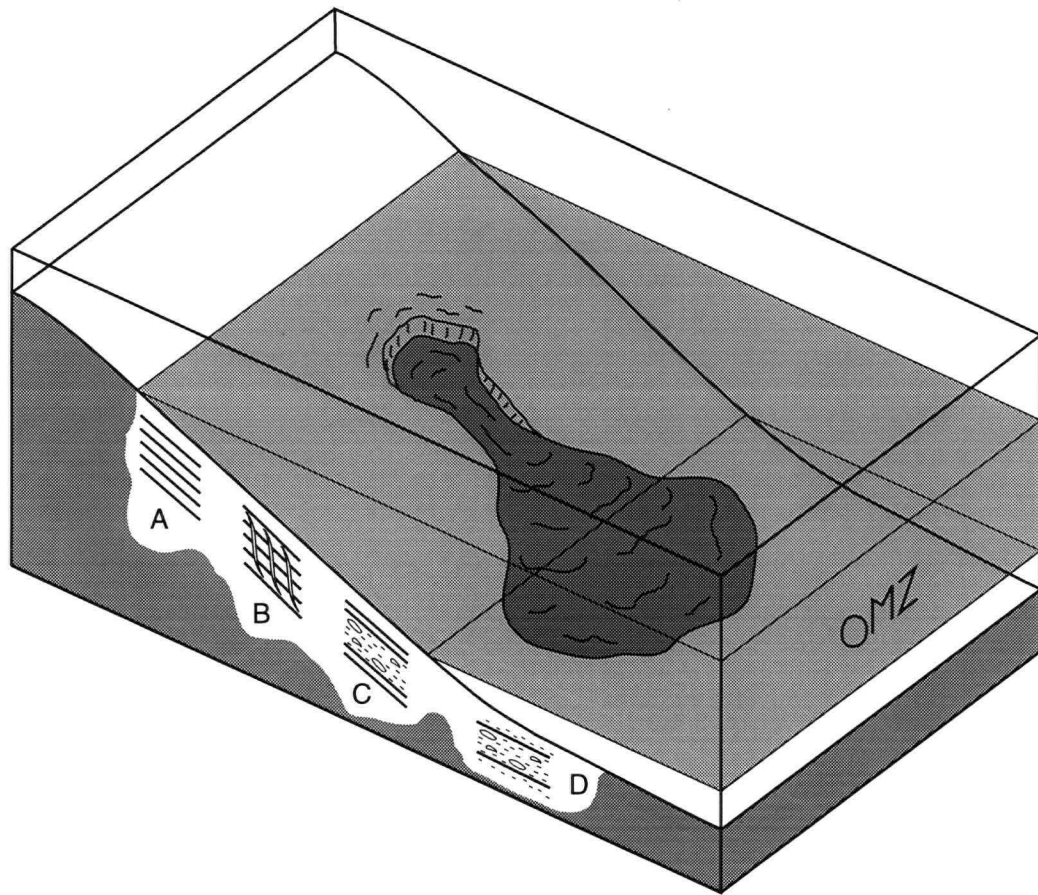
Figure 3.11. Block diagram depicting environmental setting for the formation of speckled beds. **A)** Laminateddiatomaceous sediments forming within the oxygen minimum zone (OMZ) where the lack of bioturbating macrobenthos permits the preservation of primary laminae. **B)** Slope failure (shown here as intrastratal microfracture formation and slumping) must occur within the OMZ since speckled beds are composed of disrupted laminated sediments. Failure of cohesive sediments, progressive disaggregation of laminae during transport, and mixing within high-density gravity flows produces speckles, blebs and lozenges (cf. Fig. 3.12). **C)** Bedding-parallel sedimentation of speckled beds within laminated sediments downslope. Deposition within the OMZ produces speckled beds bounded by laminated sediments. **D)** Slumped sediments deposited below the OMZ produces speckled beds within non-laminated sediments.

Blais-Stevens, in press). Regardless of the triggering force, slope destabilization caused sediments to deform hydroplastically forming tight slump folds where primary laminae were preserved but contorted (Lowe 1975; Keller 1983). Initiation of abrupt slumping or sliding of entire blocks of sediments, which in turn generated into gravity flows, may have subsequently occurred (Stow and Bowen 1980; McCave and Jones 1988; Fig. 3.12B and C). Sediment failure arose because of the naturally high sensitivity and liquid limits of the organic-rich diatomaceous sediments. When these sediments were undisturbed, they maintained their coherence and cohesiveness, but once they were disturbed, the cohesion was lost and the sediment mass began to flow (Keller 1983; Hill and Marsters 1990).

Transport.—Once the slump or glide blocks were mobilized, they progressively disaggregated and generated into gravity flows as turbulence and water content increased (Middleton and Hampton 1976; Keller 1983; Grimm and Orange 1997; Fig. 3.12D). During transport, slump or glide blocks and slump folds disintegrated to a threshold size where large blocks broke up but sand- to pebble-sized blebs and lozenges and pebble-sized laminated segments remained intact. These particles reached a maximum equilibrium size related to the intensity of the turbulence in the flow (cf. Stow and Bowen 1980). The presence of pebble-sized laminated intraclasts in some speckled beds suggests that these clasts experienced less agitation and transport than other aggregates, which in turn suggests late-stage entrainment of the laminated segments. We are presently unable to quantify the velocities and energies of the initial to final flows.

Within the turbulent gravity flow, the speckles, blebs and lozenges were well mixed. Some sediments lost all cohesiveness and disintegrated down to their basic components forming the fine mud and diatom hash matrix. As mentioned previously, a combination of gels and the interlocking meshwork of unfragmented diatom morphotaxa within diatom-rich laminae allowed large lozenges to remain intact after transport. These lozenges preserved pristine low-diversity assemblages from bloom laminae and mats laminae.

Deposition.—When flow energy dissipated, water content decreased, flow concentration and viscosity increased, and turbulence became damped (McCave and Jones 1988); the sediment mass slowed to a critical velocity and froze in place (Lowe 1982; Gorsline 1984; Fig. 3.12E). During damped turbulence, the gravity flow decelerated while continuing to flow downslope; the aggregates and matrix
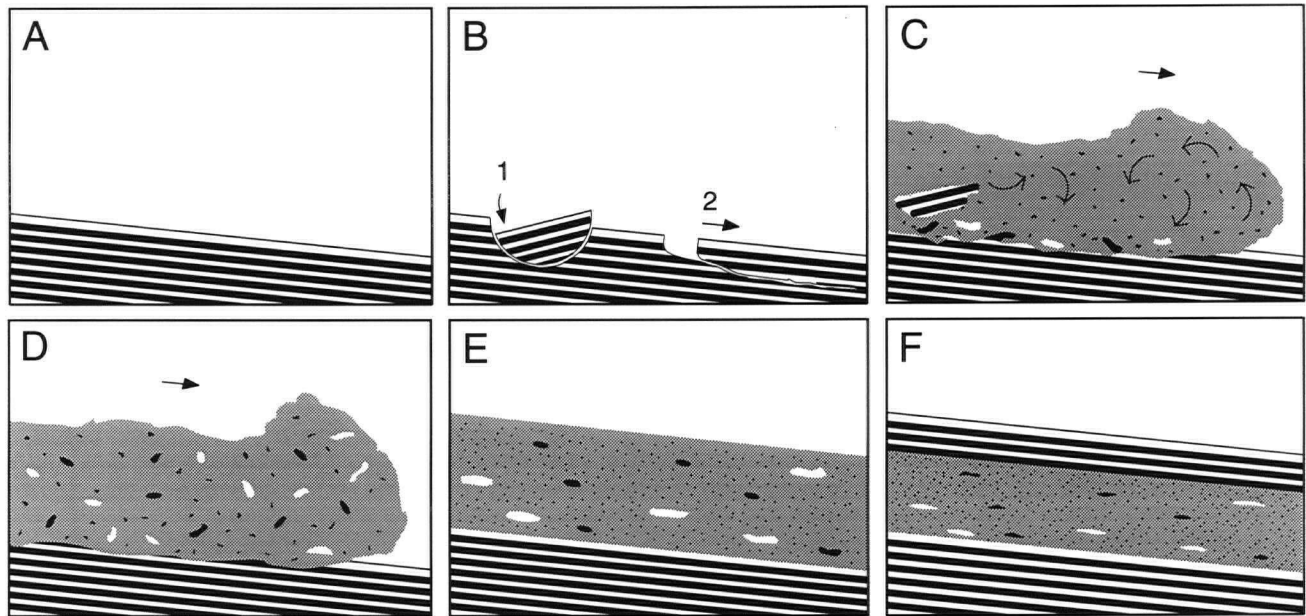
Figure 3.12.   Gravity flow hypothesis for the formation of speckled beds within the oxygen minimum zone. No scale is intended.
A) Laminated diatomaceous sediments on a subaqueous slope within the oxygen minimum zone; high cohesion and sediment strength.
B) Slope failure and laminae disturbance by (1) slumping or (2) gliding; sediment strength and cohesion lost. Slump/glide block
 evolves into a viscous gravity flow. **C)** Gravity flow disaggregates laminae, producing speckles, blebs and lozenges. **D)** Diatomaceous
and detrital aggregates are mixed gravity flow during viscous transport. Diatomaceous sediments produce larger aggregate size
than detrital-rich laminae. **E)** As current energy dissipates and the flow freezes, aggregates sediment with long axes parallel to bedding.
F) Aggregates are flattened during burial compaction, producing a speckled bed with sharp basal and upper contact.

consolidated like a static suspension where interparticle forces prevented grain sorting (McCave and Jones 1988). When frictional forces exceeded the internal kinetic energy of the flow, the flow stopped and froze as an ungraded plug (cf. Pallesen 1983; Gorsline 1984).

Elongate components—whether they were microscopic unfragmented tests and frustules or macroscopic lozenges and laminated intraclasts—sedimented with their long and intermediate axes parallel to bedding with the speckles, blebs and lozenges distributed evenly throughout the matrix. The lack of grain shape and/or size grading indicated that there was no settling of fine particles during the waning stage of the flow; hence, a high-density or hyperconcentrated turbidity current (Gorsline 1984; McCave and Jones 1988) was probably responsible for the formation and deposition of speckled beds. Numerical modeling of high-density turbidity currents by Zeng and Lowe (1990) suggested that a high suspended sediment concentration and wide grain-size range could hinder the settling of particles and inhibit dynamic sorting during deposition.

Burial and preservation.—During burial, the blebs and lozenges became flattened, enhancing the primary fabric (Fig. 3.12F). Normal sedimentation of laminae resumed and a speckled bed was produced with a sharp upper contact. Subsequent post-depositional flattening and time-enhanced compaction may have also contributed to the bedding-parallel texture.

Speckled beds represent end products in a continuum of deformation structures observed in Monterey Formation diatomites (Fig. 3.13). The abundance of these syndepositional deformational features indicates that deposition of laminated diatomites occurred in a region where active tectonism may have played a prominent role in slope destabilization (Thornton 1984; Grimm and Orange 1997). The initial signature of slope destabilization is assumed to be the formation of intrastratal microfractured zone structures (Fig. 3.13A). Alternatively, increases in the pore fluid pressures lead to planes of weakness and fluidized strata which lead to slump folding (Fig. 3.13B) in competent sediments (Grimm and Orange 1997). Stratal detachment, partial laminae disaggregation and plastic deformation of slump and glide blocks during short transport episodes, and subsequent amalgamation of laminated segments, led to the coarse slumped laminae seen in Fig. 3.13C. Transport of coarse slumped laminae, complete fluidization, and disaggregation result in the formation of speckled beds (Fig. 3.13D).

Speckled beds from the Monterey Formation resemble the "brecciated laminae" observed in

79

Figure 3.13. Outcrop photographs of progressive deformation styles in a slope destabilization continuum.

A and B) Initial steps of sediment failure:

A) Intrastratal microfractured zone. Coin=2.4 cm.

B) Slump fold. Several speckled beds of varying thicknesses are present above and below the slump.

C) Further deformation yields slumped laminae.

D) Complete failure and disaggregation of slumped laminae during transport produces speckled beds. Shown are speckled beds with laminated intraclasts. Coin=1.8 cm.
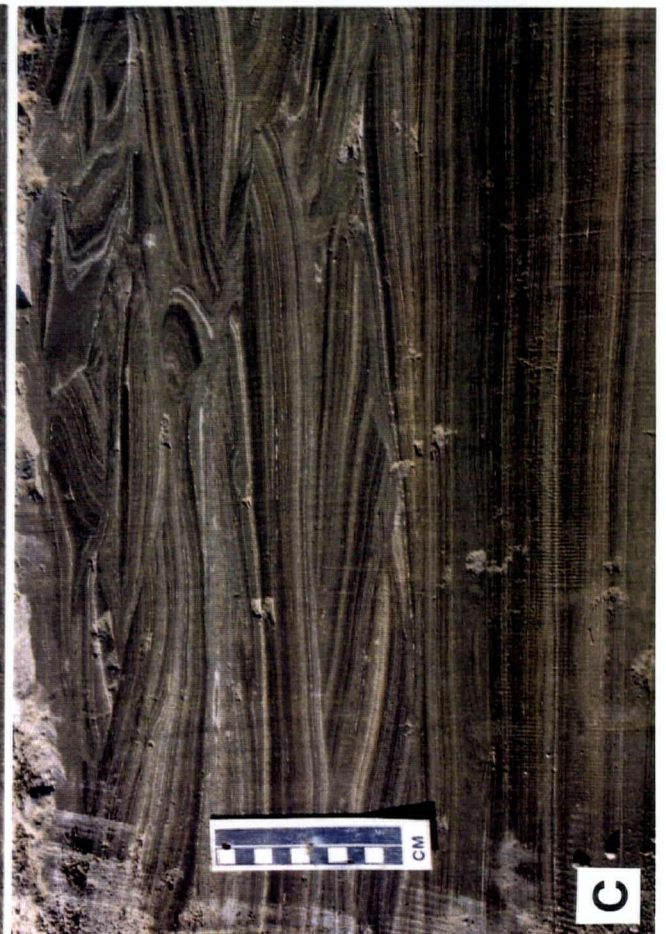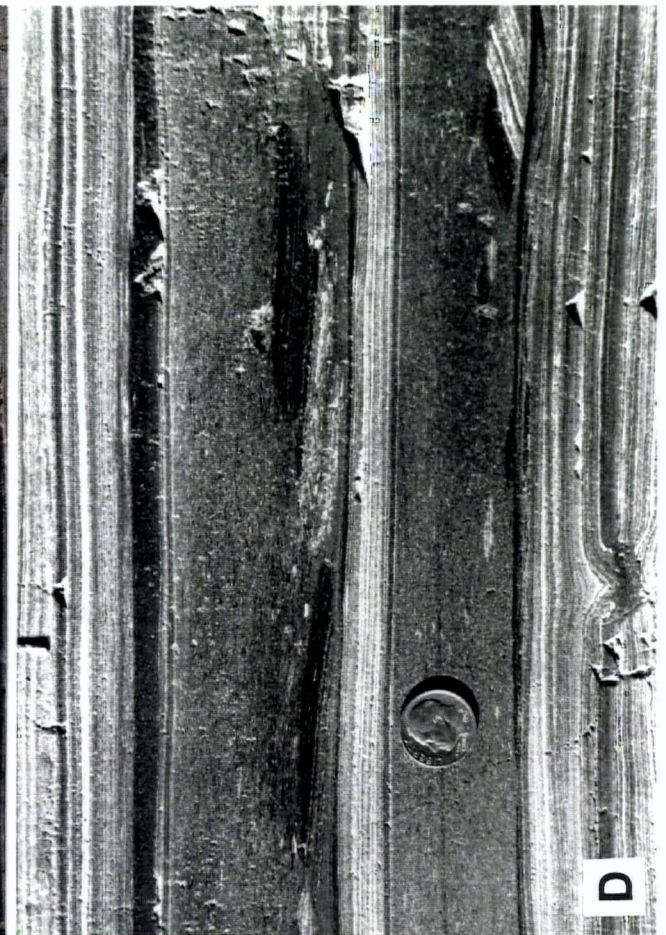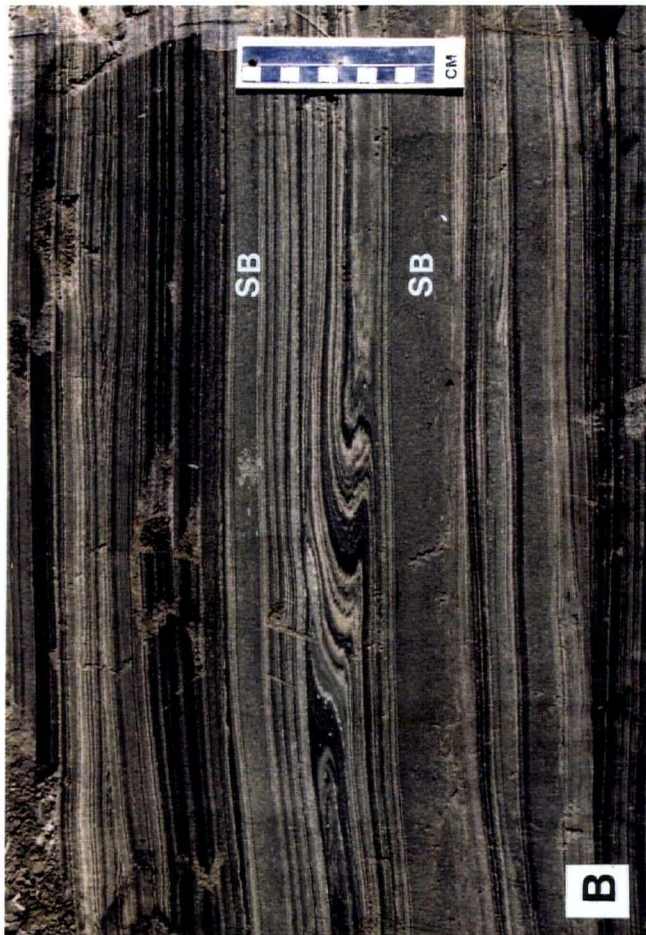
laminated diatomaceous sediments from the anoxic Saanich Inlet, British Columbia (ODP Sites 1033 and 1034; A. Chang, personal observation, 1997). Like speckled beds, brecciated laminae consist of discoid blebs and lozenges, have a flat or erosive base and are of comparable thickness. However, unlike speckled beds, there is a higher silt content, the presence of benthic forams, and normal grading of blebs and lozenges. Most brecciated laminae form the base of massive silty clay layers which are commonly capped with a distinctly thick diatomaceous lamina (Blais 1995). The formation of the massive silty clay and brecciated laminae has been attributed to seismic activity, sediment loading on the sides of the inlet, and sediment influx from ephemeral streams (Blais 1995). Since brecciated laminae commonly form the base of thicker massive units, they are interpreted to represent shear zones at the bases of debris flows (Blais 1995; Blais-Stevens et al., in press). The presence of forams and high silt content of brecciated laminae indicate provenance from *above* an oxygen minimum zone instead of within it (Blais 1995).

3.8 Conclusions

Compositional and deformational features in laminated diatomites from the Monterey Formation at Celite quarry indicate that deposition occurred in a tectonically active slope setting in a region of vigorous coastal upwelling. Complementary slump folds, intrastratal microfractured zones, coarse slumped laminae and speckled beds indicate that slope destabilization and sediment failure was a common occurrence. High organic matter content, high pore water content and low wet bulk density likely contributed to the high sensitivity of laminated diatomaceous sediments, leaving them prone to soft-sediment failure.

Three distinct types of non-laminated intervals are recognized: massive beds, bioturbated beds with *Thalassinoides* burrows and speckled beds. Speckled beds consist of uniformly distributed detritus-rich and diatom-rich aggregates produced from the disintegration of previously existing laminated sediments. Many diatomaceous blebs and lozenges contain very well-preserved monospecific diatom assemblages suggesting that these aggregates are the eroded remnants of bloom-dominated thick

diatomaceous laminae. Owing to the probable presence of gels and the ability for diatom frustules to interlock, diatomaceous laminae are apparently more cohesive than detritus-rich laminae resulting in anomalously large diatomaceous lozenges when large detrital blebs are rarely observed. The preservation of blebs and laminated fragments within speckled beds are evidence that ordinary laminated sediments are cohesive; thus, "firmground" fabrics and ichnofabrics may develop in the absence of a hiatus (cf. Ozalas et al. 1994).

The occurrence and deformation of laminated sediments are prerequisites for speckled bed formation; consequently, the presence of speckled bed fabrics within hemipelagites can be utilized to improve paleogeography of coastal upwelling-influenced deposits. The sedimentary fabric of speckled beds demands provenance of clasts from within an oxygen minimum zone in which slope destabilization and the generation of the gravity flow must occur within the oxygen minimum zone. Slope failure occurring above the oxygen minimum zone would entrain silt and benthic foram species as was observed in the Saanich Inlet brecciated laminae (ODP Sites 1033 and 1034). The occurrence of speckled bed fabrics within non-laminated hemipelagic sequences would indicate that a previously unrecognized oxygen minimum zone was situated upslope (Fig. 3.11).

The content of speckled beds, their sharp upper and lower contacts with adjacent laminae, uniform fabric, and parallel alignment of aggregates and laminated intraclasts suggests that deposition was via high-density turbidity currents which froze in place when flow energy waned. Speckled beds are part of a continuum of synsedimentary deformation and slope failure features in tectonically active borderland basin sediments (Thornton 1984). Some, and perhaps many, speckled beds and related features may record seismically triggered failure events that complement the interpretation of slumping and slope-failure events in modern laminated diatomaceous sediments at Saanich Inlet, British Columbia.

CHAPTER 4

CONCLUDING REMARKS

4.1   Summary

Diatomaceous sediments from the Miocene Monterey Formation in the Celite diatomite quarry, Lompoc, California, contain both finely laminated diatomites and non-laminated intervals that include speckled beds. Field studies, hand sample descriptions, and ecological assemblages determined by high-magnification microscope analyses reveal that the diatomites at Celite quarry were deposited on unstable low-gradient slopes within an oxygen minimum zone beneath a region of vigorous and seasonally variant coastal upwelling.

The major findings and conclusions of Chapter 2 are listed on page 45. Laminated intervals consist of fine, millimetre-scale couplets of alternating dark detrital-rich laminae, and light diatomaceous laminae. Sedimentary couplets and individual laminae record biologically mediated sedimentary processes, paleoecology and paleoenvironmental clues at subannual time scales. Detrital rich laminae contain detrital silt grains and clay, along with heavily silicified microfossils such as resting spores, benthic diatoms, and silicoflagellates. We interpret that detritus and benthic diatom species were washed off the shelf by increased duration and intensity of rainfall and coastal runoff during the fall and winter seasons. Thin biosiliceous laminae consist of a diverse ecological assemblage resulting from background primary productivity during the winter and early spring. Thick continuous diatomaceous laminae and thick discontinuous diatomaceous laminae contain pristine monospecific and near-monospecific assemblages attributable to diatom blooms and efficient export by self-sedimentation during the spring and summer upwelling seasons. Blooms and self-sedimentation permit delivery of unaltered frustules and unrecycled carbon and opal directly to the sediments. Finely hashed and concentrated frustules in macerated biosilica laminae are interpreted to result from intense dissolution and/or zooplankton grazing.

The major conclusions of Chapter 3 are outlined on page 82. High organic carbon content, high

84

porosity, and high tensile strength of diatomaceous laminae due to interlocking diatom frustules and the presence of early diagenetic gels, directly influence the physical properties of laminated diatomaceous sediments. The increased organic content influences the development of low wet bulk density, high water content, high liquid and plastic limits and high natural shear strength. These factors combine to give organic-rich hemipelagic sediments high sensitivity ratios which cause the sediments to fail abruptly upon disturbance (Grimm and Orange 1997).

The abundance of deformation structures in Celite quarry indicate that syndepositional slope instability and sediment failure were prevalent during the Miocene. Speckled beds represent end-products in a slope destabilization spectrum. Speckled beds are sharply based and abruptly overlain by undisturbed laminated diatomite. The speckled texture is produced from bedding-parallel alignment of diatom-rich aggregates, detrital-rich aggregates and pebble-sized laminated intraclasts set in a matrix of fine mud and macerated biosilica. Four main speckled bed types were classified. Unimodal speckled beds contain well-sorted diatom and detritus-rich aggregates. Bimodal speckled beds contain a unimodal speckled bed matrix and conspicuous diatomaceous lozenges. Amalgamated speckled beds consist of alternations between different speckled bed fabrics. Speckled beds with pebble-sized laminated intraclasts contain unimodal or bimodal matrices. We interpret that speckled beds were produced from the disruption of laminated sediments by slumping and gliding within the oxygen minimum zone, and laminae disaggregation during viscous transport. A gravity flow hypothesis was devised to interpret the origins and environment of speckled bed formation. Bedding-parallel alignment of aggregates and the lack of grading or sorting suggest that speckled beds were deposited by high-density turbidity currents. The presence of diatomaceous lozenges with pristine diatom assemblages suggests that they were derived from the disruption of bloom laminae from diatom-rich laminated intervals. Speckled beds in this study were always observed within laminated sediments, and contain clasts—specifically speckles, blebs, lozenges and larger intraclasts—that were clearly derived from a laminated precursor within the oxygen minimum zone.

4.2   Future Work

Lamination-scale assessment of composition and diatom ecology provides insights into subannual and subseasonal depositional processes in the Miocene Monterey Formation and provide paleoenvironmental indices that can be applied in other upwelling-influenced hemipelagites. The next step in lamination-scale research of Monterey Formation diatomites is to perform complementary geochemical analyses. Presently, we are unable to acquire accurate geochemical results from the dark-colored samples we collected in the quarry since they apparently have undergone weathering (K. Johnson, unpublished data, 1997). Cores of unweathered diatomite are required. Integration of lamination-scale geochemical analyses with paleoecological associations and sedimentary processes, and the development of a detailed time series will yield a more complete high-resolution paleoenvironmental record for the California Borderland region during the Miocene.

Analyses regarding several aspects of speckled bed fabrics, composition and formation warrants further investigation. For instance, more in-depth studies on the physical properties of organic-rich laminated diatomites are necessary to gain a better understanding of their effects on sediment failure. Also, physical and/or numerical modeling can be used to test the gravity flow hypothesis, to understand the mechanics of speckled bed deposition via high-density turbidity currents. Furthermore, we require a larger sampling set by examining laminated sediments from ODP cores from active upwelling regions such as the Peru margin (Leg 112) and Benguela Current off southwest Africa (Leg 175) for evidence of speckled beds within and below the oxygen minimum zone. Speckled bed-type fabrics have already been observed in non-laminated intervals from diatomaceous Holocene laminites from Saanich Inlet, British Columbia (ODP Sites 1033 and 1034) where these non-laminated intervals have been attributed to coseismic mass wasting processes. Speckled beds may be used to refine paleogeography of oxygen minimum zones, and to interpret recurrence intervals of slope failure events and perhaps seismic activity in the Miocene Monterey Formation and other hemipelagic deposits.

REFERENCES

Algeo, T. J., Phillips, M., Jaminski, J. and Fenwick, M. 1994. High-resolution x-radiography of laminated sediment cores. *Journal of Sedimentary Research*, A64(3): 665-703.

Alldredge, A. L. and Gottschalk, C. C. 1989. Direct observations of the mass flocculation of diatom blooms: characteristics, settling velocities and formation of diatom aggregates. *Deep-Sea Research*, 36: 159-171.

Anderson, R. Y. 1986. The varve microcosm: propagator of cyclic bedding. *Paleoceanography*, 1(4): 373-382.

Anderson, R. Y., Hemphill-Haley, E. and Gardner, J. V. 1987. Persistent Late Pleistocene-Holocene seasonal upwelling and varves off the coast of California. *Quaternary Research*, 28: 307-313.

Archer, D., Lyle, M. Rodgers, K. and Froelich, P. 1993. What controls opal preservation in tropical deep-sea sediments? *Paleoceanography*, 8(1): 7-21.

Barber, T. B. and Chavez, F. P. 1983. Biological consequences of El Niño. *Science*, 228: 1203-1210.

Barron, J. A. 1983. Diatoms. In: Lipps, J. H. (ed.), *Fossil Prokaryotes and Protists*. Blackwell Scientific Publications, Boston. pp. 155-167.

Barron, J. A. and Keller, G. 1983. Paleotemperature oscillations in the middle and late Miocene of the northeastern Pacific. *Micropaleontology*, 29(2): 150-181.

Barron, J. A. and Baldauf, J. G. 1989. Tertiary cooling steps and paleoproductivity as reflected by diatoms and biosiliceous sediments. In: Berger, W. H., Smetacek, V. S. and Wefer, G. (eds.), *Productivity of the Oceans: Present and Past*. John Wiley & Sons Limited. pp. 341-354.

Barron, J. A. and Isaacs, C. M. In press. Updated chronostratigraphic framework for the California Miocene. In: Isaacs, C. M. and Rullkvtter, J. (eds.), *The Monterey Formation in the Santa Maria and Ventura Basins, California—An Integrated Paleoenvironmental and Petroleum Geochemical Assessment*. Columbia University Press.

Baumgartner, T., Ferreira-Bartrina, V., Schrader, H. and Soutar, A. 1985. A 20-year varve record of siliceous phytoplankton variability in the central Gulf of California. *Marine Geology*, 64: 113-129.

Behl, R. J. 1995. Sedimentary fabrics and sedimentology of the late Quaternary Santa Barbara Basin, Site 893. *Proceedings of the Ocean Drilling Program, Scientific Results*, 146: 295-308.

Behl, R. J. and Hughen, K. A. 1997. Ultra-high-resolution stratigraphic methods for paleoclimate and paleoceanography studies. *American Association of Petroleum Geologists Bulletin*, 81(4): 679.

Blais, A. 1995. Foraminiferal biofacies and Holocene sediments from Saanich Inlet, B. C.: implications for environmental and neotectonic research. Unpublished Ph. D. dissertation, Carleton University, Ottawa. 275 pp.

Blais-Stevens, A., Clague, J. J., Bobrowsky, P. T. and Patterson, R. T. In press. Late Holocene sedimentation in Saanich Inlet, British Columbia and its paleoseismic implications. *Canadian Journal of Earth Sciences*.

Blake, G. H. 1981. Biostratigraphic relationship of Neogene benthic foraminifera from the California outer continental borderland to the Monterey Formation. In: Garrison, R. E., Douglas, R. G., Pisciotto, K. A., Isaacs, C. M. and Ingle, J. C. (eds.), *The Monterey Formation and Related Siliceous Rocks of California*. Society of Economic Paleontologists and Mineralogists, Pacific Section, Special Publication No. 15: 1-14.

Bodén, P. & Backman, J. 1996. A laminated sediment sequence from the northern North Atlantic Ocean and its climate record. *Geology*, 24: 507-510.

Brodie, I. and Kemp, A. E. S. 1994. Variation in biogenic and detrital fluxes and formation of laminae in late Quaternary sediments from the Peruvian coastal upwelling zone. *Marine Geology*, 116: 385-398.

Brodie, I. and Kemp, A. E. S. 1995. Pelletal structures in Peruvian upwelling sediments. *Journal of the Geological Society, London*, 152: 141-150.

Bull, D. and Kemp, A. E. S. 1995. Composition and origins of laminae in Late Quaternary and Holocene sediments from the Santa Barbara Basin. *Proceedings of the Ocean Drilling Program, Scientific Results*, 146(Pt. 2): 77-87.

Busch, W. H. and Keller, G. H. 1981. The physical properties of Peru-Chile continental margin sediments—the influence of coastal upwelling on sediment properties. *Journal of Sedimentary Petrology*, 51: 705-719.

Chang, A. S. 1995. Investigation of laminated Miocene diatomites—exploring a high-resolution climate record. Unpublished Bachelor's thesis, University of British Columbia, 63 pp.

Chang, A. S., Johnson, K. M. and Grimm K. A. 1997. Speckled beds in diatomites of the Miocene Monterey Formation, California, USA: distinctive gravity flow deposits in finely-laminated diatomaceous sediments. *American Association of Petroleum Geologists Bulletin*, 81(4): 681.

Cleve-Euler, A. 1968. Die Diatomeen von Schweden und Finnland. In: Cramer, J. (ed.), *Bibliotheca Phycologica*. Wheldon & Wesley, Ltd. New York, NY, vol. 2(1), 163 pp.

Collins, A. D. 1996. Hi-resolution paleoclimatic reconstruction from annually-laminated sediments, Saanich Inlet, B. C. Unpublished M. Sc. thesis, University of Victoria, Victoria, British Columbia, Canada, 233 pp.

Föllmi, K. B. and Grimm, K. A. 1990. Doomed pioneers: gravity-flow deposition and bioturbation in marine oxygen-deficient environments. *Geology*, 18: 1069-1072.

Gardner, J. V. & Hemphill-Haley, E. 1986. Evidence for a stronger oxygen-minimum zone off central California during the late Pleistocene to early Holocene. *Geology*, 14: 691-694.

Garrison, R. E., Douglas, R. G., Pisciotto, K. E., Isaacs, C. M. and Ingle, J. C. (eds.) 1981. *The Monterey Formation and Related Siliceous Rocks of California*. Society of Economic Paleontologists and Mineralogists, Pacific Section, Special Publication No. 15, 327 pp.

Gorsline, D. S. 1984. A review of fine-grained sediment origins, characteristics and transport. In: Stow, D. A. V. and Piper, D. J. W. (eds.), *Fine-grained Sediments: Deep-water Processes and Facies*. Blackwell Scientific Publications, p. 17-34.

Gorsline, D. S., Kolpack, R. L, Karl, H. A., Drake, D. E., Fleischer, P., Thornton, S. E., Schwalbach, J. R. and Savrda, C. E. 1984. Studies of fine-grained sediment transport processes and products in the California Continental Borderland. In: Stow, D. A. V. and Piper, D. J. W. (eds.), *Fine-grained Sediments: Deep-water Processes and Facies*. Blackwell Scientific Publications, p. 395-415.

Govean, F. M. and Garrison, R. E. 1981. Significance of laminated and massive diatomites in the upper part of the Monterey Formation, California. In: Garrison, R. E., Douglas, R. G., Pisciotto, K.E., Isaacs, C. M. and Ingle, J. C. (eds.), *The Monterey Formation and Related Siliceous Rocks of California*. Society of Economic Paleontologists and Mineralogists, Pacific Section, Special Publication No. 15: 181-198.

Grimm, K. A. 1992a. High-resolution imaging of laminated biosiliceous sediments and their paleoceanographic significance (Quaternary, Site 798, Oki Ridge, Japan Sea). *Proceedings of the Ocean Drilling Program, Scientific Results*, 127/128, Pt. 1: 547-557.

Grimm, K. A. 1992b. Preparation of weakly-consolidated hemipelagic sediment for high-resolution electron microanalysis: and analytical method. *Proceedings of the Ocean Drilling Program*, 128: 57-62.

Grimm, K. A. and Föllmi, K. B. 1994. Doomed pioneers: allochthonous crustacean tracemakers in anaerobic basinal strata, Oligo-Miocene San Gregario Formation, Baja California Sur, Mexico. *Palaios*, 9: 313-334.

Grimm, K. A. Lange, C. B. & Gill, A. S. 1996. Biological forcing of hemipelagic sedimentary laminae: evidence from ODP Site 893, Santa Barbara Basin, California. *Journal of Sedimentary Research*, 66: 613-624.

Grimm, K. A. and Orange, D. L. 1997. Synsedimentary fracturing, fluid migration, and subaqueous mass wasting: intrastratal microfractured zones in laminated diatomaceous sediments, Miocene Monterey Formation, California, USA. *Journal of Sedimentary Research*, 67(3): 601-613.

Grimm, K. A. Lange, C. B. & Gill. A. S. 1997. Self-sedimentation of fossil phytoplankton blooms in the geologic record. *Sedimentary Geology*, 110: 151-161.

Hagadorn, J. W., Stott, L. D., Sinha, A. and Rincon, M. 1995. Geochemical and sedimentologic variations in inter-annually

laminated sediments from Santa Monica Basin. *Marine Geology*, 125: 111-131.

Hargraves, P. E. and French, F. W. 1983. Diatom resting spores: significance and strategies. In: Fryxell, G. A. (ed.), *Survival Strategies of the Algae* . Cambridge University Press, New York, pp. 49-68.

Hill, P. R. and Marsters, J. C. 1990. Controls on physical properties of Peru continental margin sediments and their relationship to deformational styles. *Proceedings of the Ocean Drilling Program, Scientific Results*, 112: 623-632.

Honjo, S. 1982. Seasonality and interaction of biogenic and lithogenic particulate flux at the Panama Basin. *Science*, 218: 883-884.

Hülsemann, J. and Emery, K. O. 1961. Stratification in recent sediments of Santa Barbara Basin as controlled by organisms and water character. *Journal of Geology*, 69: 279-290.

Ingle, J. C., Jr. 1981. Origin of Neogene Diatomites around the North Pacific Rim. In: Garrison, R. E., Douglas, R. G., Pisciotto, K.E., Isaacs, C. M. and Ingle, J. C. (eds.), *The Monterey Formation and Related Siliceous Rocks of California*, Society of Economic Paleontologists and Mineralogists, Pacific Section Special Publication No. 15: 159-179.

Isaacs, C. M. and Garrison, R. E. (eds.) 1983. *Petroleum Generation and Occurrence in the Miocene Monterey Formation, California*. Society of Economic Paleontologists and Mineralogists, Pacific Section. 228 pp.

Isaacs, C. M. and Petersen, N. F. 1987. Petroleum in the Miocene Monterey Formation, California. In: Hein, J. R. (ed.), *Siliceous Sedimentary Rock-Hosted Ores and Petroleum*. Van Nostrand Reinhold Company, New York. pp. 83-116.

Isaacs, C. M., Baumgartner, T. R., Tennyson, M. E., Piper, D. Z. and Ingle, J. C., Jr. 1996. A prograding margin model for the Monterey Formation, California. *AAPG-SEPM Annual Meeting Abstracts* —American Association of Petroleum Geologists-Society foe Economic Paleontologists and Mineralogists, 5: 69.

Johnson, K. M., Chang, A. S. and Grimm, K. A. 1997. Lamination-scale, multi-tracer geochemistry of organic-rich diatomites of the Monterey Formation: implications for organic carbon richness and speciation. *American Association of Petroleum Geologists Bulletin*, 81(4): 688.

Keller, G. H. 1983. Coastal upwelling: its influence on the geotechnical, properties and stability characteristics of submarine deposits. In: Thiede, J. and Suess, E. (eds.), *Coastal Upwelling: Its Sediment Record, Part A*. Plenum Press, New York, p. 181-199.

Kemp, A. E. S. 1995. Laminated sediments from coastal and open ocean upwelling zones: what variability do they record? In: Summerhayes, C. P., Emeis, K. C., Angel, M. V., Smith, R. L. and Zeitzschel, B. (eds.), *Upwelling in the Ocean: Modern Processes and Ancient Records*. John Wiley and Sons, Ltd. pp. 239-257.

Kemp, A. E. S. and Baldauf, J. G. 1993. Vast Neogene laminated diatom mat deposits from the eastern equatorial Pacific

Ocean. *Nature*, 362: 141-143.

Kemp, A. E. S, Baldauf, J. G. and Pearce, R. B. 1995. Origins and paleoceanographic significance of laminated diatom ooze from the Eastern Equatorial Pacific Ocean. *Proceedings of the Ocean Drilling Program, Scientific Results*, 138: 641-645.

Kennett, J. P., Baldauf, J. G. et al.. 1994. *Proceedings of ODP Site 893 Initial Results*, 146 (Part 2): 15-50.

Lange, C. B., Berger, W. H., Burke, S. K., Casey, R. E., Schimmelmann, A., Soutar, A. and Weinheimer, A. L. 1987. El Niño in Santa Barbara Basin: diatom, radiolarian and foraminiferan responses to the "1983 El Niño" event. *Marine Geology*, 78: 153-160.

Lange, C. B., Burke, S. K. and Berger, W. H. 1990. Biological production off Southern California is linked to climate change. *Climate Change*, 16: 319-329.

Lee, H. J, Kayen, R. E., and McArthur, W. G. 1990. Consolidation, triaxial shear-strength, and index-property characteristics of organic-rich sediment from the Peru continental margin: results from Leg 112. *Proceedings of the Ocean Drilling Program, Scientific Results*, 112: 639-651.

Lowe, D. R. 1975. Water escape structures in coarse-grained sediments. *Sedimentology*, 22: 157-204.

Lowe, D. R. 1982. Sediment gravity flows: II. Depositional models with special reference to the deposits of high-density turbidity currents. *Journal of Sedimentary Petrology*, 52(1): 279-297.

McCave, I. N. and Jones, K. P. N. 1988. Deposition of ungraded muds from high-density non-turbulent turbidity currents. *Nature*, 333: 250-252.

Middleton, G. V. and Hampton, M. A. 1976. Subaqueous sediment transport and deposition by sediment gravity flows. In: Stanley, D. J and Swift, D. J. P. (eds.), *Marine Sediment Transport and Environmental Management*. John Wiley & Sons, Inc. New York, p. 197-218.

Mullins, H. T., Thompson, J. B., McDougall, K. and Vercoutere, T. L. 1985. Oxygen minimum zone edge effects: evidence from the central California coastal upwelling system. *Geology*, 13: 491, 494.

Munsell Color Company, 1971. *Munsell® Soil Color Chart*, Munsell Color Company, Inc. Baltimore, Maryland, USA.

Ozalas, K. 1993. Character and paleoenvironmental implications of bioturbated event beds in the siliceous facies of the Monterey Formation (Miocene), Lompoc area, central California. Unpublished M. Sc. thesis, Auburn University, Auburn, AL. 173 pp.

Ozalas, K. Savrda, C. E. and Fullerton, R. R. 1994. Bioturbated oxygenation-event beds in siliceous facies: Monterey

Formation (Miocene), California. *Palaeogeography, Palaeoclimatology, Palaeoecology*, 112: 63-83.

Pallesen, T. R. 1983. *Turbidity currents*. Institute of Hydrodynamics and Hydraulic Engineering, Technical University of Denmark, Series Paper No. 2. 115 pp.

Pearce, R. B., Kemp, A. E. S., Baldauf, J. G. and King, S. C. 1995. High-resolution sedimentology and micropaleontology of laminated diatomaceous sediments from the Eastern Equatorial Pacific Ocean. *Proceedings of the Ocean Drilling Program, Scientific Results*, 138: 647-663.

Pike, J. & Kemp, A. E. S. 1996a. Records of seasonal flux in Holocene laminated sediments, Gulf of California. In: Kemp, A. E. S. (ed.), *Palaeoclimatology and Palaeoceanography from Laminated Sediments*, Geological Society Special Publication No. 116: 157-169.

Pike, J. and Kemp, A. E. S. 1996b. Silt aggregates in laminated marine sediment produced by agglutinated foraminifera. *Journal of Sedimentary Research*, 66: 625-631.

Pike, J. & Kemp, A. E. S. 1997. Early Holocene decadal-scale ocean variability recorded in Gulf of California laminated sediments. *Paleoceanography*, 12: 227-238.

Pisciotto, K. A. and Garrison, R. E. 1981. Lithofacies and depositional environments of the Monterey Formation, California. In: Garrison, R. E., Douglas, R. G., Pisciotto, K.E., Isaacs, C. M. and Ingle, J. C. (eds.), *The Monterey Formation and Related Siliceous Rocks of California*, Society of Economic Paleontologists and Mineralogists, Pacific Section Special Publication No. 15: 97-122.

Prior, D. B. and Coleman, J. M. 1984. Submarine slope instability. In: Brunsden, D. and Prior, D. B. (eds.), *Slope Instability*. John Wiley & Sons Ltd., New York, p. 419-455.

Reimers, C. E. 1982. Organic matter in anoxic sediments off central Peru: relations of porosity, microbial decomposition and deformation properties. *Marine Geology*, 46: 175-197.

Round, F. E., Crawford, R. M. and Mann, D. G. (eds.). 1990. *The diatoms: biology and morphology of the genera*. Cambridge University Press, Cambridge, 747 pp.

Sancetta, C. 1989. Processes controlling the accumulation of diatoms in sediments: a model derived from British Columbian fjords. *Paleoceanography*, 4: 235-251.

Sancetta, C. and Calvert, S. E. 1988. The annual cycle of sedimentation in Saanich Inlet, British Columbia: implications for the interpretation of diatom fossil assemblages. *Deep-Sea Research*, 35(1): 71-90.

Sancetta, C., Villareal, T. and Falkowski, P. 1991. Massive fluxes of rhizosolenid diatoms: a common occurrence? *Limnology and Oceanography*, 36: 1452-1457.

Sancetta, C., Lyle, M. and Heusser, L. 1992. Late-glacial to Holocene changes in winds, upwelling and seasonal production of the northern California current system. *Quaternary Research*, 38: 359-379.

Sautter, L. R. and Sancetta, C. 1992. Seasonal associations of phytoplankton and planktic foraminifera in an upwelling region and their contribution to the seafloor. *Marine Micropaleontology*, 18: 263-278.

Savrda, C. E. 1995. Ichnologic applications in paleoceanographic, paleoclimatic and sea-level studies, *Palaios*, 10: 565-577.

Savrda, C. E., Bottjer, D. J. and Gorsline, D. S. 1984. Development of a comprehensive oxygen-deficient marine biofacies model: evidence from Santa Monica, San Pedro, and Santa Barbara Basins, California Continental Borderland. *American Association of Petroleum Geologists Bulletin*, 68: 1179-1192.

Savrda, C. E., Bottjer, D. J. and Gorsline, D. S. 1985. An image-enhancing technique for friable diatomaceous rocks. *Journal of Sedimentary Petrology*, 55: 604-605.

Savrda, C. E. and Bottjer, D. J. 1987. The exaerobic zone, a new oxygen-deficient marine biofacies. *Nature*, 327: 54-56.

Savrda, C. E. and Ozalas, K. 1993. Preservation of mixed-layer ichnofabrics in oxygenation-event beds. *Palaios*, 8: 609.613.

Schimmelmann, A. Lange, C. B. and Berger, W. H. 1989. Climatically controlled marker layers in Santa Barbara Basin sediments and fine-scale core-to-core correlation. *Limnology and Oceanography*, 35(1): 165-173.

Schimmelmann, A., Lange, C. B., Berger, W. H., Simon, A., Burke, S. K. and Dunbar, R. B. 1992. Extreme climatic conditions recorded in Santa Barbara Basin laminated sediments: the 1835-1840 *Macoma* event. *Marine Geology*, 106: 279-299.

Schrader, H., Kelts, K., Curray, J., Moore, D., Aguayo, E., Aubry, M., Einsele, G., Fornari, D., Giekes, J., Guerrero, J., Kastner, M., Lyle, M., Matoba, Y, Molina-Cruz, A., Niemitz, J., Rueda, J., Saunders, A., Simoneit, B. and Vaquer, V. 1980. Laminated diatomaceous sediments from the Guaymas Basin slope (central Gulf of California): 250,000-year climate record. *Science*, 207: 1207-1209.

Schwarz, H. U. 1982. Subaqueous slope failures—Experiments and modern occurrences. *In* Füchtbauer, H., Lisitzyn, A. P., Milliman, J. D. and Seibold, E. (eds.), *Contributions to Sedimentology 11*, Stuttgart, Schweizerbart'sche Verlagbuchhandlung, 166 pp.

Smetacek, V. S. 1985. Role of sinking in diatom life history cycles: ecological, evolutionary and geological significance. *Marine Biology*, 84: 239-251.

Soutar, A. and Crill, P. A. 1977. Sedimentation and climatic patterns in the Santa Barbara Basin during the 19th and 20th

centuries. *Geological Society of America Bulletin*, 88: 1161-1172.

Soutar, A., Johnson, S. R. and Baumgartner, T. R. 1981. In search of modern depositional analogs to the Monterey Formation. In: Garrison, R. E., Douglas, R. G., Pisciotto, K.E., Isaacs, C. M. and Ingle, J. C. (eds.), *The Monterey Formation and Related Siliceous Rocks of California*, Society of Economic Paleontologists and Mineralogists, Pacific Section Special Publication No. 15: 123-147.

Stow, D. A. V. and Bowen, D. J. W. 1978. Origin of laminae in deep sea, fine-grained sediments. *Nature*, 274: 324-328.

Stow, D. A. V. and Bowen, A. J. 1980. A physical model for the transport and sorting of fine-grained sediment by turbidity currents. *Sedimentology*, 27: 31-46.

Thornton, S. E. 1984. Basin model for hemipelagic sedimentation in a tectonically active continental margin: Santa Barbara Basin, California Continental Borderland. In: Stow, D. A. V. and Piper, D. J. W. (eds.), *Fine-grained Sediments: Deep-Water Processes and Facies*, Blackwell Scientific Publications, p. 377-394.

Vercoutere, T. L., Mullins, H. T., McDougall, K. and Thompson, J. B. 1987. Sedimentation across the central California oxygen minimum zone: an alternative coastal upwelling sequence. *Journal of Sedimentary Petrology*, 57: 709-722.

Villareal, T. A. and Carpenter, E. J. 1989. Nitrogen fixation, suspension characteristics, and chemical composition of *Rhizosolenia* mats in the central north Pacific gyre. *Biological Oceanography*, 6: 327-345.

Villareal, T. A., Altabet, M. A. and Culver-Rymsza, K. 1993. Nitrogen transport by vertically migrating diatom mats in the North Pacific Ocean. *Nature*, 363: 709-712.

White, L. D. 1989. Chronostratigraphic and paleoceanographic aspects of selected chert intervals in the Miocene Monterey Formation, California. Unpublished Ph. D. dissertation, University of Santa Cruz, California.

White, L. D. and Alexandrovich, J. M. 1992. Pliocene and Pleistocene abundance and preservation of siliceous microfossil assemblages from Sites 794, 795, and 797: implications for circulation and productivity in the Japan Sea. Proceedings of the Ocean Drilling Program, v. 127/128: 341-357.

White, L. D., Garrison, R. E. and Barron, J. A. 1992. Miocene intensification of upwelling along the California margin as recorded in siliceous facies of the Monterey Formation and offshore DSDP sites. In: Summerhayes, C. P, Prell, W. L and Emeis, K. C. (eds.), *Upwelling Systems: Evolution Since the Early Miocene*. Geological Society Special Publication No. 64: 429-442.

Yoder, J. A., Ackleson, S. G., Barber, R. T., Flamnet, P. and Balch, W. M. 1994. A line in the sea. *Nature*, 371: 689-692.

Zeng, J. and Lowe, D. R. 1990. A numerical model of high-density turbidity current sedimentation. *American Association of Petroleum Geologists Bulletin*, 74: 685.

APPENDIX 1

Sample Catalogue
(cf. Figure 2.2)

Abbreviations: LB=low bimodality; MB=moderate bimodality; HB=high bimodality; SB=speckled bed; IMZ=intrastratal microfractured zone

Sample	Position (m)	Thickness (cm)	Sample description
2-2	6.33	35.4	closely-spaced bloom laminae and intrastratal slumping with thin speckled beds (SBs); sample not described in detail
2-3	6.51	29.5	bioturbated bed; mud-dominated, closely spaced LB-MB couplets and isolated laminae disrupted by burrowing; minor SBs undisturbed by burrowing
2-4	8.17	42.0	four distinct 2-mm thick bloom laminae; sample not described in detail (Fig. 2.6C)
2-5	10.57	27.6	mud-dominated to subequal closely spaced HB couplets and bundles; SBs from ≤5 mm to >1 cm thick, some with scoured bases; bloom laminae at 7.5 cm
2-7B	15.06	31.7	mud-dominated to subequal MB-HB closely to widely spaced razor to chalk-striped couplets; abundant thin muddy turbidites, SBs, bloom laminae and bloom lozenges; occasional slumped laminae
2-8	15.49	17.7	thick Chaetoceros setae lamina (5 mm by 15 cm); subequal closely spaced razor to chalk-striped MB couplets, minor muddy turbidites and SBs
2-9	15.77	37.0	mud-dominated to subequal closely spaced razor to pin-striped LB-HB couplets and packets; abundant SBs, bloom laminae lozenges and mats
M-2	19.20	26.7	mud-dominated, closely-spaced, LB-MB couplets; laminae thicknesses range from razor- to pin-stripe; minor SBs and disrupted laminae
M-3	20.40	23.3	subequal to mud-dominated, closely- to moderately-spaced MB-HB couplets; most laminae are razor-to pin-striped; upper 8 cm contains SBs of variable composition
M-6	22.41	28.0	mud-dominated, closely- to widely-spaced, LB-HB couplets; laminae thickness is pin to chalk-striped; some distinct bloom laminae; muddy turbidites ≤5 mm thick
M-7/8	23.47	35.0	mainly mud-dominated with minor diatom-dominated bundles; indistinct pin to chalk-striped LB-MB couplets; several SBs and bloom laminae

M-10/11	26.62	49.6	domination ranges; mud-dominated: razor- to chalk-striped LB-MB laminae with variable spacing, muddy SBs common; subequal: razor to chalk-striped MB-HB couplets with variable spacing; diatom-dominated: closely spaced pin to chalk striped MB-HB couplets, bloom laminae and lozenges common
M-12	27.15	25.0	overall subequal with closely to moderately spaced MB-HB pin-striped couplets; thin SBs except for SB-dominated upper 2 cm of sample; distinct bloom lamina at 17.2 cm; bloom lozenges present
M-13/14	28.57	42.6	bioturbated interval; mostly mud-dominated to subequal; mud-dominated sections are not laminated and contain burrowed horizon; subequal sections are laminated with closely spaced, razor and pin-striped MB couplets; burrowing disrupts and crosscuts laminated sections but SBs are absent
M-16	33.37	33.5	subequal, closely spaced LB-HB couplets with variable thicknesses; muddy SB from 2.4-5.3 cm; prominent bloom lamina at 18.7 cm; S-shaped slump folds at 13.8 and 23 cm
M-18/19	39.00	29.6	subequal to diatom-dominated, closely spaced, razor to pin-striped HB couplets; SBs ≤1 cm; bloom lamina at 2.1 cm and lozenges at 19.5 cm; this sample was waterlogged and its appearance altered from that of other samples
M-21	41.22	21.0	"silver sand" ash horizon and adjacent laminae
M-22	53.40	42.4	bioturbated bed; sample not described in detail
M-26	50.77	77.8	amalgamated bioturbated beds; sample not described in detail
M-29	53.49	63.6	IMZs; sample not described in detail
M-BP	59.14	17.8	mud-dominated to diatom-dominated, distinctive closely spaced, razor and pin-striped LB-HB couplets; very finely laminated; minor thin SBs and disrupted laminae; thin 1 mm black waxy layer at 11 cm

APPENDIX 2

X-radiograph contact prints of slabbed samples
and subsample locations

(see App. 3 for symbols)

APPENDIX 2A. Sample M-3 is subequal to mud-dominated with closely to moderately spaced MB-HB couplets. Most laminae are razor- to pin-striped. The upper portion of this sample contains a diatom-rich SB with laminated intraclasts, and two unimodal SBs.

APPENDIX 2B. Sample M-6 is a muddy sample with numerous low bimodality (LB) to moderate bimodality (MB) couplets. Numbered black arrows indicate locations where images from Figures 2.8A and 2.9A were taken.

APPENDIX 2C. Sample M-BP contains alternating intervals of mud-dominated and diatom-dominated packets. Laminae are distinctively closely-spaced and razor-striped (cf. Fig. 2.4). There are minor SBs. A thin 1-mm black "waxy" lamina of unknown composition occurs at the 11-cm position on the slab.

APPENDIX 2D. Sample 2-8 is a relatively diatom-rich sample with razor to pin-striped laminae. The lower portion of this sample has indistinct pin-striped laminae whereas the upper portion has distinct razor-striped laminae. Black hollow arrows point toward thick discontinuous diatomaceous lamina (cf. Figs. 2.10A and 2.11); asterisks show positions where images from Figures 2.7 and 2.8D were collected.

APPENDIX 2E. Sample 2-9 contains mud-dominated to subequal couplets and numerous macerated biosilica laminae. Couplets are LB to HB and laminae are razor- to chalk-striped. A 4-cm thick bimodal SB at 20.2-23.0 cm contains *Chaetoceros* setae-rich lozenges (cf. Fig. 3.5B).
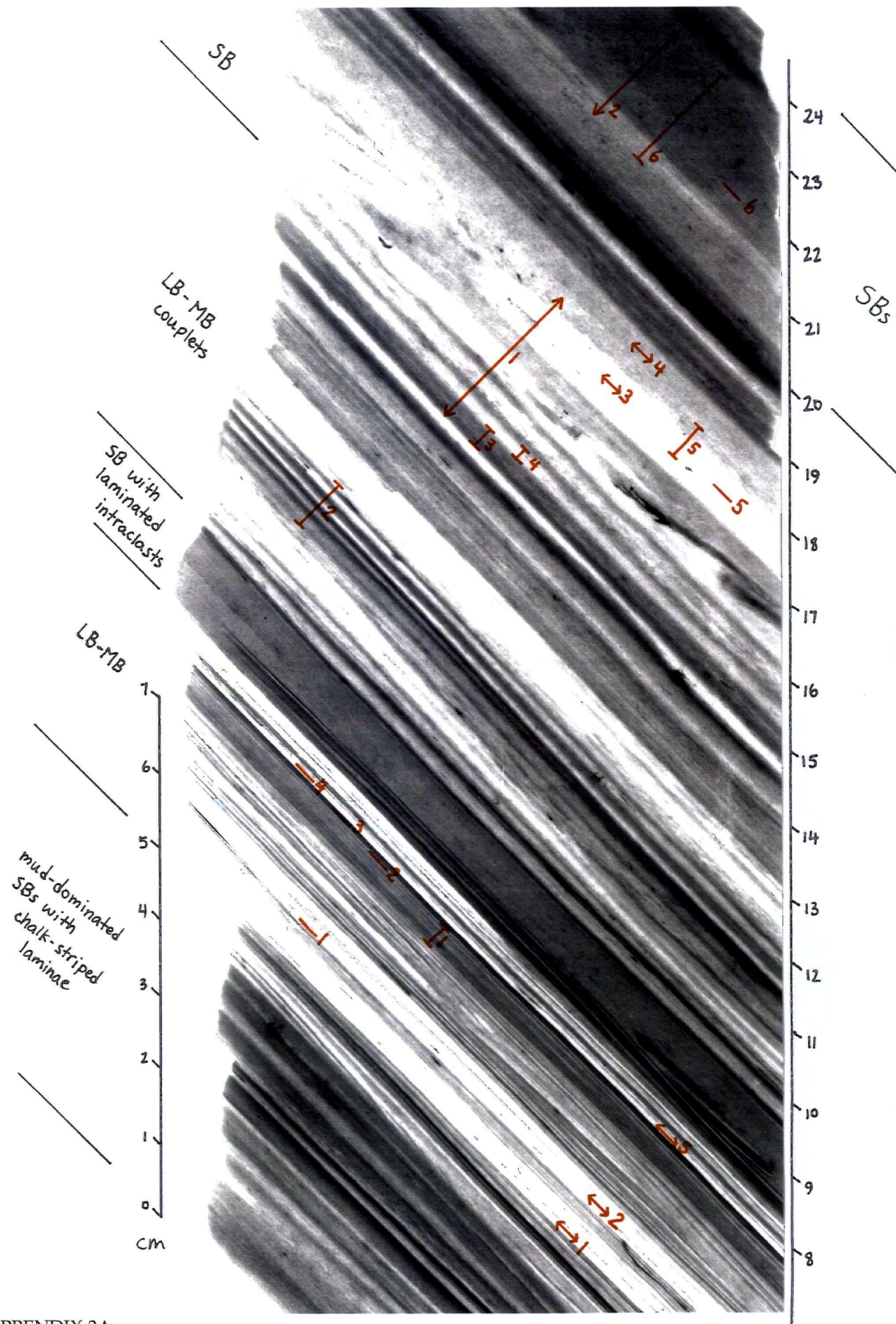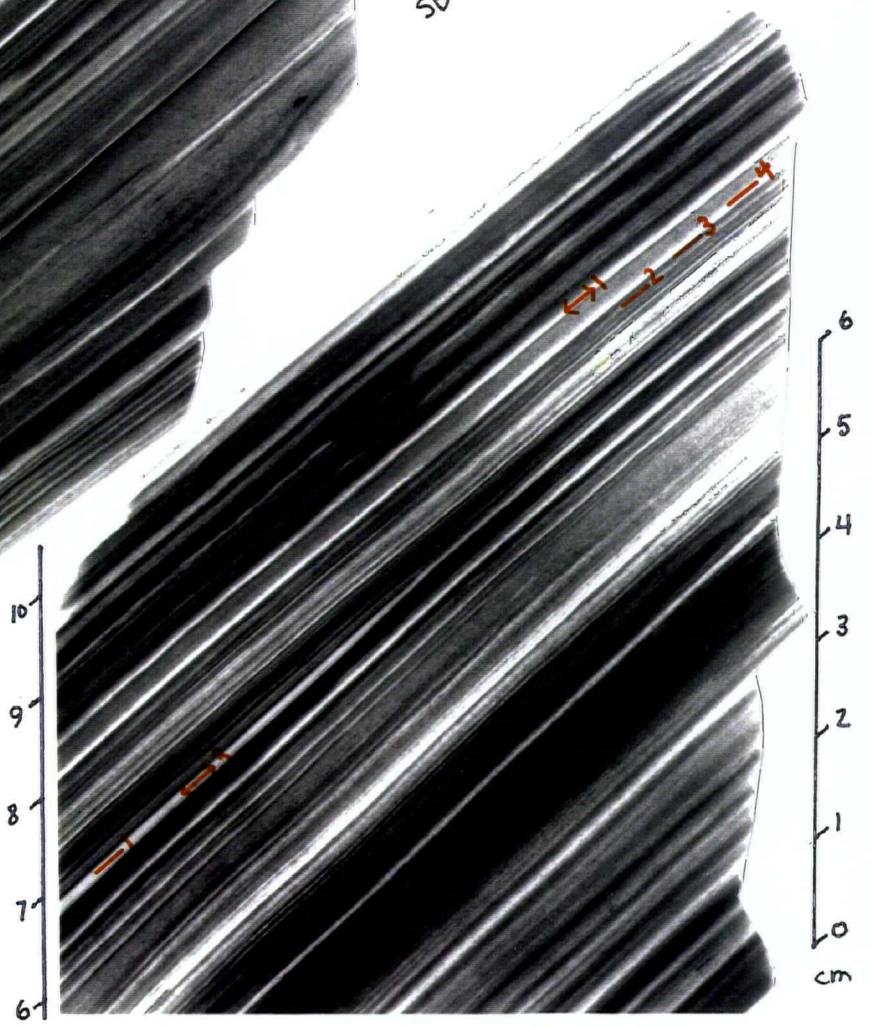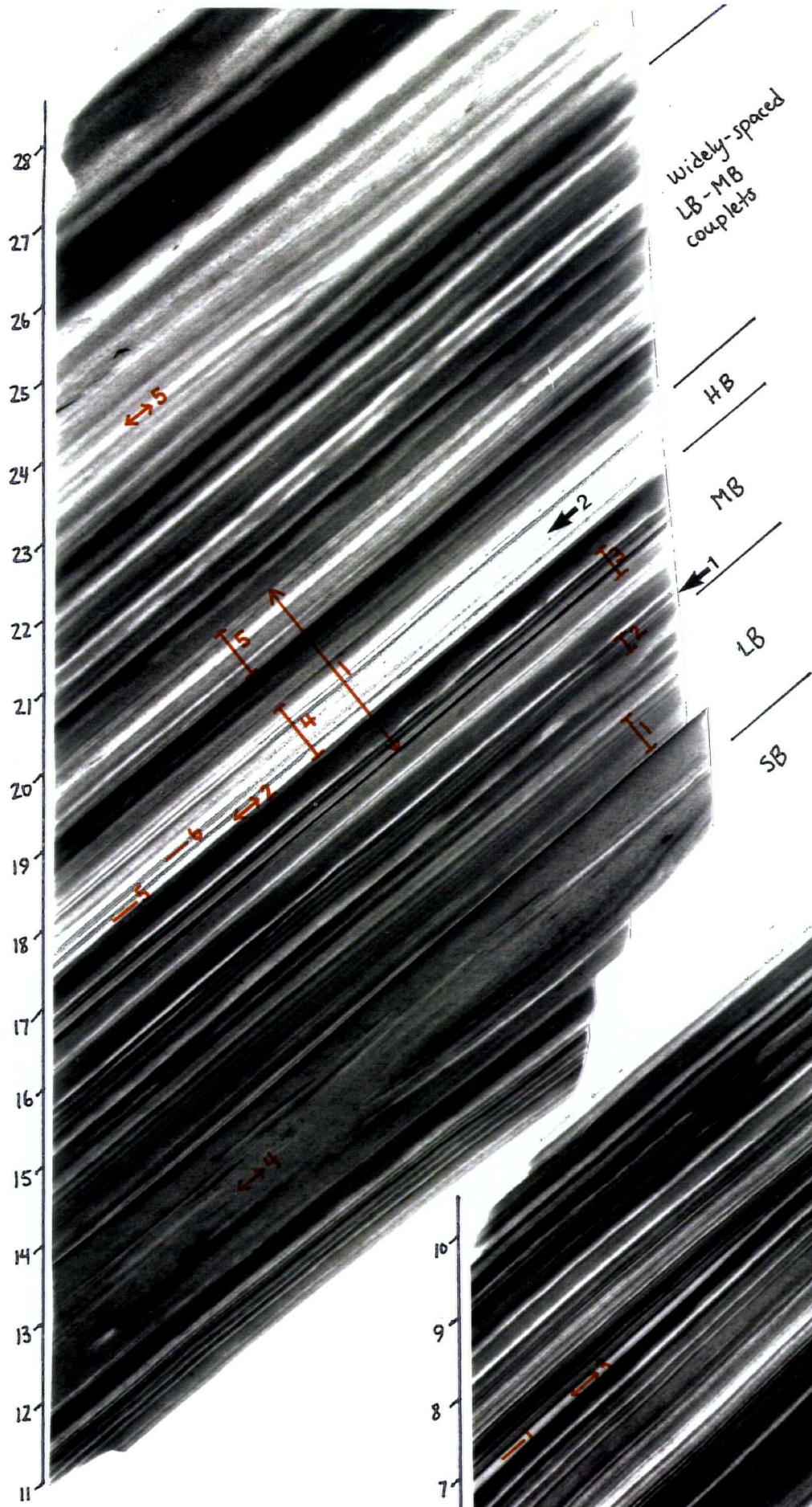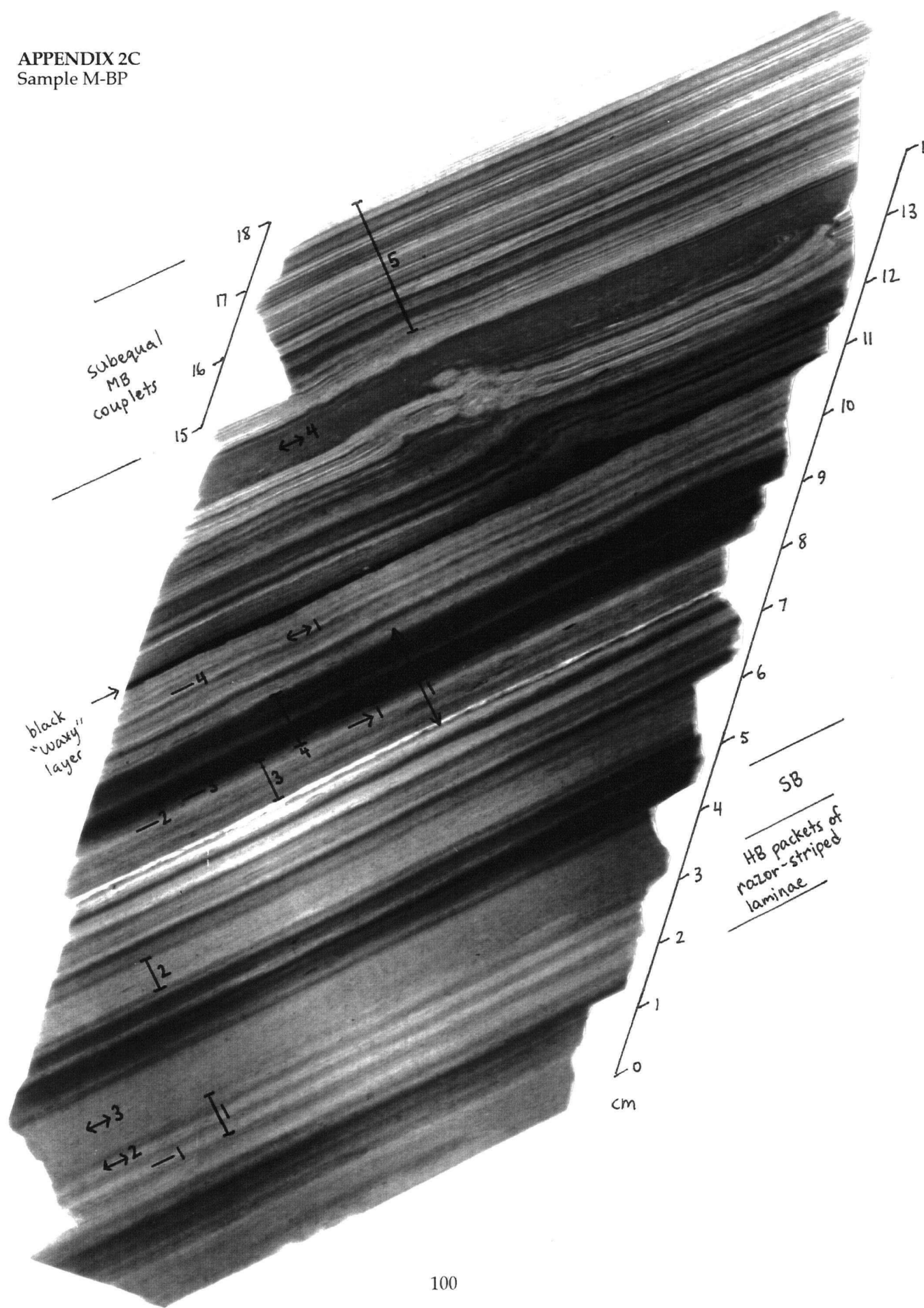
SB

LB - MB
couplets

SB with
laminated
intraclasts

LB-MB

mud-dominated
SBs with
chalk-striped
laminae

SBs

APPENDIX 2A
Sample M-3

Widely-spaced
LB-MB
couplets

HB

MB

LB

SB

APPENDIX 2B
Sample M-6

99

APPENDIX 2C
Sample M-BP

100

APPENDIX 2D
Sample 2-8

razor-striped laminae

macerated biosilica lamina

bimodal SB

thick macerated
biosilica lamina

MB-HB
couplets;
pin- to
chalk-striped
laminae
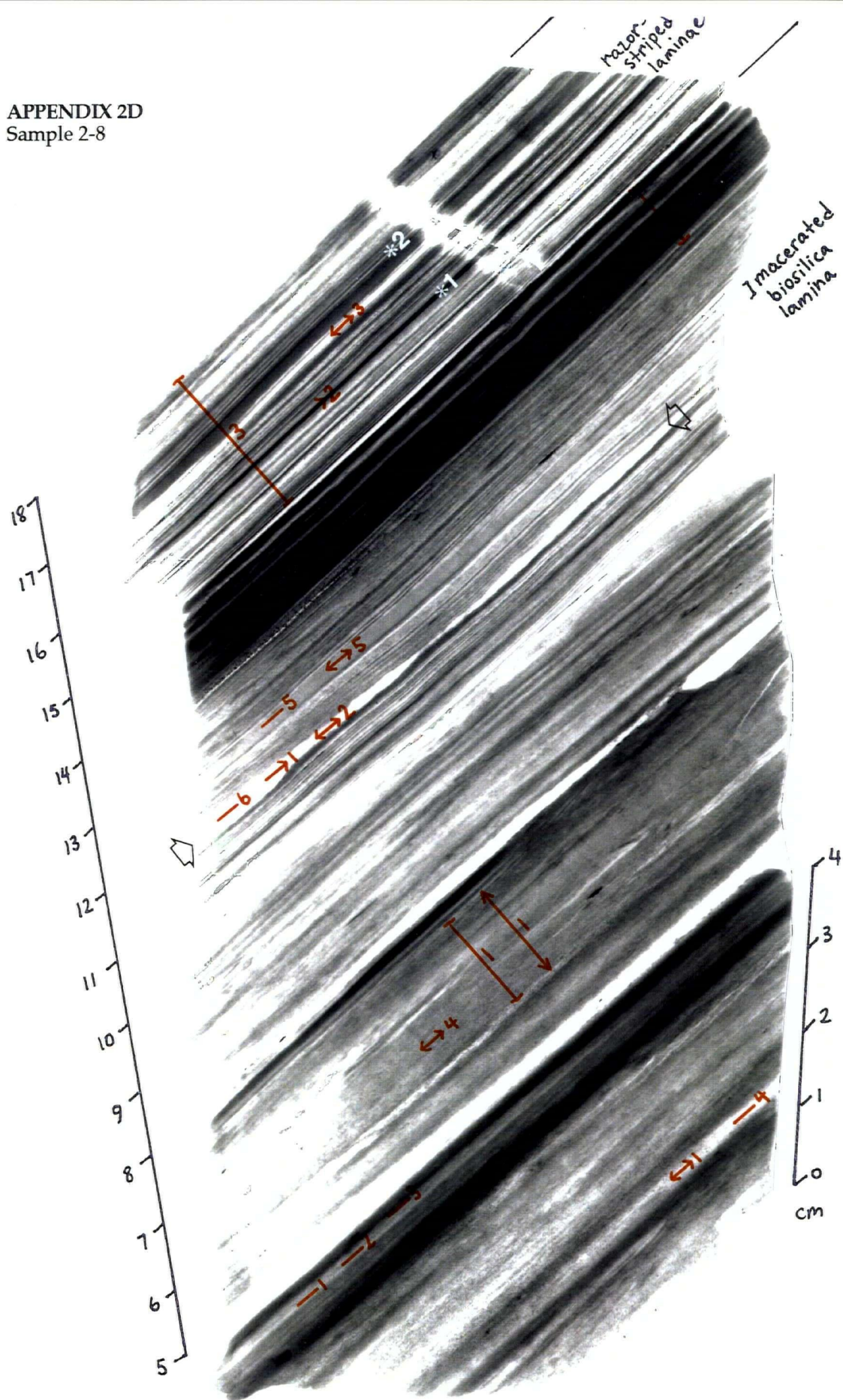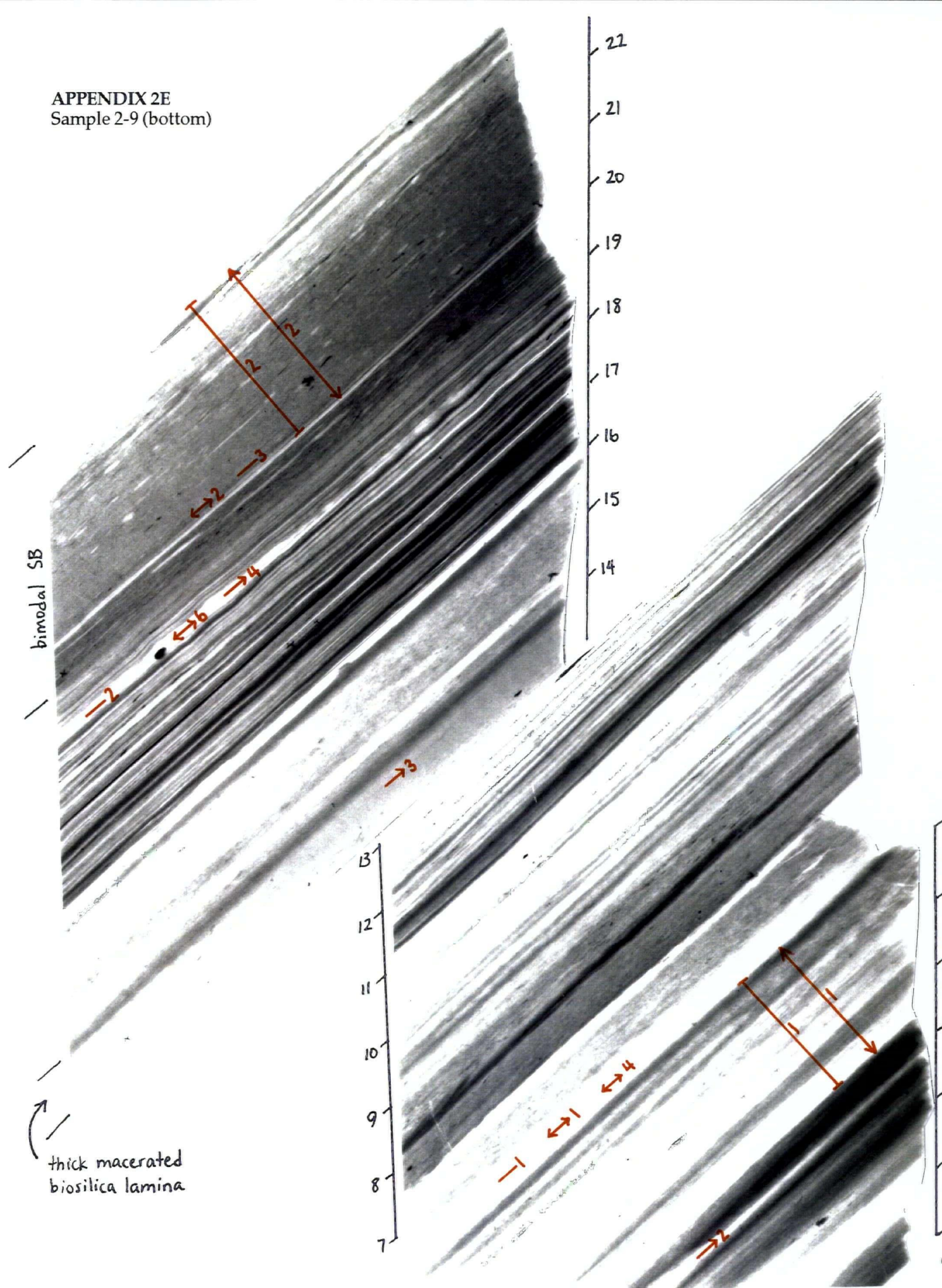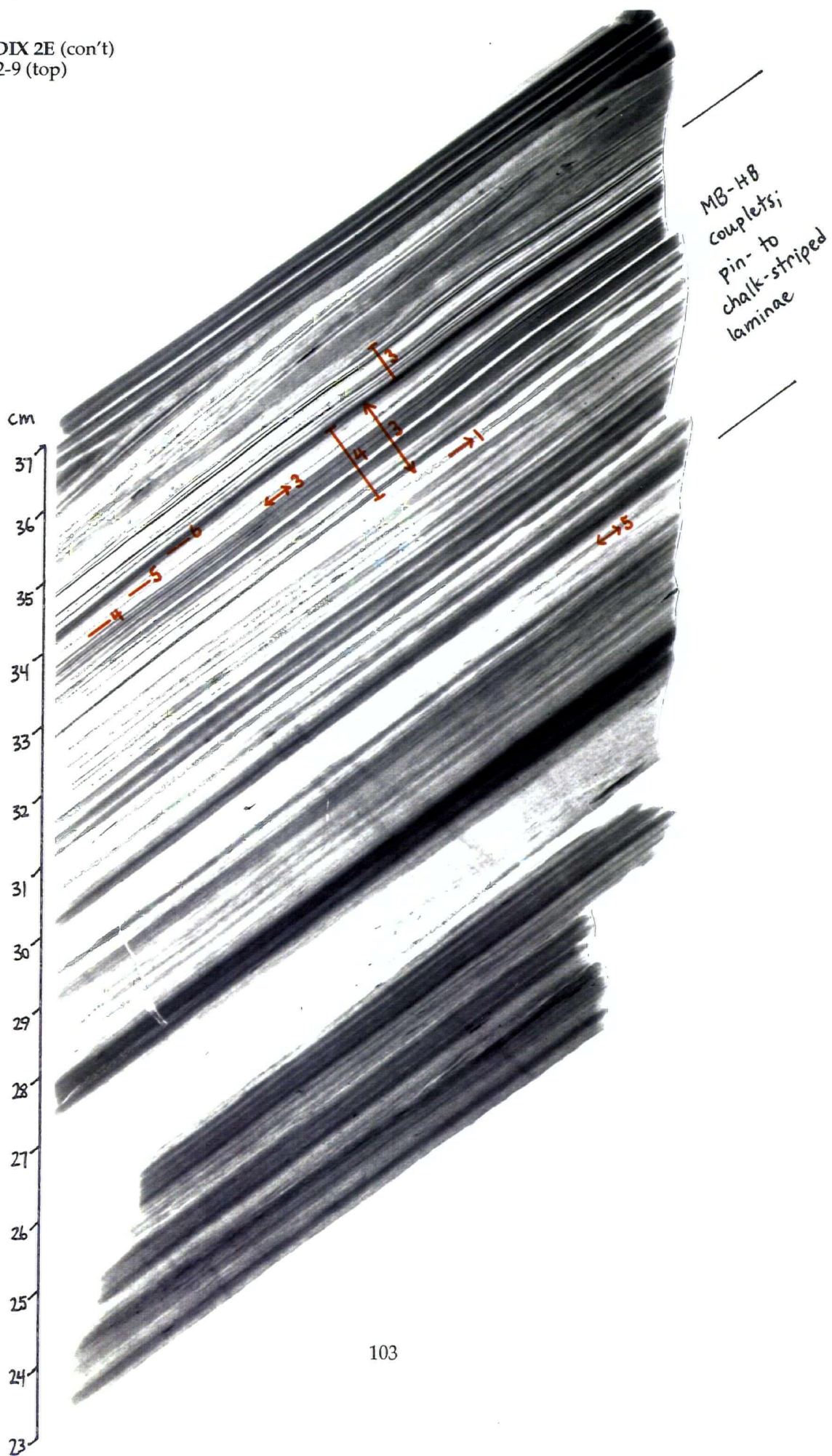
APPENDIX 3A

Smear Slide Catalogue
(symbol: —)

Abbreviations: LB=low bimodality; MB=moderate bimodality; HB=high bimodality; SB=speckled bed

Sample	Position on x-ray (cm)	Comments
M-3		
M-3.1	6.1	macerated biosilica lamina
M-3.2	7.8	MB diatomaceous lamina: high diversity
M-3.3	7.9	detrital lamina of HB couplet: typical winter assemblage
M-3.4	8.0	diatomaceous lamina of HB couplet: various diatoms, abundant silicoflagellates (*Dictyocha*)
M-3.5	17.2-17.9	diatom-rich unimodal SB matrix: abundant silt, high diversity, poor preservation
M-3.6	21.4-24.5	detritus-rich unimodal SB matrix: abundant silt, high diversity
M-6		
M-6.1	7.0	macerated biosilica lamina
M-6.2	7.9	diatomaceous lamina of LB couplet [referred to hereafter as "LB diatomaceous lamina"]: abundant silt, high diversity, abundant silicoflagellates
M-6.3	8.0	LB diatomaceous lamina: similar to M-6.2 but with more silt
M-6.4	8.1	bloom lamina: *Rouxia californica*
M-6.5	17.5	HB diatomaceous lamina: high diversity but *Thalassiosira* and *Chaetoceros* resting spores dominate
M-6.6	17.7	MB diatomaceous lamina: high diversity, silt common
M-BP		
M-BP.1	2.5	MB diatomaceous lamina: high diversity, poor preservation
M-BP.2	8.5	HB biosiliceous lamina: silicoflagellate bloom
M-BP.3	8.6	LB diatomaceous lamina: high diversity, silicoflagellates common
M-BP.4	10.5	background diatomaceous lamina: abundant *Thalassiosira antiqua*
2-8		
2-8.1	4.4	HB diatomaceous lamina: high diversity; *Chaetoceros* setae common
2-8.2	4.5	LB diatomaceous lamina: abundant *Chaetoceros* setae and *Thalassiothrix*; poor preservation
2-8.3	4.6	MB diatomaceous lamina: high diversity
2-8.4	1.5	high diversity diatomaceous lamina
2-8.5	13.2	macerated biosilica lamina
2-8.6	11.5	*Chaetoceros* setae lens
2-9		
2-9.1	6.5	*Rouxia californica* bloom lamina
2-9.2	18.7	bloom lamina: abundant *Chaetoceros* setae
2-9.3	20.3	bloom bleb in bimodal SB: abundant *Chaetoceros* setae; other diatoms minor
2-9.4	33.7	HB diatomaceous lamina: abundant *Thalassiosira, R. californica, Nitzschia*
2-9.5	33.9	MB diatomaceous lamina: high diversity
2-9.6	34.1	LB diatomaceous lamina: high diversity

APPENDIX 3B

Strewn Slide Catalogue
(symbol: ➡)

Abbreviation: SB=speckled bed

Sample	Smear Slide equivalent	Position on slab (cm)	Comments
M-BP			
M-BP.1	M-BP.2	8.5	thin biosiliceous lamina
2-8			
2-8.1	2-8.6	11.5	thick *Chaetoceros* setae lamina
2-8.2	—	15.8	detrital lamina
2-9			
2-9.1	—	32.4	detrital lamina
2-9.2	—	2.7	thin macerated biosilica lamina
2-9.3	—	13.3-14.0	thick macerated biosilica lamina
2-9.4	2-9.2	18.7	irregular bloom lamina

Reconnaissance samples:

Sample	Smear Slide equivalent	Position on slab (cm)	Comments
94-L			
94-L.1	—	3.8	*Denticulopsis* / coccolithophore bloom lamina
94-L.2	—	0.0-3.0	dark, detritus-rich coarse SB
94-M			
94-M.1	—	10.1	2-mm thick *Denticulopsis* bloom lamina
94-M.2	—	4.0-7.0	coarse diatom-rich SB from amalgamated SB fabric; wisps composed of *Denticulopsis*
94-N			
94-N.1	—	0.5	2-mm thick *Denticulopsis* bloom laminae
94-N.2	—	2.0-5.0	coarse diatom-rich SB from amalgamated SB fabric; wisps composed of *Denticulopsis*

APPENDIX 3C

Secondary Electron Microscopy Catalogue
(symbol: ↔)

Abbreviations: SB=speckled bed; HB=high bimodality

Sample	Position on x-ray (cm)	Comments
M-3		
M-3.1	5.2	bloom lamina: large fragmented centrics (*Coscinodiscus* and *Ethmodiscus*)
M-3.2	6.0	macerated biosilica lamina
M-3.3	17.5	diatom-rich SB matrix: high diversity
M-3.4	18.5	SB bleb: high diversity, poor preservation, silicoflagellates common
M-3.5	8.0	background HB diatomaceous lamina: *Thalassiothrix* common
M-6		
M-6.1	8.4	bloom lamina: fragmented *Coscinodiscus*
M-6.2	17.4	bloom lamina: abundant *Coscinodiscus* and *Thalassiothrix*; good preservation
M-6.3	7.0	macerated biosilica lamina
M-6.4	11.5-14.0	unimodal SB matrix: abundant well preserved *Coscinodiscus* and *Thalassiosira*
M-6.5	23.7	diffuse chalk-striped diatomaceous lamina: high diversity and fragmentation
M-BP		
M-BP.1	10.5	bloom lamina: abundant *Thalassiothrix* and *Thalassiosira*
M-BP.2	3.0	background diatomaceous lamina: silicoflagellate-rich, high diversity
M-BP.3	3.0-4.0	unimodal SB matrix: fragmented, high diversity assemblage
M-BP.4	13.6-14.3	unimodal SB matrix: silt grains and fragmented diatoms
2-8		
2-8.1	1.5	high diversity diatomaceous lamina: various centrics and *Chaetoceros cinctum* resting spores
2-8.2	11.5	*Chaetoceros* setae lens; good preservation
2-8.3	16.5	HB background diatomaceous lamina: high diversity, moderate preservation
2-8.4	6.0-8.0	unimodal SB matrix: *R. californica* and various other diatom and resting spore species
2-8.5	12.1	macerated biosilica lamina
2-9		
2-9.1	6.5	bloom lamina: *R. californica*
2-9.2	20.3	bimodal SB bleb and matrix: high diversity and abundant *Thalassiothrix* (rafts)
2-9.3	33.7	HB diatomaceous lamina: high diversity, pollen common
2-9.4	6.4	macerated biosilica lamina
2-9.5	29.7	macerated biosilica lamina
2-9.6	18.7	irregular bloom lamina: *Thalassiosira* dominant with various other diatoms

Backscattered Scanning Electron Microscopy Catalogue
(symbol: I)

Vacuum impregnation was attempted three times for the sediment to become properly impregnated. In the first two attempts, Spurr resin was used (cf. Grimm 1992b). Samples were placed into a teflon tray, the epoxy was poured in and the sediments were evacuated at a pressure of 15 torr for 2 hours. Afterwards, the epoxy-impregnated sediment was baked at 70 °C for 3 hours. This technique did not work as the epoxy did not fully penetrate the sediments. A second attempt to prepare the same samples failed. For the third, successful trial, all new samples were cut and then vacuum-impregnated with Struers brand Epofix at 172 kPa and left to set overnight.

Abbreviations: LB=low bimodality; MB=moderate bimodality; HB=high bimodality; SB=speckled bed

Sample	Position on x-ray (cm)	Comments
M-3		
M-3.1	7.5-8.0	pin and chalk-striped LB couplets
M-3.2	11.5-12.5	chalk-striped HB couplets: *Thalassiothrix* and *Ethmodiscus* laminae
M-3.3	14.7-15.2	mud-dominated laminae: silty with macerated diatoms and sponge spicules
M-3.4	15.2-15.5	diatom dominated laminae: large, porous *Coscinodiscus* frustules
M-3.5	17.5-18.5	diatom-rich unimodal SB: fragmented diatoms and silt aggregates
M-3.6	21.0-23.0	two textures of unimodal SBs: silt and silt aggregates common, diatom blebs, fish scales
M-6		
M-6.1	14.0-14.5	razor-striped LB couplets: very silty with razor-striped *Coscinodiscus* laminae
M-6.2	15.3-15.6	razor-striped LB couplets: very silty with razor-striped *Coscinodiscus* laminae
M-6.3	16.5-17.0	pin-striped MB couplets
M-6.4	17.4-18.3	pin-striped, diatom-rich HB couplets with *Coscinodiscus* bloom (black arrow)
M-6.5	19.2-20.0	closely spaced, mud-dominated razor-striped couplets
M-BP		
M-BP.1	2.3-3.0	closely spaced razor/pin-striped MB couplets with pristine *Chaetoceros* floc
M-BP.2	5.6-6.2	closely spaced diatom-rich razor/pin-striped MB couplets
M-BP.3	8.0-8.7	closely spaced razor/pin-striped HB couplets
M-BP.4	8.7-9.5	closely spaced mud-rich razor/pin-striped LB couplets
M-BP.5	15.0-17.5	closely spaced razor/pin-striped MB couplets, *Coscinodiscus* laminae and sponge spicule flocs
2-8		
2-8.1	6.0-7.5	unimodal SB: silt-sized speckles of various composition
2-8.2	10.5-11.8	widely spaced mud-rich chalk-striped LB couplets: silt aggregates common, *Chaetoceros* resting spore laminae (CRSL)
2-8.3	15.0-18.0	close to moderately spaced, razor/pin-striped MB/HB couplets: silicoflagellate laminae, pelletal structures and CRSL
2-8.4	4.0-5.7	HB couplets: diatom laminae=CRSL and *Thalassiothrix*
2-9		
2-9.1	3.0-6.0	moderately spaced diatom-rich couplets: *Ethmodiscus* and *Coscinodiscus* blooms
2-9.2	20.2-23.0	bimodal SB: *Chaetoceros* setae blebs and lozenges; pellets, silt and macerated biosilica in matrix
2-9.3	34.1-34.8	closely spaced, razor/pin-striped HB couplets: *Chaetoceros* setae blebs and *Thalassiothrix* laminae
2-9.4	32.5-34.1	MB couplets

APPENDIX 3E

Thin Section Catalogue
(symbol: ↕)

Abbreviations: LB=low bimodality; MB=moderate bimodality; HB=high bimodality; SB=speckled bed

Sample	BSEM sample equivalent	Position on x-ray (cm)	Comments
M-3			
M-3.1	M-3.3/4/5	14.7-18.5	mud-dominated and diatom-dominated packets, and diatom-rich unimodal SB
M-3.2	M-3.6	21.0-23.3	mud-rich and diatom-rich unimodal SBs: sharp contact visible
M-6			
M-6.1	M-6.3/4/5	16.5-20.0	mud-dominated MB and diatom-dominated HB razor-striped packets
M-BP			
M-BP.1	M-BP.3/4	8.0-9.5	LB couplets and HB couplets comparison
2-8			
2-8.1	2-8.1	6.0-7.5	unimodal SB
2-9			
2-9.1	2-9.1	3.0-6.0	moderately spaced diatom-rich couplets
2-9.2	2-9.2	20.2-23.0	bimodal SB
2-9.3	2-9.4	32.5-34.1	MB couplets

APPENDIX 4

Diatom abundances and ecology from a detrital lamina

	Strewn sample	2-8.2	
	Position on slab (cm)	15.8	
I. Diatom flora		Abundance	Ecology
Actinoptychus			coastal neritic diatom washed off from shelf (1)
A. splendens		R	
A. undulatus		C	
benthics		R	e.g. Arachnodiscus (Fig. 2.7B) and Navicula; from shelf
Chaetoceros			resting spore survival strategy
C. cinctum		F	
C. debilis		R	
C. diadema		R	
C. radicans		R	
C. vanheurkerii		C	
Coscinodiscus marginatus		A	ubiquitous; robust forms are produced throughout the winter
Ethmodiscus		F	background primary productivity
Hemiaulus		R	background primary productivity
Hemidiscus cuniformis		R	background primary productivity
Nitzschia		F	background primary productivity
Rhaphoneis		F	background primary productivity
Rouxia californica		R	fragments may actually be derived from summer laminae
Stephanopyxis turris		C	resting spore
Thalassiothrix longissima		F	fragments may actually be derived from summer laminae
II. Other microfossils			
Silicoflagellates		F	winter-dominant (2); ubiquitous
III. Preservation			
Lightly silicified		P	poor preservation due to dissolution and grazing
Heavily silicified		M-G	

References: (1) Pike and Kemp 1996, (2) Sautter and Sancetta 1992

Taxa and abundances from diatomaceous laminae.

Sample	Stratigraphic Interval (m)	Lamina type	Actinocyclus	Actinoptychus	Asteromphalus	Chaetoceros setae	Chaetoceros	Coscinodiscus	Denticulopsis hustedtii	Ethmodiscus	Hemiaulus	Hemidiscus cuniformis	Leptocylindrus	Nitzschia	Rhaphoneis	Rhizosolenia styliformis	Rouxia californica	Stephanopyxis turris	Thalassiosira antiqua	Thalassiothrix longissima	benthic diatom taxa	Silicoflagellates	Radiolaria	Coccoliths	Preservation
MBP	59.14-59.32																								
MBP-4		thin HB	-	F	R	C	C	F	-	R	R	R	-	A	R	R	-	-	A	A	-	F	-	-	P
MBP-3		thin LB	-	F	-	A	A	F	-	R	-	-	-	F	-	-	R	-	C	C	-	C	-	-	P
MBP-2		thin HB	-	F	-	A	C	F	-	R	-	-	-	C	-	-	-	-	A	A	-	A	-	-	M
MBP-1		thin MB	F	C	-	A	C	C	-	F	R	-	-	F	R	-	F	-	C	C	-	C	R	-	P
M-6	22.41-22.69																								
M-6.6		thin MB	F	F	-	A	A	A	-	A	-	R	-	C	-	-	F	-	A	A	-	F	-	-	P
M-6.5		thick continuous	-	R	-	C	C	A	-	C	-	-	-	C	F	-	F	-	C	A	-	F	-	-	P
M-6.4		thick continuous	-	-	-	F	F	A	-	A	-	-	-	F	-	R	R	-	F	C	-	C	-	-	M
M-6.3		thin LB	-	R	-	F	A	A	R	R	-	-	-	F	R	-	F	-	A	A	-	R	-	-	M
M-6.2		thin LB	-	F	-	C	A	A	-	R	-	-	-	C	F	R	R	-	C	A	-	F	-	-	P
M-6.1		macerated	-	R	-	A	A	A	-	R	-	-	-	F	F	R	-	-	A	A	-	F	-	-	P
M-3	20.40-20.63																								
M-3.2		thin MB	R	R	-	C	F	A	-	R	R	F	-	R	R	-	-	-	F	F	-	F	-	-	P
M-3.1		macerated	-	R	-	A	C	A	-	C	-	-	-	C	R	R	R	-	A	C	-	F	-	-	M
2-9	15.77-16.14																								
2-9.6		thin LB	-	C	R	C	C	F	-	-	R	-	R	C	R	R	R	R	F	C	-	F	R	-	P
2-9.5		thin MB	-	F	-	A	A	F	-	-	-	-	-	A	R	-	C	F	C	C	-	R	-	-	P
2-9.4		thick continuous	-	-	-	C	F	F	-	-	F	-	-	C	-	-	A	R	C	F	-	R	-	-	M
2-9-4s		thick discontinuous	-	R	-	A	F	F	-	F	R	R	-	C	R	-	C	F	A	F	R	F	-	-	M
2-9-3s		macerated	-	F	-	F	C	F	-	-	R	R	-	C	R	-	R	F	A	C	R	F	-	-	M
2-9-2s		macerated	-	C	F	F	C	-	-	F	R	-	-	A	R	-	-	R	C	C	-	F	-	-	M
2-8	15.49-15.67																								
2-8.5		macerated	-	F	R	C	C	F	-	F	R	R	-	C	R	-	C	-	C	C	-	F	-	-	M
2-8-1s		thick discontinuous	-	F	R	A	C	F	-	R	R	-	-	A	R	-	-	C	C	C	R	F	R	-	G
2-8.3		thin MB	-	F	-	C	C	C	-	-	R	R	-	C	-	-	-	-	C	C	-	F	-	-	M
2-8.2		thin LB	-	F	-	F	F	F	-	F	-	-	-	C	-	-	-	R	C	A	-	-	-	-	P
2-8.1		thin HB	-	F	-	A	A	F	-	R	-	R	-	C	R	-	R	R	C	C	-	-	-	-	P
2-8.4		thick continuous	-	F	F	A	A	R	-	F	R	-	-	A	F	R	A	R	A	C	-	F	-	-	G
94L-1s	reconnaissance	thick continuous	R	C	-	R	C	R	A	R	R	-	-	A	-	A	-	-	A	C	-	A	R	A	M
94M-1s	reconnaissance	thick continuous	-	-	-	-	-	R	A	-	-	-	-	-	-	C	-	R	-	-	-	F	-	-	G
94N-1s	reconnaissance	thick continuous	-	-	-	-	C	F	A	-	-	-	-	-	-	-	-	-	C	-	-	-	-	-	M

Abundance: A=abundant; C=common; F=few; R=rare; '-'=barren

Preservation: G=good; M=moderate; P=poor

s=strewn slide; all other analyses from smear slides

APPENDIX 6

Full quantitative diatom counts from smear slides (see App. 3A)

An average of 300 diatoms were counted per slide; values given per species are percentages normalized to 100%

(Counting courtesy L. D. White)

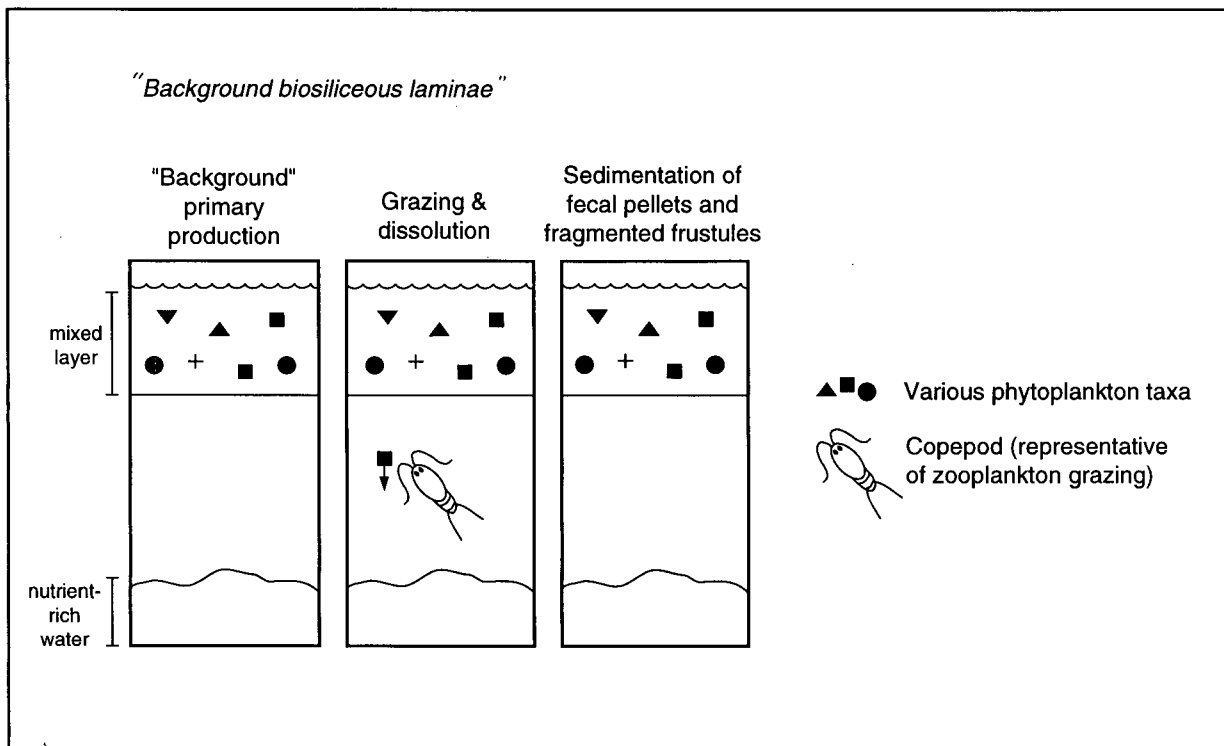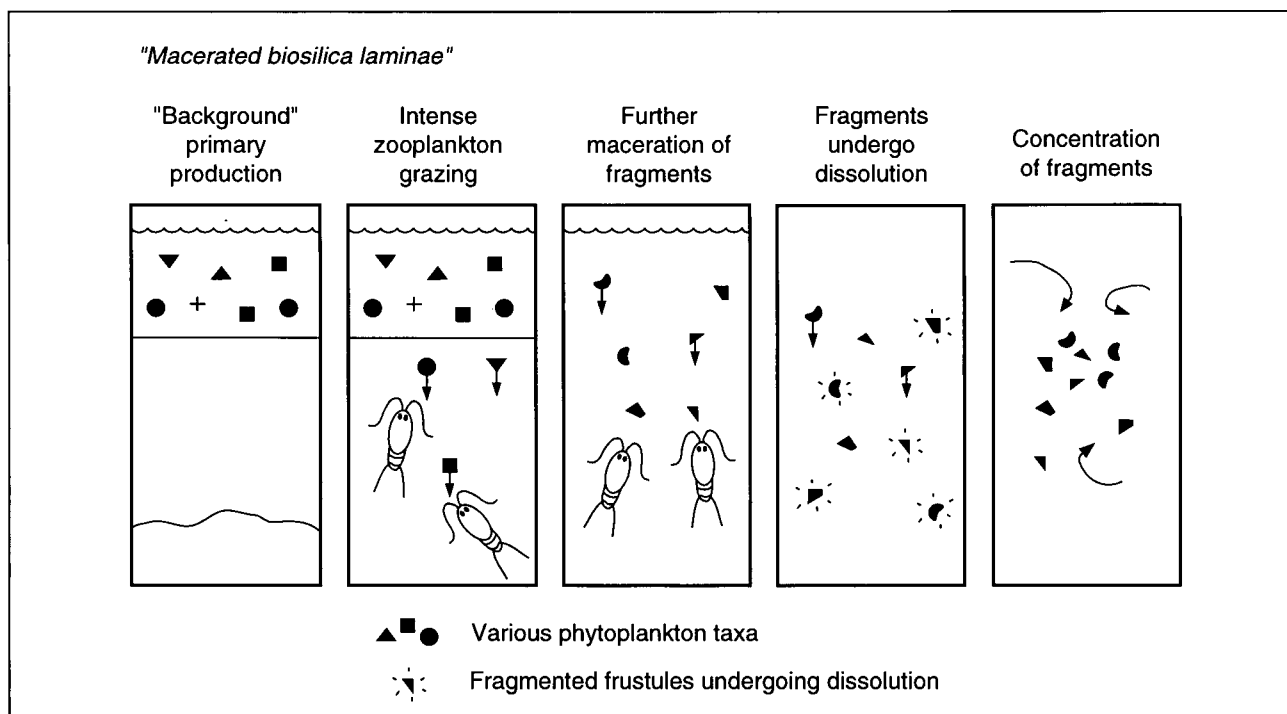| Sample	Comments	Abundance	Preservation	Actinocyclus ellipticus	Actinocyclus spp.	Actinoptychus senarius	Asteromphalus spp.	Chaetoceros setae	Coscinodiscus marginatus	Coscinodiscus nodulifer	Coscinodiscus spp.	Denticulopsis hustedtii	Hemidiscus cuniformis	Nitzschia reinholdii	Rouxia californica	Thalassionema nitzschioides	Thalassionema schraderi	Thalassiosira antiqua	Thalassiosira nativa	Thalassiosira sp.	Thalassiothrix longissima	Benthics (other than A. senarius)	Total Diatoms Counted (normalized to 100%)
2-8.6	Chaetoceros setae lens	G	A					64						1		31		1		1	2		438
2-9.1	Rouxia californica bloom lamina	G	A			*			*			*		*	77	8	1	6	1	4		1	310
2-9.3	Chaetoceros setae-rich bleb in speckled bed	A	G					78				*	*	7	2	8		3			2		405
M-3.3	Detrital lamina: fragments of C. marg. & T. ant.	C	M	*	*	6		3	21		2		*			28		34		2		3	248
M-3.4	Detrital lamina: fragments of T. nitz. and T. ant.	C	M		*	2		4	15	1	2		*			44		24			1	2	292
M-3.6	Detritus-rich speckled bed: C. marg. dominates	C	M	1	*	2	1		37		2			2		15	2	23	4	2	3	5	207

* less than 1%

111

APPENDIX 7

Formation of diatomaceous laminae

The following 5 panels are interpretive cartoons which outline the possible mechanisms by which each type of diatomaceous laminae may have formed; these hypotheses reflect work in progress.
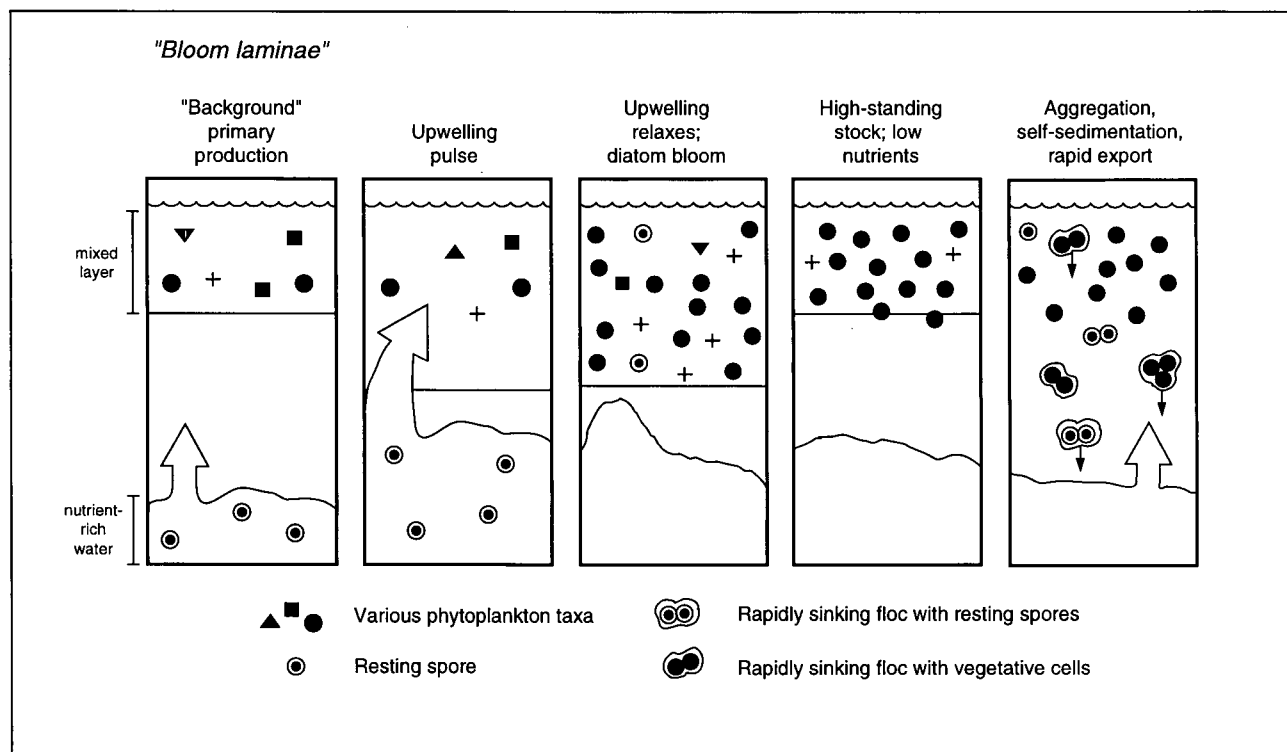
APPENDIX 7A. Formation of thin biosiliceous laminae. The diverse diatom assemblages, poor to moderate states of frustule preservation, and minor detrital content in these laminae are interpreted to represent intervals of lower, or "background," primary productivity. Upwelling was likely weak or non-existent, nutrient levels in the mixed layer were generally low and relative rates of zooplankton grazing and dissolution were high. Thin biosiliceous laminae are interpreted to have formed during the late winter or early spring and can be considered "background bsiliceous laminae."

"Background biosiliceous laminae"

"Background" primary production

Grazing & dissolution

Sedimentation of fecal pellets and fragmented frustules

mixed layer

nutrient-rich water

▲■● Various phytoplankton taxa

Copepod (representative of zooplankton grazing)

APPENDIX 7B . Formation of macerated biosilica laminae. These laminae contain highly fragmented components of frustules from a variety of morphotaxa (cf. Grimm 1992a) and minute amounts of detritus. The high diversity assemblage suggests that background primary production was occurring; poor preservation of frustules can be attributed to intense zooplankton grazing and dissolution. Macerated biosiliceous laminae are interpreted to form when primary production rates were closely coupled with grazing rates, perhaps in the late summer.

"Macerated biosilica laminae"

"Background" primary production — Intense zooplankton grazing — Further maceration of fragments — Fragments undergo dissolution — Concentration of fragments

▲■● Various phytoplankton taxa

⋰⋱ Fragmented frustules undergoing dissolution

APPENDIX 7C. Formation of thick continuous diatomaceous laminae (modified from Grimm et al. 1996). Monospecific and monogeneric diatom assemblages dominate this lamina type. The low diversity assemblages and excellent state of frustule preservation indicates strong upwelling and nutrient delivery to the surface waters, optimal blooming, and efficient self-sedimentation (Grimm et al. 1997). Strong upwelling and diatom blooms usually occur in the spring and early summer seasons; thus we consider thick continuous diatomaceous laminae as "bloom laminae."

"Bloom laminae"

"Background" primary production — Upwelling pulse — Upwelling relaxes; diatom bloom — High-standing stock; low nutrients — Aggregation, self-sedimentation, rapid export

mixed layer

nutrient-rich water

▲■● Various phytoplankton taxa

◉ Resting spore

◉◉ Rapidly sinking floc with resting spores

●● Rapidly sinking floc with vegetative cells

APPENDIX 7D. Formation of thick discontinuous diatomaceous laminae I: *Thalassiothrix* mats. The macroscopically crinkled appearance of these laminae and the presence of pristine monospecific assemblages of interwoven *Thalassiothrix* suggest that these laminae resulted from the sedimentation of *Thalassiothrix* mats. Differing strategies for nutrient uptake govern mat development: (1) the development of oceanic fronts from the subduction of colder surface waters in which mats congregate on the warm side (Yoder et al. 1994); or (2) strongly stratified water column which allow mats to form in the surface waters (Villareal et al. 1993). A combinationof these scenarios may also operate. In both scenarios, mats regulate their buoyancy to photosynthesize and uptake nutrients at the nutricline.
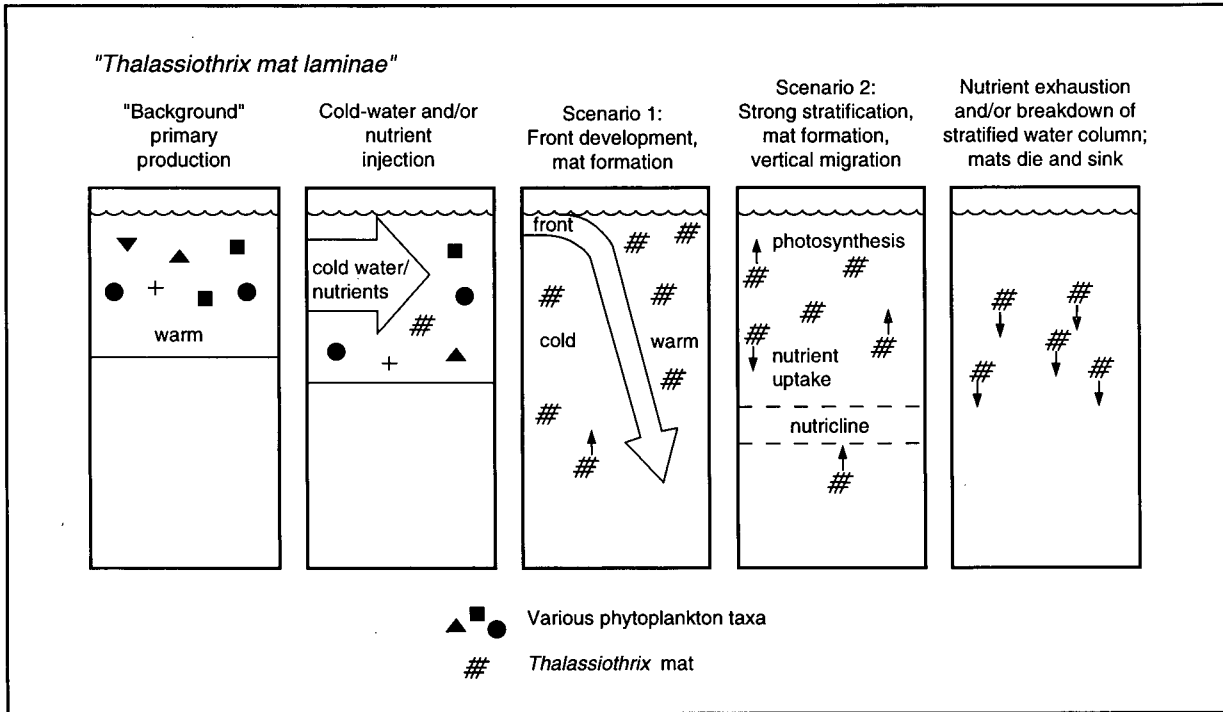
APPENDIX 7E. Formation of thick discontinuous diatomaceous laminae II: *Chaetoceros* setae. These laminae contain well-preserved *Chaetoceros* setae. Other diatom taxa and *Chaetoceros* resting spores are present but are minor components. The formation of setae-rich laminae is interpreted to begin with a *Chaetoceros* bloom. Interpretations regarding the isolation of setae from vegetative cells and subsequent concentration is speculative. We hypothesize that the vegetative cells were grazed but the setae were discarded by zooplankton. The robust setae may also survive dissolution better than vegetative fragments (Pike and Kemp 1996a). Setae may have been concentrated by currents, facilitating aggregation and rapid sinking.